2012-10-19

Thermodynamic Kinetics and Efficiency Analysis of Methyl Viologen

Chang Chen
Brigham Young University - Provo

Thermodynamic, Kinetic and Efficiency Analysis of Methyl Viologen

Chang Chen

A thesis submitted to the faculty of
Brigham Young University
in partial fulfillment of the requirements for the degree of

Master of Science

Randy S. Lewis, Chair
Dean R. Wheeler
Julianne H. Grose
Larry L. Baxter

Department of Chemical Engineering

Brigham Young University

October 2012

ABSTRACT

Thermodynamic, Kinetic and Efficiency Analysis
of Methyl Viologen

Chang Chen
Department of Chemical Engineering, BYU
Master of Science

Methyl Viologen (MV) is an electron mediator that has great possibilities to be used with an electrode system in which the electrode system provides electrons towards reducing MV species. MV has three redox states and they can be converted to each other via redox reactions on the surface of the electrode. The concentration of the three species of MV was related to the voltage potential applied to the system through a thermodynamic model. With the thermodynamic model the concentration of the three species can be predicted with different applied voltage potentials towards providing guidance for controlling the redox state of MV in a system. The kinetic rates of MV reduction were also assessed using a preliminary kinetic model. The kinetic model predicted all three species concentration changes with time although only the MV^+ concentration was measured with time. Analysis revealed that the rate of MV reduction was three orders of magnitude slower than the rate of electrons required for bioethanol production. However, increasing the affinity of MV^+ on the surface and blocking the H^+ on the surface potentially can increase the reduction rate of MV by up to three orders of magnitude and can potentially enable MV to be used in commercial applications. As for the efficiency study, the coloumbic efficiency was less than 22% which was much lower than the efficiency of more than 85% observed in other studies for the direct electron transfer between electrode and bio organism. The efficiency was lowered mainly by the reduction of H^+ and minimizing H^+ on the electrode can largely increase the efficiency. Medium used for cell growth can also affect the efficiency through medium species consuming electrons provided by the electrode. Electron mediators, such as MV, have potential promise in applications such as microbial fuel cells, biofuel formation, and waste water treatment. However, engineering analysis of electron mediators is critical to provide better engineering control, design, and economic analysis for future applications.

Keywords: Chang Chen, methyl viologen, engineering analysis, thermodynamic, kinetic, efficiency

ACKNOWLEDGEMENTS

I am very grateful for the opportunity to work with Dr. Randy Lewis. I have appreciated his guidance and direction, patience and encouragement, and willingness to listen. I'm also grateful to a wonderful advisory committee, Dr. Dean R. Wheeler, Dr. Julianne H. Grose and Dr. Larry Baxter for their assistance and advice. I have enjoyed the company of many other great students in the lab, who have increased the quality of my research through their probing questions, and willingness to work hard. A special thanks to my wonderful husband, Fangyuan Zhou, without whom, the completion of this work would not have been possible.

TABLE OF CONTENTS

LIST OF TABLES

LIST OF FIGURES

1 INTRODUCTION

1.1 Biofuel as an alternative fuel

The energy crisis and global warming are among the most severe issues that threaten the development of the economy. World energy consumption has increased by 4.2 percent from 495 quadrillion Btu in 2007 to 516 quadrillion Btu in 2010 [1, 2]. Among energy sources, liquid fuels remain the world's largest energy source. World use of liquids and other petroleum grew 3.4 percent per year from 2007 to 2010 [1, 2]. Consequently, the rising worldwide demand for oil will collide with falling availability. Although the U.S. is still the world's second-largest producer of oil, about a third of the US demand must be imported [1]. The same report also indicated that in 2001, the U.S. imported 6 million barrels of oil, about half the total amount consumed; this makes an average 3 gallons per person per day. Over time, governments, corporations, and individuals continue to compete for the shrinking supply.

In addition to the energy crisis, global climate change has gained more attention. Over the past century, the Earth has increased in temperature by about 0.5 °C partly due to the "greenhouse gas effects" [3]. The same report also showed that in 2009, total U.S greenhouse gas emissions of CO were 6.6×10^{15} g CO, which increased by 7.4 percent from 1990 to 2009.

One proposed method to reduce the impact of global warming and the energy crisis is the production and utilization of biofuels obtained from renewable resources. The idea of biofuels was first introduced in 1912 when the first microbial biofuel cell was demonstrated by Potter [4]. Biofuels are fuels produced from renewable biological resources like starch crops, trees and grasses, vegetable oils, and animal fats. [5]. Biofuels are renewable, meaning their carbon sources can often be regrown. Since the energy demands are expanding and the fossil fuels are depleting, biofuels have the potential to make a difference in helping to meet the world's future energy needs as an alternative energy source. In addition, advanced biofuels can offer environmental benefits such as lower carbon and sulfur emissions when compared with conventional petroleum-based fuels [6].

Typical biofuels include biodiesel [7], bio-alcohol [8] and bio-gasoline [9]. Biodiesel is a diesel fuel produced from natural oils such as animal fats or vegetable oils through a chemical process involving transesterification. The process produces two products—methyl esters (i.e. biodiesel) and glycerin (a valuable byproduct that can be used to make soaps and other products). Biodiesel can be blended at any level with petroleum diesel to create a biodiesel blend. It can be used in compression-ignition (diesel) engines with little or no modifications. Biodiesel is simple to use, biodegradable, nontoxic, and essentially free of sulfur and aromatics. Biodiesel is the most common biofuel used in Europe [10]. However, there are concerns with the competition with food, the compatibility with existing engines, and lower heat of combustion than traditional gasoline [7, 8]. Bench work on new kind of biofuels like bio gasoline is aimed at solving these problems [9] but there is still a long way to go.

Bio-alcohol is an alcohol fuel derived from sugarcane, wheat, corn and biomass which can be blended with conventional petroleum to improve its octane level and reduce its greenhouse gas emissions. Bio-alcohol, especially ethanol, is the most common biofuel worldwide [8]. Ethanol fuel can be formed via two main processes: sugar/starch crop fermentation and lignocellulosic processes. The most prevalent lignocellulosic processes for ethanol production includes fermentation of sugars and fermentation of syngas [11]. Syngas is a mixture of principally CO, CO_2, and H_2, which can be obtained by gasification of coal, petroleum, biomass or steam reforming of natural gas. To convert sugars and syngas to alcohol during fermentation, electrons are essential for the metabolic processes associate with fermentation.

Biodiesel and bio-alcohol have difficulties in energy-density and compatibility when used in traditional engines. Bio-gasoline is liquid hydrocarbons identical to those currently used which is converted from biodiesel or bio-alcohol chemically. The bio-gasoline system includes hydrotreating, advanced microbial synthesis and chemical converting.

1.2 **Electron mediators**

In biological processes, electrons for product formation and bio-organism growth are often supplied by reduced species (e.g. glucose, H_2, CO, etc.) [12-16]. However, a recent focus has also been on the use of electrodes to replace the use of reduced species for supplying electrons for enzymatic or cellular processes [17-21]. When using electrodes, electrons can either be transferred to cells or enzymes by an external electron mediator or, in some cases, directly transferred to cells immobilized on an electrode. Several classes of external chemical electron

mediators that have been used in biological processes include, but are not limited to, viologen, phenoxazine, phenothiazine, phenazine, indophenol and bipyridilium derivatives [22]. Specific examples include methyl viologen (MV) [18], neutral red [20], AQDS [23], resazurin [24], and phenosafranin [25]. However, challenges of using external mediators have included toxicity [16], mediator inactivation [26] and low energy efficiency [27].

As for direct electron transfer from electrodes , Nevin et al. recently reported that some bacteria can utilize electrons directly from an electrode to convert CO_2 to valuable organic chemicals [28, 29]. For this study, the efficiency of electrons directly transferred from the electrode was reported to reach as high as 85%. Although the mechanisms of direct electron transfer are still under question, the current hypothesis is that key enzymes are critical for direct electrode utilization to occur [30, 31]. Yet, it is unclear as to whether all bacteria are capable of directly utilizing electrons since only a few cases have been reported. Several challenges that exist with direct utilization include mass transfer associated with biofilms, potential limitations of bacterial growth and unclear electron transfer mechanisms between the bacteria and electrode.

As noted, there are many examples of using electrodes for providing electrons in biological processes, although there are still several challenges including scale-up and economic issues. Most engineering analysis has been associated with either the kinetics of redox reactions between electron mediators and enzymes without an electrode [12, 32] or with electron mediators' chemical electrochemical properties [33, 34] using cyclic voltammetry. The cyclic voltammetry studies can only provide limited guidance for future biofuel production applications due to the significant differences in system settings between the applied system and the cyclic voltammetry system. The differences include temperature, stirring rate and electrode surface area.

Thus, there is great potential in using electrodes but a more rigorous engineering analysis is needed to design and control electrode-mediated biological processes that are sustainable. Specifically, this work focuses on characterizing the thermodynamics and kinetics of methyl viologen (MV) in an electrode system in order to better understand the potential limitations of using MV as an external electron mediator in biological processes. MV was chosen as a result of several studies noted below in which MV had a beneficial effect on the biological processes.

For biofuels applications, there is an opportunity to provide electrons from off-grid energy like energy from a wind mill. The energy from the wind mill is usually difficult to use in many applications because of the unstable current supply and low potential. However, with a biological system, there is an opportunity to use the off-grid energy since biological systems can remain dormant during non-use.

1.3 **Methyl viologen**

Methyl viologen (MV), also known as N,N′-dimethyl-4,4′-bipyridinium dichloride or Paraquat, has been demonstrated as an extracellular electron mediator to promote biological redox reactions. Three redox states of methyl viologen, MV^{2+}, MV^{+} and MV^{0}, can exist. MV^{2+} is the easiest to be reduced, MV^{0} is the hardest to be reduced and the MV^{+} is between the two extremes.

Several studies have successfully utilized MV in biological processes. From testing with *Clostridium acetobutylicum*, it was reported that MV can act as an external electron donor to increase ethanol yields either from glucose [35] or in an electrode system [36, 37]. Tatsumi et al. [38] demonstrated the MV can react with the *hydrogenase* enzyme to promote the electron

transfer. Additionally, in another study using *Dehalococcoides*, MV was applied as an external electron mediator for cell fermentation of Trichloroethene [17]. Unlike the first two studies, this latter study used an electrode to continuously provide electrons.

However, some adverse effects of MV on cell growth have been reported with *Clostridium ragsdalei* [16]. For example, an immediate decline of cell mass was observed when MV was added. However, the cell mass eventually reached steady state at a lower cell mass and an increase of ethanol production was observed, a condition which demonstrated that the cells were still active. As is evident, MV has promising potential as an external electron mediator, although a better understanding of the underlying engineering principles would provide more guidance as to the potential use of MV in these systems. This study focuses on the thermodynamic and kinetic characterization of MV in an electrode system to provide a foundation that can lead towards better control and design of biological systems utilizing extracellular electron mediators.

1.4 **Objective**

The objective of the project is to perform thermodynamic, kinetic, and efficiency studies for the extracellular electron mediator MV. The thermodynamic study provides the analysis of the minimum required external energy input to reduce MV^{2+} in the solution to useable MV species that can donate electrons and provides guidance on the applied potential needed to control the types of MV species that are present. The kinetic analysis provides information of the MV reduction rate (or electron transfer rate), which is valuable when assessing the feasibility of future cellular applications based on required cellular electron consumption rates. For efficiency

studies, where the electron efficiency is defined as the ratio of the electrons acquired by the reducing MV versus the electrons provided by external power, the efficiency helps in the analysis of the economic feasibility in future biofuel production with an electrode system.

The experimental system of a Bio Electrochemical Reactor (BER) used for all work is depicted in Figure 1.1. In the cathode chamber, MV^{2+} and MV^{+} are reduced by electrons to become MV^{+} and MV^{0}, respectively. In the anode chamber, water is electrolyzed to O_2 and H^{+}. Details of the system are described in Chapter 3.

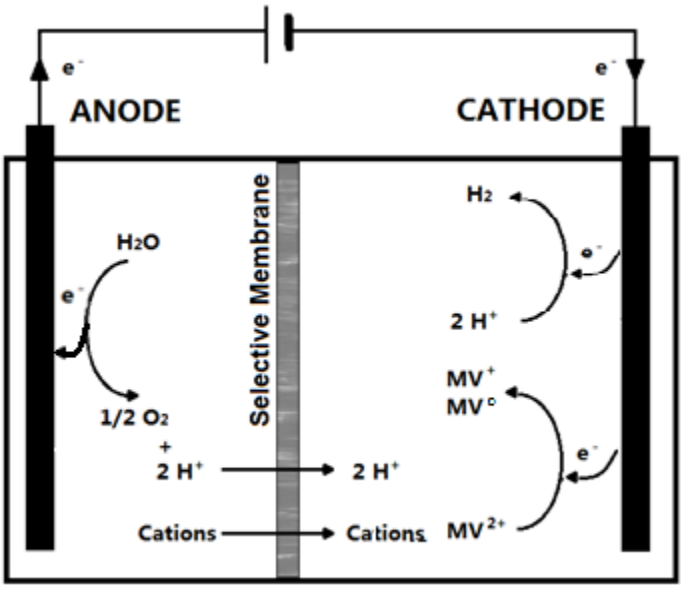

Figure 1.1 Experimental system

1.4.1 Objective 1: Thermodynamic modeling

MV has three redox species, MV^{2+}, MV^{+} and MV^{0}. MV^{+} and MV^{0} have the potential to donate electrons in biological fermentations. Since the three species can be interconverted by

redox reactions, the concentrations of the three species in the solution were studied in relation to the potential applied to the system. By imposing an optimal potential, concentrations of the three species in solution can be controlled. A model was developed using the Nernst Equation to predict the relationship between MV concentrations change with the potential. Several experiments at various potentials were performed to test the MV thermodynamic model.

1.4.2 Objective 2: Kinetic modeling

Reduction of MV is a two-step electrochemically reaction. The understanding of the kinetics of electron mediator reduction needs to be addressed for proper design of potential industrial applications. The speed and total yield of desired product formation could be limited if the speed of recycling the electron mediator is slower than that of the enzyme or cellular system. The kinetics of MV reduction was always considered as diffusion limiting in cyclic voltammetry studies based on the limiting current measurement in stagnant solution [6-8] such that the kinetic-limiting reaction rates were not studied. For commercial biofuels production, it is important to know the kinetic-limiting reaction rate to aid in the design or analysis of potential commercial systems. In this study, the kinetics of MV reduction in the absence of diffusion limitations were studied using a well-stirred system. For the two-step reduction of MV; each step is a surface reaction which is composed of three stages: reactant adsorption, surface reaction, and product desorption. Due to previous research in our lab, the reaction is limited by the surface reaction.

1.4.3 Objective 3: Efficiency analysis

The efficiency of electron utilization (Coulombic efficiency) when reducing MV is defined as the ratio of the moles of electrons used to reduce MV to the moles of electrons provided by the applied external potential. The efficiency can be lowered by side reactions, such as hydrogen formation, medium reduction, and potential other side reactions that can compete with MV reduction. The electrons utilized and provided were calculated separately. Electron utilization with time was calculated with experimental data and the kinetic model developed in Objective 2 and electrons provided were calculated by monitoring the current with time.

2 LITERATURE REVIEW

The purpose of the work presented in this dissertation is to characterize the thermodynamics, kinetics, and efficiency of electron transfer to methyl viologen (MV) in an electrode system in order to better understand the potential limitations of using MV as an external electron mediator in biological processes. The following literature review and preliminary studies outlines the current state of using MV as an electron mediator for biological systems, particularly with the potential application for producing biofuels such as ethanol.

2.1 Production of bioethanol

2.1.1 Starch/sugar crops fermentation

Starch fermentation to produce ethanol is considered a first generation biofuel process. Starch and sugar crops contain the simplest source of sugars and fermentation of starch/sugar crops is one of the easiest methods of biofuel production. Starch contains a polysaccharide of glucose residues and sugar crops contains mostly sucrose, both of them can be used by bio organism directly with little pretreatment. Disadvantages of this process include the competition with food, high cost of enzymes, and the need for economic subsidies [39].

2.1.2 Lignocellulosic processes

Ethanol production using lignocellulosic materials, compared with using starch, has several advantages including a cheaper feedstock, better carbon conversion, and non-competition with food [40]. The downside is that lignocellulosic materials are more complex for fermentation applications which require complicated pretreatments [41].

New technology is being developed to implement lignocellulosic ethanol production. The most prevalent lignocellulosic processes for ethanol production include: fermentation of sugars, metal catalysis of syngas, and fermentation of syngas [11]. For the process involving fermentation of sugars, there are three main steps in ethanol production: biomass pretreatment, cellulose saccharification, and fermentation. Pretreatment of the lignocellulosic material is necessary due to the crystalline structure of the lignocellulosic material. Pretreatment processes of cellulosic and hemi-cellulosic components often include two steps, first with chemicals such as acid, ammonia, steam, or alkaline [42, 43] to remove the lignin shell outside the cellulosic and hemi-cellulosic components then with enzymes called cellulases and xylanases to hydrolyze the lignocellulosic material to fermentable sugars. The sugars are then fermented to ethanol using bio organisms such as genetically-engineered *Escherichia Coli* [44], *Saccharomyces Cerevisiae* [45] and *Zymomonas Mobilis* [46]. For the syngas processes, lignocellulosic is first gasified to produce syngas. Syngas is composed mostly of CO_2, CO and H_2, but will include a variety of additional major and minor species depending on the feedstock and type of gasifier [47, 48]. Following syngas generation, syngas is converted to ethanol and other products using either metal catalysts or fermentation. Syngas fermentation is the focus of the research and more details are introduced in the following sections.

2.2 Syngas utilization

Syngas can be obtained by gasification of coal, petroleum, biomass or steam reforming of natural gas [49]. Syngas is an intermediate product in the formation of a number of useful products, including additional H_2, Fischer-Tropsch liquids, methane, electricity, and ethanol [50]. Syngas can be converted to ethanol and a variety of chemicals through two main processes: metal catalysis and syngas fermentation.

2.2.1 Metal catalysis

Catalytic conversion of syngas is a primary industrial method to convert syngas to ethanol fuel using metal catalysts, such as Fe, Co, Ru and Ni [51]. The most common process is Fischer-Tropsch Synthesis (FTS). FTS is used for the production of liquid hydrocarbons from CO and H_2 mixtures over a transition metal catalyst. The potential exists for using cellulosic-generated syngas for large-scale commercial processes, although syngas is not currently used [52]. The FTS process can produce either gasoline or diesel depending on the catalyst used and the operating temperature. For iron based catalysts and a high operating temperature (330-350 ^{o}C), the process will produce mostly light hydrocarbons where the final product will be mostly gasoline [53]. A low H_2/CO ratio syngas is optimal for this process. For cobalt based catalysts, a lower operating temperature (200 ^{o}C) will produce heavier hydrocarbons and the final product will be mostly diesel [54]. This process is optimal with a high H_2/CO ratio syngas which is usually generated with natural gas or oil. The first FTS plant began operation in Germany in 1938 [50], playing an important role in supplying the fuel for Germany during World War II. In 1955, Sasol (South Africa) launched the first large-scale FTS operation in the

world. Currently, many oil companies such as Shell Oil, Chevron, ExxonMobil and ConocoPhillips have been conducting research and have built pilot plants [50].

With regards to FTS using lignocellulosic-generated syngas, there are still some obstacles. The severe reaction conditions with high temperature and pressure limit the applications and require high energy inputs. The heat removal duty resulting from the strong exothermal reactions during the process are also a serious challenge [55]. In addition, the selectivity of catalytic conversion is low [52] and some catalysts are very sensitive to biomass-generated syngas contaminants and are easily poisoned [51]. Besides catalytic conversion of syngas, syngas fermentation is another method to produce ethanol from syngas.

2.2.2 Syngas fermentation

Syngas fermentation is a microbial process using syngas as the carbon and energy sources to convert CO_2, CO and H_2 into fuels and chemicals. CO_2 and CO can act as the carbon sources and CO and H_2 can act as the electron sources. Similar to using metal catalysis with FTS, there are several bio-catalysts that can also produce fuels and chemicals from syngas by fermentation. These microorganisms are mostly known as acetogens including *Clostridium ljungdahlii* [56], *Clostridium autoethanogenum* [57], *Eurobacterium limosum* [58], *Clostridium carboxidivorans* P7 [59], *Peptostreptococcus* products [60], and *Butyribacterium methylotrophicum* [61].

One particular microbe, known as *Clostridium Ragsdalei* P11, can produce ethanol from syngas under conditions of 37 °C, 1 atm, and pH 6. The metabolic pathway follows the Wood-Ljungdahl pathway shown in Figure 2.1 [62, 63].

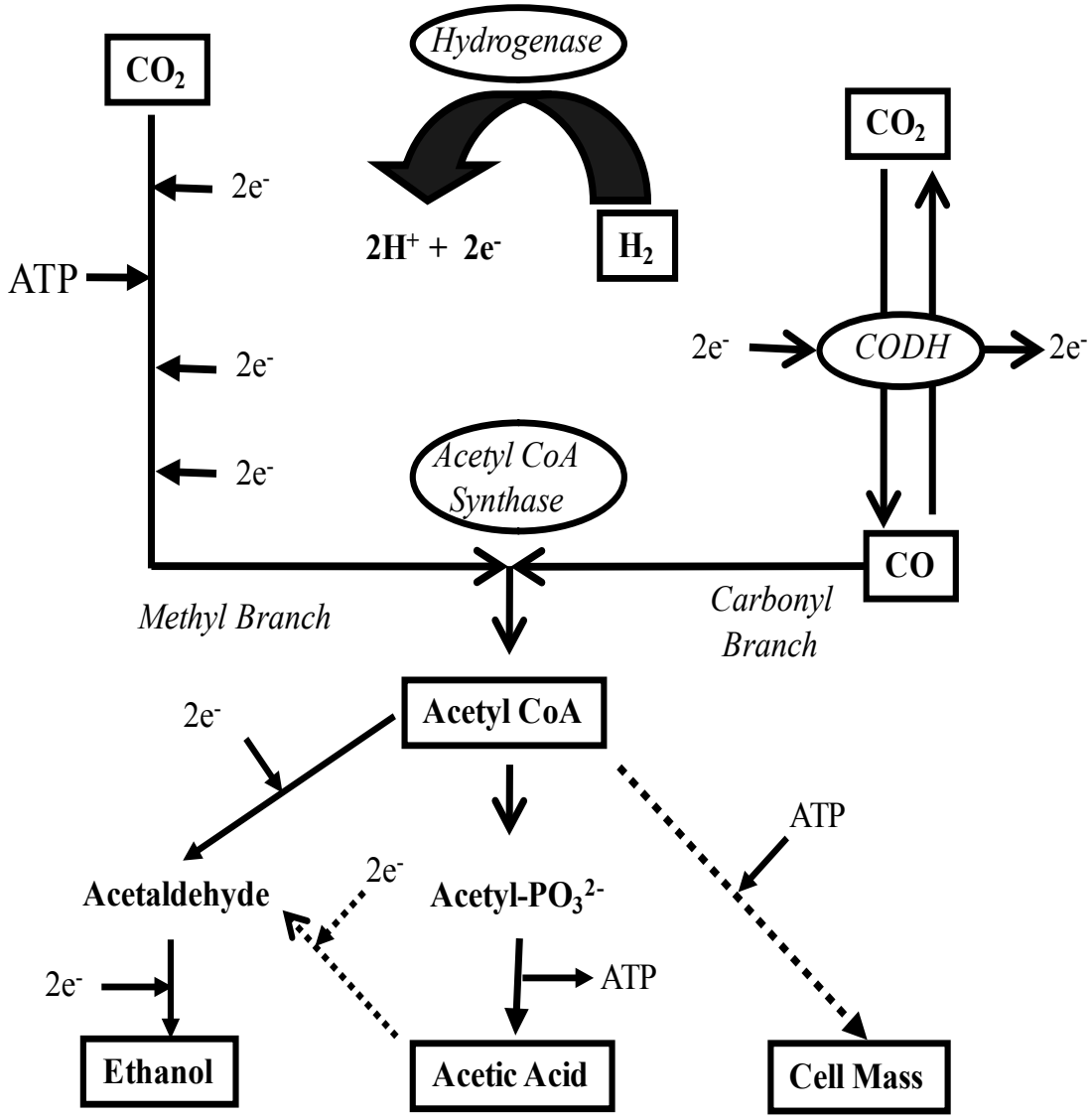

Figure 2.1 Modified Wood-Ljungdahl metabolic pathway [41]

In this metabolic pathway, shown in Figure 2.1, two molecules of CO2 are reduced to acetyl-CoA, following which acetyl-CoA is used by bacteria for product formation (e.g. ethanol and acetic acid) or cell growth or both [64]. In the fermentation process, acetyl CoA can be converted to the targeted product ethanol or acetic acid. In the methyl branch, one CO_2 molecule

is converted to a methyl moiety consuming one ATP and six electrons. In the carbonyl branch, two electrons are utilized to reduce one CO_2 molecule to CO which is then incorporated with the methyl moiety to form acetyl-CoA. Twelve electrons are needed to reduce two molecules of CO_2 to acetyl-CoA. Previous experiments demonstrated that cells can grow and produce ethanol and acetic acid from a headspace composed purely of H_2 and CO [63] or purely of H_2 and CO_2 [65]. H_2 and CO acted as the electron source. Nevertheless, using CO_2 as the sole carbon source rather than syngas could provide an additional avenue of biofuel production since the amount of CO_2 produced in industry every year is much higher compared to that of CO. Additionally, CO_2 is the waste gas for many fermentation processes and utilization of CO_2 could enhance the economics of a biological process using syngas. When using CO_2 as the sole feed gas species, an external electron source is required. One possible solution is that electrons can be created by an external power source using a specially designed Bio Electrochemical Reactor.

2.3 **Bio electrochemical reactors (BERs)**

A bio electrochemical reactor, shown in Figure 2.2, is a reactor that uses external electricity to enhance biological processes. The reactor can either use direct electricity for electrons or use biologic processes to produce electrons. For the latter case, chemicals like glucose are feed to bio organisms or enzymes and electrons from the substrate are donated to the anode and then transferred to the cathode to make product. In all cases, electrons are transported from the cathode to the bio organism(s) or enzyme for product formation. Sometimes, a selective membrane is constructed between the two electrodes to increase the selectivity by avoiding

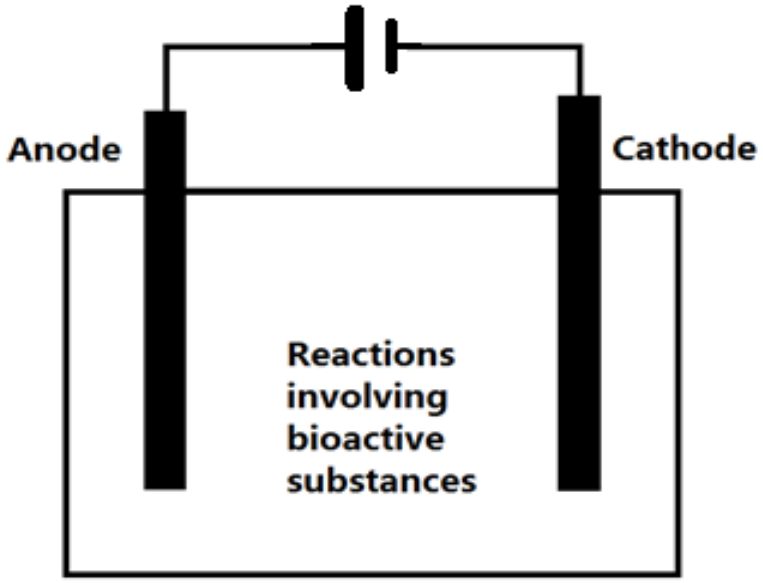

Figure 2.2 Bio electrochemical reactors

homogeneous side reactions. The idea of BERs first occurred thirty years ago [66] with various applications. The most recent uses have focused on waste treatment [67-69] using external electricity or fuel cells [70-72] to produce electricity. Some studies have addressed the metabolic changes that affect product distributions of these systems [73]. A few kinetic studies have reported the kinetic rate constants of electron transfer for bio electrochemical reactions in binary organic solvent-water media [74]. However, research is still needed to characterize the reactions that take place in these reactors [65].

One important characteristic of BERs for future implementation is their ability to induce oxidation-reduction reactions. For example, cell growth and fermentation demand electrons to provide a chemical reducing potential for product formation. Electrical energy provided by the BERs can be converted directly to certain kinds of bacteria immobilized on the electrode surface

or via electron transfer to a suitable electron carrier and subsequently to metabolite production. For directly electron transfer, certain bacteria can utilize electrons directly from the electrode and convert CO_2 to valuable organic chemicals [28, 29]. Liao et al. also demonstrated that CO_2 can be converted to 1-butanol [14]. The efficiency of electrons directly from an electrode could reach as high as 85% while the process was limited by the low variety of qualified bacteria, low reaction rate, non-specificity of products produced and high cathode expense.

Thus, it is not evident as to the extent to which direct electrode utilization can be applied to a wide variety of bacteria. Therefore, it is feasible to explore the use of external chemical electron mediators for a wider application to the numerous bacteria that are available. However, low efficiency of the external mediator process is a huge obstacle and improvement of the efficiency and an understanding of the underlying engineering principles are important to study.

2.4 **Electron mediator**

2.4.1 Methyl viologen

Methyl viologen (MV) is also known as N,N′-dimethyl-4,4′-bipyridinium dichloride or by the trade name Paraquat. Three redox states of MV, structures shown in Figures 2.3 – 2.5 [75, 76], can exist via during electron transfer reactions. The colorless di-cation (MV^{2+}), the blue-colored radical cation (MV^{+}) and the yellow-colored neutral species (MV^{0}) are shown in reactions 2.1 and 2.2, with the standard potential (U_{θ}) shown relative to Ag/AgCl reference electrode. A negative standard potential for reaction 1 indicates that the redox reaction is not thermodynamically favorable when coupled with an Ag/AgCl reference electrode such that

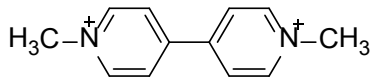

Figure 2.3 Structure of MV^{2+}

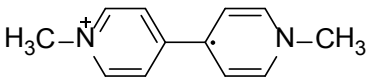

Figure 2.4 Structure of MV^{+}

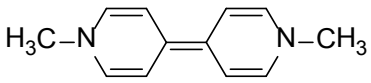

Figure 2.5 Structure of MV^{0}

the MV^{2+} will not reduce to MV^{+} spontaneously but require an external power to drive the reaction. Thus, MV^{2+} is the easiest species to be reduced and MV^{+} is more difficult.

$$MV^{2+} + e^{-} \leftrightarrow MV^{+} \qquad U_{\theta 1} = -0.646\ V \qquad (2\text{-}1)$$

$$MV^{+} + e^{-} \leftrightarrow MV^{0} \qquad U_{\theta 2} = -0.960\ V \qquad (2\text{-}2)$$

MV has been shown to be an effective extracellular electron carrier to promote redox reactions involving bio-catalysis [12, 17, 18, 77]. In 1986, Rao and Mutharasan [36] reported that MV can act as an electron mediator and increase the ethanol yield from 0.001 g/ g glucose to 0.134 g/g glucose. Aulenta et al. [17] also presented an application of MV as an artificial electron mediator for cell fermentation with an efficiency of 20%-60%. Yukihiro Tashiro [38] demonstrated that with MV as the electron mediator, the yield of butanol increased from 0.577 mol/mol without the electron mediator to 0.671 mol/mol with the mediator. These results all focused on the yield of the product which is the material efficiency while ignoring the ratio of the energy input verses the energy output—this is critical for the economics of the process. Further, there are many more reports, with little information of the material or energy efficiency, that simply illustrate the positive effects of MV on electron transport and product formation [12, 13, 18, 33, 78-81].

On the other hand, some reports show that certain amounts of MV will sharply decrease the growth of some cells and inactivate enzymes [16, 82]. The conclusion that all extracellular MV species are toxic to cells has been made by some researchers, which is not convincing since experimental results indicate the viability of using the extracellular MV species as electron donors without any toxicity. The possibility that not all MV species have negative effects on the cells is supported by the following evidences. First, the redox state (MV^{2+}, MV^{+}, MV^{0}) of MV used in the reports is not always clearly stated. Second, MV^{2+} is possibly the species initially used in the reports, because the commercially sold MV is often in the form of MV^{2+}. Third, MV^{2+} can react with NADH inside the cells forming MV^{+} and MV^{0} [82]. The conclusion is that although MV^{2+} is the only species added to the system, all three species can be present in the solution due to the redox reactions. Thus, it's highly possibly that one or more forms of extracellular MV is toxic while the other forms are harmless to cell growth and fermentation.

2.4.2 Neutral red

Neutral red (NR), shown in Figure 2.6, is also able to promote electron transfer in a cellular system. NR is a natural reducing agent since, unlike methyl or benzyl viologen, it is non-toxic to cells. NR can promote the growth of cells by replacing menaquinone in the membrane-

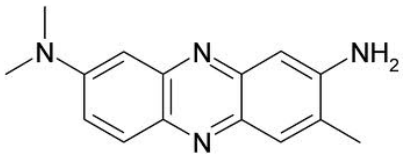

$$NR^{+} + H^{+} + 2e^{-} \leftrightarrow NRH \quad E^{0} = -446\ mV$$

Figure 2.6 Neutral red

bound complex. For example, the *A. succinogenes* mutant strain FZ-6 did not grow on fumarate alone unless electrically reduced NR or hydrogen was present as the electron donor for succinate production [20]. Furthermore, the NR can act as the sole electron source for cell growth and fermentation [83]. Since one mole of NR can only carry one mole of electrons while onemole of MV can carry two moles of electrons at one time, the electron "carrying capacity" of NR is lower than that of MV.

2.4.3 NADH

NADH, shown in Figure 2.7, is a natural electron carrier that is widely used by microorganisms for growth and fermentation. NADH is also used in some cell-free bio-catalysis

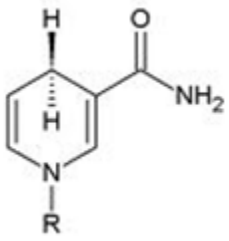

$$NAD^+ + H^+ + 2e^- \leftrightarrow NADH \quad E^0 = -320\ mV$$

Figure 2.7 NADH

redox reactions [82]. However, several problems occur when using NADH in cellular redox systems. First, the NADH molecule is too large to be transported across the cell membrane. NADH will be broken into two parts when cells try to transport it through cell membranes.One part is the pyridine structure, the other is a long carbon chain (represented by "R" in Figure 2.7), and neither of them is active enough for redox reactions inside cells. This makes NADH

impossible to be used in cellular systems. Second, NADH will dimerize on electrodes when reducing NAD^+ to NADH [26]. As shown in Figure 2.8, two units of NADH will react with each other and lose their ability to participate in redox reactions. Without solving these two problems, NADH would be difficult to use as an external electron donor in syngas fermentation.

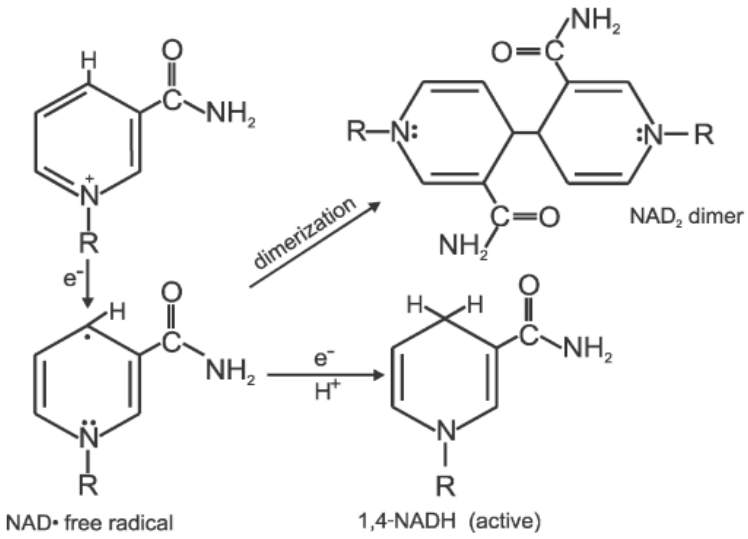

Figure 2.8 Dimerization of NADH on the electrode [26]

In summary, MV as an electron carrier possesses two encouraging advantages: 1. MV can easily move in and out the cells carrying and transferring electrons to active sites. 2. The "carrying capacity" of two electrons per MV is advantageous. On the other hand, the toxicity of MV might be a potential problem for some bio-organisms. It's obvious that MV has promising potential as an external electron mediator although a better understanding of the underlying engineering principles involving thermodynamics, kinetics, and transport would provide more guidance as to the potential uses of MV as an external electron mediator in biological systems. For such applications, a continual source for MV reduction, such as an externally supplied energy source, would be important.

2.5 **Engineering analysis of methyl viologen**

2.5.1 Thermodynamics

Thermodynamic studies have significant importance in the applications of continuous production, system scale-up and exploring of suitable products without conducting experiments. As for syngas fermentation using MV as an electron mediator in a BER system, thermodynamic studies provide a solid theoretical understanding for choosing optimal operating conditions, such as the potential imposed on the system. For example, to reduce the MV^{2+} using electricity, an optimal potential value is important since a potential above a certain threshold in one direction may not reduce the MV^{2+} while an increasingly more negative potential would cost too much energy and investment. Early MV thermodynamic research focused on the measurement of equilibrium potential [84]. Reduction of MV^{2+} to MV^{+} has a standard potential of -646 mV vs $AgCl/Cl^{-}$, and the reduction of MV^{+} to MV^{0} has a standard potential of -960 mV vs $AgCl/Cl^{-}$ [84]. Shebadeh et.al [85] presented the equilibrium constant values for homogeneous chemical reactions between MV and macrocycliccomplexes.. MV thermodynamic work is of significant importance but little has been reported, especially the thermodynamic work for MV in an electrode system. Thermodynamics for MV in an electrode system is quite different from the thermodynamics in a homogeneous solution, because the external power provided by the electrode can largely influence the whole system. One of the objectives of this work is to look into the MV thermodynamics and develop a quantitative expression for the relationship between MV concentration and the potential applied to the system.

2.5.2 Kinetics

MV has three redox species where the two reduced species, MV^+ and MV^0, can act as an electron donor in a number of systems, both in non-biological and biological systems. Kinetic studies of non-biological chemical reactions between MV and reducing agents have shown that MV can be reduced by H_2 [12, 86], dithionite [87], water [33, 34, 78], and O_2 [88]. Kim et al. [33] reported the second-order rate constants for the reactions of MV^0 with H^+, CH_3COOH, $ClCH_2CH_2COOH$, and HCOOH in stagnant aqueous media. MV^{2+} can also form charge-transfer complexes with various chemicals [34, 75, 89]. Monk et al. demonstrated [75] that the charge-transfer complexes formed between MV^+ and solvent ions is essential in evaluation of the reduction rate of MV^{2+}. In this latter study, kinetic data of MV^{2+} reduction and properties of charge-transfer complexes were determined and it was demonstrated that the rate of MV^{2+} reduction depended on the dissociation rate of the charge-transfer complexes, rather than the electron-transfer complexation equilibrium constant [75].

Besides non-biological chemical reaction studies, the kinetics of reactions involving bio-organisms have also been reported [13, 32]. Llobell et al. [13]. reported an enzymatic reduction of glutathione disulfide by electrochemically reduced MV as an electron donor. The *Glutathione Reductase* used in the experiments followed a standard Michaelis-Menten kinetics; a Km = 230 μM for reduced MV was determined. The enzyme demonstrated specificity to MV by a significant lower activity. The activity of the enzyme increased 1.5% with reduced MV at the same operation conditions, compared to using reduced benzyl viologen as the electron donor.

The kinetics of electrochemically reducing MV with an electrode system has always been considered as diffusion limiting in cyclic voltammetry studies, however, the kinetic in a well

stirred system has never been studied. For commercial biofuels production, it is important to know the kinetic-limiting reaction rate to aid in the design or analysis of potential commercial systems. In this study, the kinetics of MV reduction in the absence of diffusion limitations were studied using a well-stirred system to fill in the gap. The understanding of the kinetics of electron mediator reduction needs to be addressed for industrial applications to occur. The speed and total yield of desired product could be limited if the speed of recycling the electron mediator is slower than that of the enzyme or cellular system. Identification of the kinetic mechanism and quantification of kinetic parameters are keys to gaining understanding required for future implementation of MV.

2.5.3 Other engineering analysis

Diffusion analysis for MV [90, 91] has also been reported. Schröder et al. [90] reported that water has a dramatic acceleration effect on the diffusion of MV in ionic liquids. The photoinduced diffusion of MV^{2+} from the inner to outer vesicle surface as an electron mediator is also reported by Lee et al. [91]. The bilayer diffusion is influenced by temperature and buffer. Only at temperatures above 30 ^{o}C and in the presence of the amine buffer is the transmembrane diffusion rapid. At a temperature below 30 ^{o}C, passive diffusion of MV^{2+} across the bilayer is quite slow [91].

In summary, there is great potential in using MV as electron mediators but a more rigorous engineering analysis is needed to design and control MV-mediated biological processes that are sustainable. This work focuses on characterizing the thermodynamics, kinetics, and electron efficiency of methyl viologen (MV) in order to better understand potential limitations of

using MV in an electrode system. MV was chosen as a result of several studies discussed above in which MV had a beneficial effect on the biological process.

3 THERMODYNAMICS STUDY

MV has been used as an electron donor for biofuel production in the lab [17]. MV has three redox species, MV^{2+}, MV^{+} and MV^{0}. MV^{2+} is potentially toxic to bio-organisms by depleting NAD^{+} and ATP [16]. On the other hand, MV^{+} and MV^{0} are potentially beneficial to bio-organisms due to their ability to donate electrons. As all the three species can be present in a system because of redox reactions, a thermodynamic study was performed to assess and model the concentrations of the three species in a solution as a function of the potential applied to the system.

3.1 Material and methods

3.1.1 Bio electro reactor (BER)

A Bio-electric Reactor (BER) for anaerobic system was used for the experiments (Figure 3.1). The BER is made of Pyrex glass and contains two 50mm ID jacketed glass chambers which are connected with a 30-mm diameter pinch clamp. The chambers are separated by a cation selective membrane of Nafion with thickness of 25.4 μm (Fuel Cell Store, San Diego, CA) where no chemicals or metabolites can be transferred across the Nafion membrane except protons and cations. Each chamber was constructed with two gas ports on the upper part of the

chamber in which gas tubing with inner diameter of 0.25 inches (Masterflex Tubing Puri-Flex, L/S® 17,Cole-Parmer, Vernon Hills, IL) is inserted into the chamber above the solution for the gas inlet and outlet. There are two liquid ports at the bottom of each chamber for to use for the reference electrode, pH buffer control, and liquid sampling.

The anode and cathode were made from unpolished graphite 2.5cm x 1.25cm x 7.5cm (G-10, Graphite Engineering and Sales, Greenville, MI). The electrodes were connected to the wires (single solid line in Figure 3.1) with graphite epoxy. The wires then went through the butyl rubber stoppers in the top of each chamber and connected to the potentiostat.

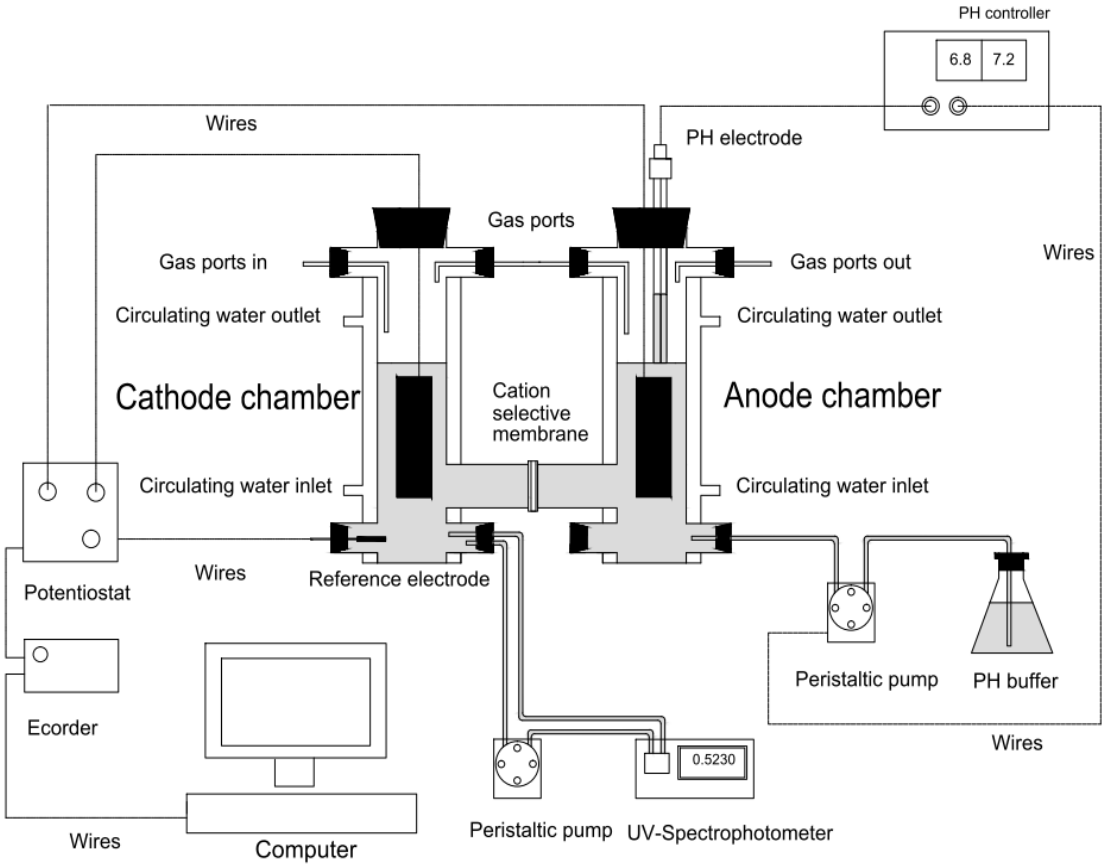

Figure 3.1 Bio-electric reactor

A potentiostat (Potentiostat EZ161, eDAQ, Colorado Springs, CO) connected to an Ecorder (Ecorder ED821, eDAQ, Colorado Springs, CO) and interfaced with Chart® (version 5.0, eDAQ, Colorado Springs, CO) was used to maintain the voltage potential of the cathode relative to a reference Ag/AgCl electrode (non-leaking Ag/AgCl reference electrode, Warner Instruments, Hamden, CT). Potentials ranging from -0.65 to -1.1 V were studied.

Throughout the study, the cathodic chamber contained 20 mL dimethylformamide (DMF) and 180 mL water and a final concentration of 0.1 mM MV^{2+} (0.0051g). The concentration was chosen to be 0.1 mM because a higher concentration would lead to noticeable dimerization of MV^{+} [33]. The anodic chamber contained 200 mL of 100 mM KCl solution. All solutions were fresh-made and adjusted to pH to 7. All solutions in the BER were maintained at pH 7 using a pH control system. The pH was measured with a pH probe (Mettler Toledo, Columbus, OH) and controlled by a controller which connects to a peristaltic pump (Cole Parmer, Vernon Hills, IL). The controller turns on the pump when the solution pH is lower than 6.8, resulting in the addition of a pH buffer (5M KOH) to the anodic chamber to adjust the pH. In experiments, the pH will drop if there is no control because more H^{+} is produced in the anode chamber than consumed in cathode chamber. Reaction conditions were maintained anaerobic by purging N_2 gas before each run for 2 hours and then continuously purging N_2 gas in the headspace throughout the duration of the experiments. The purging occurred through the cathode chamber and then the anode chamber to help maintain an anaerobic environment since O_2 is a byproduct of the reaction in the anode chamber. All experiments were maintained at 37 °C by flowing 39.2°C water through the outer jacket of each reaction chamber before each run for 2 hours and during the experiments.

Continuous photometric analysis of MV^+ was performed by continuously flowing the cathodic solution through a flow-cell in the UV-spectrophotometer (1700 UV-spectrophotometer, Shimadzu, Columbia, MD). The flow-through system consisted of Viton® pump tubing with an inner diameter tubing of 0.06 inches (Cole Parmer, Vernon Hills, IL) connected to a pump (Cole Parmer, Vernon Hills, IL), and sealed to a flow-through cuvette (585.3-SOG, Starna Cells, Atascadero, CA) which was kept at reaction temperature in the spectrophotometer. The extinction coefficient for MV^+ at 606 nm is reported by Thorneley et al. as 13000 M^{-1} cm^{-1} [88]. MV^{2+} and MV^0 do not absorb light at the chosen wavelength. The UV spectrophotometer was blanked with the initial solution containing MV^{2+}.

After each experiment, the BER was disassembled and every piece was cleansed and dried separately. Different parts needed to be rinsed with DI water before and after each step. Graphite electrodes were cleansed with soap and immersed into 5M HCl for two hours. After that, the graphite electrodes were immersed in 500 mL DI water for at least 10 hours. pH indicator paper was used to test the pH of the graphite surface to make sure HCl was fully removed. The pH should be around 7 before graphite electrodes can be used again. The pH probe was washed with soap and stored in 3M KCl solution. The two glass chambers were brushed with soap and immersed in an acid bath for 10 hours. The gas tubes and rubber stoppers were washed with soap. To clean the residue, the stoppers were boiled in 10 vol% Multi-Terge (Harleco, Gibbstown, NJ) for 10 minutes and boiled in DI water for 10 minutes. The reference electrode was washed with soap and stored in DI water. The tube between the chambers and the UV-spectrophotometer was cleansed by flowing 500 mL of clean of DI water through the tube.

In the BER, the external power drives the electrochemical reaction in the system. On the anode, water electrolysis occurs and donates electrons to the anode. H^+ and O_2 are formed from water electrolysis. O_2 is purged out of the system with N_2 and H^+ immigrates to the cathode chamber through the cation selective membrane under the influence of a potential difference. In the cathode chamber, MV^{2+}, MV^+ or sometimes H^+ are reduced when electrons are transferred to these species on the cathode.

3.1.2 Overcoming system problems

3.1.2.1 Oxygen

One of the problems that had to be overcome in order to achieve repeatable, realistic, and reliable data was oxygen contamination in the system. The development of the flow-through spectrophotometric system was used to minimize oxygen contamination in the MV^+ analysis. Viton® tubing was used for the tubing to/from the spectrophotometer since it has a low oxygen permeability of 2.8×10^{-7} cm^3 s^{-1} [92]. The only drawback for Viton® is that it cannot be autoclaved, which is unimportant in this experiment, but should be noted for any cellular experiments that may be performed in the apparatus in the future. Also, every connection was checked to make sure they were sealed before beginning the experiments.

3.1.2.2 pH influence

Without pH control, the pH in the solution would decrease with time as protons were continuously produced at the anode while only a small or negligible amount was consumed at the cathode. In preliminary experiments without a pH control system, the pH dropped to around pH 2 in 10 hours with an MV concentration of 0.01 M. A pH around 2 indicates that the H^+

concentration is 0.01 M, consistent with the amount of MV reduced on the cathode (0.01 M). Since the pH has a significant influence on the system, including the reference electrode potential, homogeneous reactions with MV, and in the future, cell growth and fermentation, a pH control system described above was utilized to maintain the system pH at 7.

3.1.2.3 Reference electrode

At first, the system used a reference electrode of Ag/AgCl (E255 Ag/AgCl wire electrode, Warner Instruments, Hamden, CT) instead of a sealed, non-leaking reference electrode. The wire reference electrode was completely exposed in the solution and it degraded with time. As an example, the potential difference between a new wire electrode and a 30-hour used wire electrode was 0.3 mV. When using the wire electrode the potential of the reference electrode is controlled by maintaining a constant Cl^- concentration (100 mM) in the solution. However, since the MV in the cathode chamber can influence the potential of a wire reference electrode, the wire electrode had to be placed in the anodic chamber. The potential that drives a reaction (which for this study is a desired parameter to select) is the potential difference between the potential on the electrode surface of interest and the potential in the solution close to the electrode. For the system of this study, the working electrode of interest is the electrode in which it is desirable to reduce MV (i.e. cathode). Thus, the best location of a reference electrode is close to the cathode. Since the potential in different places in the solution would be different, placing the reference electrode in the anodic chamber not only included the potential difference between the cathode and the solution near the cathode but also the potential difference between the solution near the cathode and the solution near the reference electrode. The additional potential difference adds additional terms for thermodynamic and kinetic calculations, making the system much more

difficult to accurately model. To minimize the electrode problem, a new reference electrode that is sealed and non-leaking was placed close to the cathode in the cathodic chamber.

3.1.2.4 Clean electrode

Clean electrodes are critical for an electro chemical system since all reactions occur on the surface of the electrode and contamination would result in unrepeatable, unrealistic, and unreliable results. The cathode and anode are made of graphite which has a porous surface structure. Porous structures make the cleaning more difficult to accomplish. Initially, the two electrodes were only rinsed for 10 minutes after immersing the electrode in acid for 2 hours. The rinsing was not enough to clean all of the acid from the porous structures. A new method of immersing the electrode into large amounts of DI water (800 mL) for at least 10 hours after the acid wash was developed. The pH of the electrode surface was tested and the pH reached 7. A pH of 7 indicates that most of the acid is removed from the surface and the electrodes are clean.

3.1.2.3 Nafion®

The cation selective membrane is made of Nafion®, which usually has high selectivity for cations and a long working life that is easy to maintain. For a system using MV, MV^{2+} and MV^{+}, these cations may clog the Nafion® pores (unpublished results from a student in Dr. Wheeler's group). For the studies in this thesis, MV^{2+} and MV^{+} are attracted to the cathode by the potential difference, which lead to a lower possibility that they will clog the membrane.

3.2 **Results and discussions**

3.2.1 Experimental results

At applied potentials more negative than -650 mV vs Ag/AgCl (Ag/AgCl is 200mV vs SHE), MV^{2+} can be electrochemically reduced to MV^{+} according to the one-electron transfer reaction since for the reaction $MV^{2+} + e^{-} \leftrightarrow MV^{+}$. At applied potentials more negative than -960 mV vs Ag/AgCl (3.4 M), MV^{+} can undergo a second, one-electron, transfer reaction of $MV^{+} + e^{-} \leftrightarrow MV^{0}$. At a potential of -1100 mV, MV^{2+} can be completely reduced to MV^{0}. When the potential was more negative than -1100 mV (e.g. -1500 mV) production of H_2 ($E°' = -642$ mV vs Ag/AgCl (3.4 M)) may occur and noticeable bubbles, likely H_2, gas was observed.

Electrochemical reduction of MV at potentials of -1100 mV, -1000 mV, -900 mV, -800 mV, -700 mV, and -650 mV with an initial MV^{2+} concentration of 0.1 mM was studied to assess the thermodynamics of MV reduction. Results of the MV^{+} concentration with time are shown in Figure 3.2 for the various applied voltages.

A potential of -650 mV cannot reduce MV^{2+} and no MV^{+} was produced. For the reduction at potentials from -700 mV to -900 mV, the MV^{+} concentration changes have two regimes. In the first regime, the concentration increased, in the second regime, the concentration reached steady state. Both of the rate of concentration change in the first regime and the steady state concentration for the second regime increased when the potential became more negative. As seen, the initial change in MV^{+} concentration for -800 to -1100 mV appeared to be similar although the reduction rate decreased as the potential changed from -1100 to -800 mV.

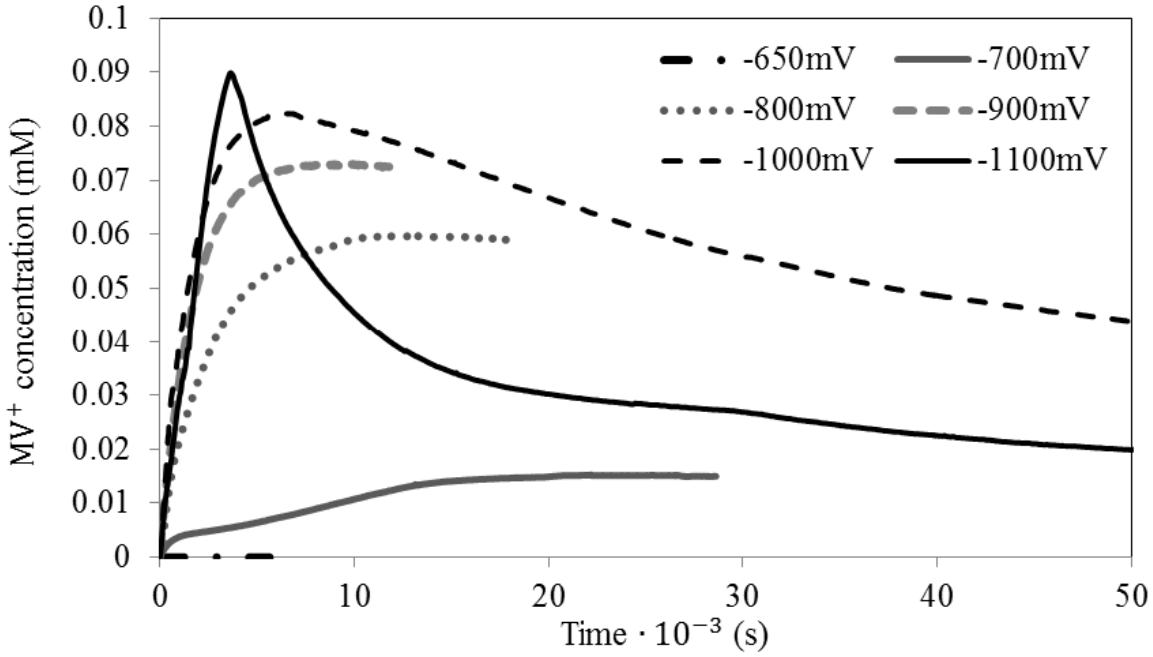

Figure 3.2 Reduction of MV under different potential

At a potential of -1000 and -1100 mV, the MV^+ concentration data demonstrated that MV^{2+} was first reduced to MV^+ since the concentration of MV^+ increased with time. After that, the MV^+ concentration decreased slowly because MV^+ was further reduced to MV^0. This two electron reduction was expected since the potential was more negative than -960 mV. The MV^+ concentration stabilized at around 0.01 mM for -1000 mV and about 0 mM for -1100 mV after long times (not shown on graph).

Repeated experiments for -900 mV and -800 mV shown in Figure 3.3 and Figure 3.4 demonstrated repeatability for the experiments.

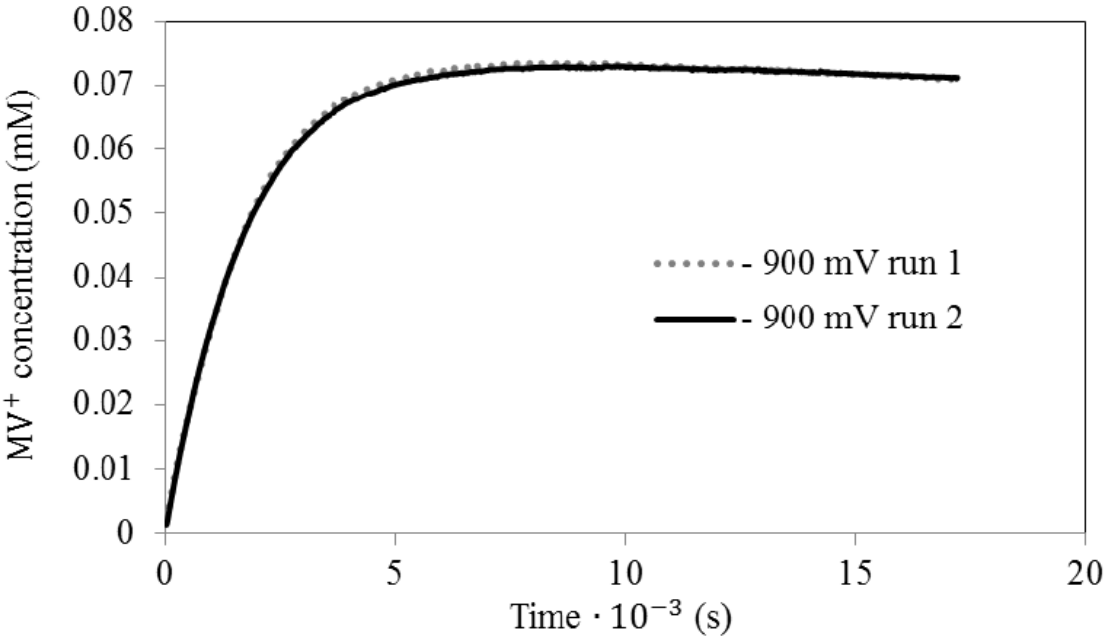

Figure 3.3 Repeat experiments on potential of -900 mV

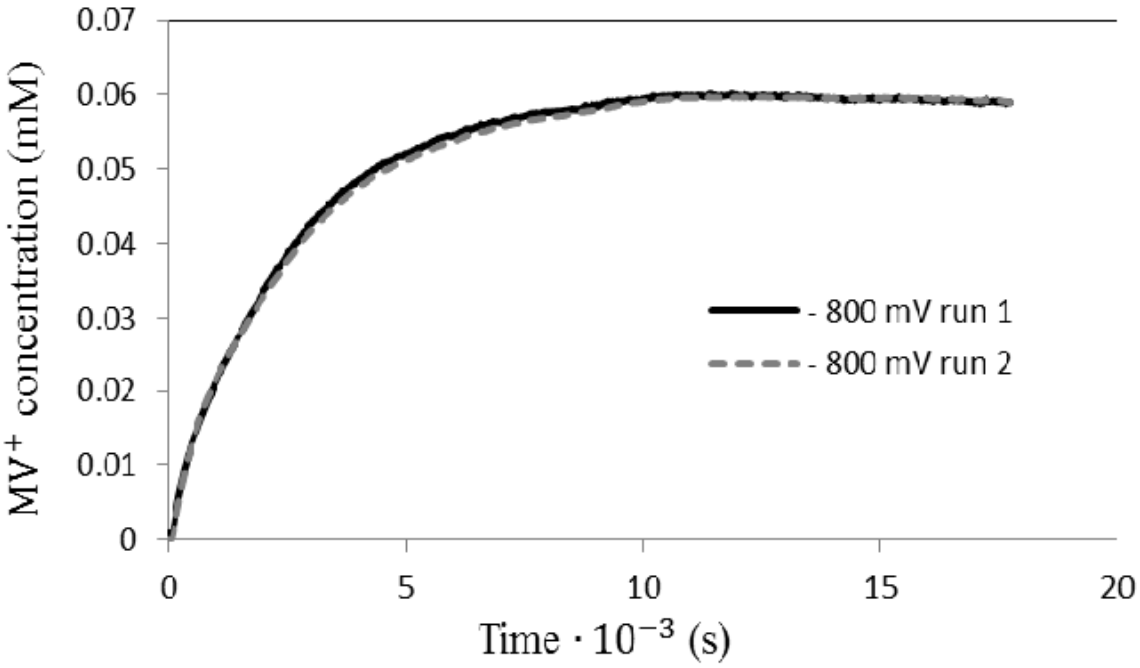

Figure 3.4 Repeat experiments on potential of -800 mV

The measured MV^+ equilibrium concentration data appear in Figure 3.5 together with modeled results with respect to each potential. The model shown is described later. As shown in Figure 3.5, the equilibrium MV^+ concentration has a Gaussian-type distribution. The model below shows this distribution. This type of figure is helpful in designing engineering systems with MV since it is important to control the type of MV state that can exist in an applied system.

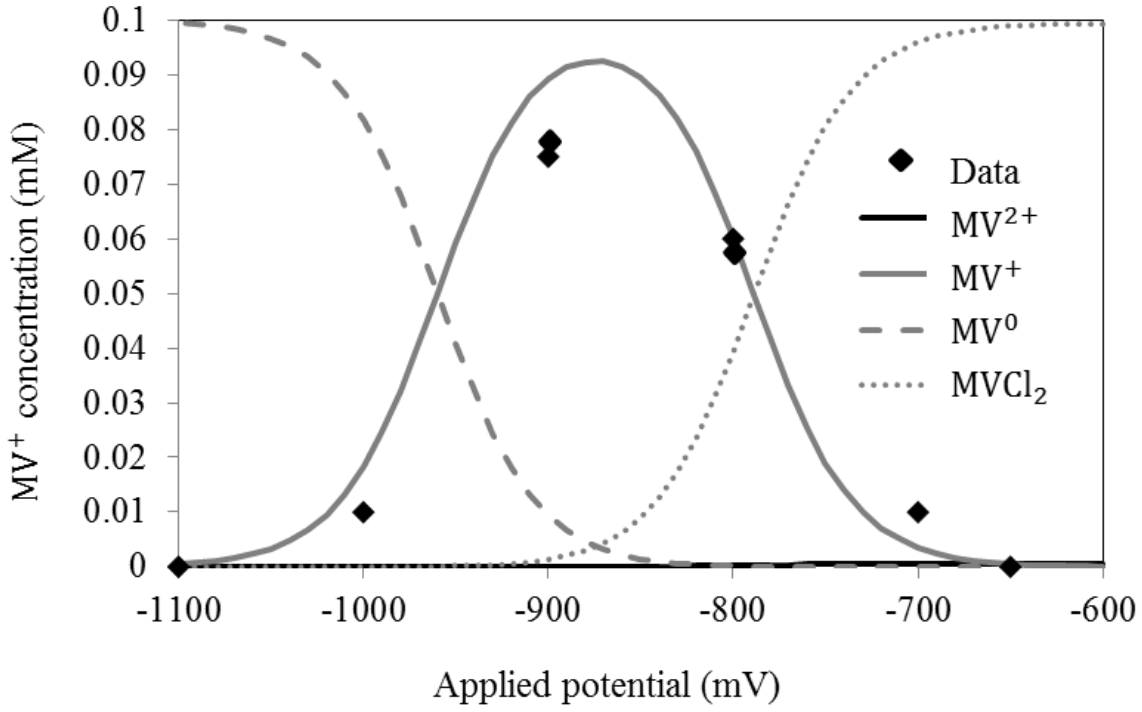

Figure 3.5 Comparison of experimental data and the model

The model below shows this distribution. This type of figure is helpful in design engineering systems with MV since it is important to control the type of MV state that can exist in an applied system.

3.2.2 The model

The equilibrium concentrations of three species in the solution are related to the potential applied to the system, though only MV^+ was experimentally measured. A thermodynamic model was developed using the Nernst Equation which describes the relationship between equilibrium chemical concentrations and the applied potential. This model was derived with the understanding that the reduction of MV can be treated as a cell with MV reduction occurring on the working electrode (cathode) and the Ag/AgCl electrode acting as the reference electrode. The reference electrode was used to control the potential of the cathode relative to the reference electrode using a potentiostat. Controlling relative to a reference electrode is much better than controlling relative to the anode since the potential of a reference electrode is relatively fixed, while the potential of an anode can vary with time as a result of changing conditions around the anode. It should be noted that different reference electrodes can be used in different systems (e.g. wire electrode, sealed electrode, etc.) though the sealed Ag/AgCl reference electrode is used in this study for reasons noted above. However, the same model calculations can be performed accordingly with any electrode.

3.2.2.1 Model derivation

To illustrate the development of the model to predict equilibrium MV concentrations as a function of applied potential ($U_{\text{external power}}$), the first reduction from MV^{2+} to MV^+ is used as an example. It is important to note that for an electrochemical system with a working electrode and a reference electrode, the open circuit potential for the MV reaction (U_{MV}) is defined as:

$$U_{MV} = \phi_{WE} - \phi_{RE} \tag{3-1}$$

Here, U_{MV} is the open circuit electrical potential of the electrode, in this case the working electrode (WE) relative to the reference electrode (RE). Similar to the relation of gravitational potential change and the work done by gravity, the Gibbs free energy change for the open circuit (ΔG_{cell}) can be expressed by the electrical potential difference between the two positions according to:

$$\Delta G_{cell} = z_{e^-} \cdot F \cdot (\phi_{WE} - \phi_{RE}) = z_{e^-} \cdot F \cdot U_{MV} \quad (3\text{-}2)$$

where z_{e^-} is the charge number of the electron, which is -1, and F is Faraday's constant of 9.65 x 10^4 C/mol.

A positive value of U_{MV} indicates that MV^{2+} reduction can occur spontaneously ($\Delta G<0$) if a wire is connected between the two electrodes. Conversely, a negative value of U_{MV} means that the MV^{2+} reduction of the redox reaction cannot occur spontaneously. For the reduction of MV^{2+} to MV^{+}, U_{MV} at standard conditions is -0.646V which indicates that MV^{2+} reduction is a nonspontaneous reaction. To drive the reaction, an external power source must be applied to the system. The external power source can be treated as another cell with the opposite working and reference electrode. Thus, the energy balance of the system is

$$\Delta G_{system} = -F \cdot U_{MV} - \left(-F \cdot U_{external\ power}\right) \quad (3\text{-}3)$$

In order for reactions to occur spontaneously in the system, which includes both an external power source and the redox reaction in the solution, a negative ΔG_{system} is required. The condition for ΔG_{system} being negative for the system is that $U_{external\ power}$ is more negative than U_{MV}. In the experimental data shown in Figure 3.2, a more negative potential like -700 mV, -800

mV and -900 mV can drive the reduction of MV^{2+} but a less negative potential of -650 mV cannot drive the reduction. Once equilibrium is achieved, $FU_{MV} = FU_{external\ power}$.

To utilize the chemical potential for the electrochemical cell in the model, the difference between the chemical potentials (μ) for a charged species (electrons for example) at two positions (such as working and reference electrodes) can be expressed as the Gibbs free energy of the electrochemical cell (ΔG_{cell}) of moving reversibly, at constant temperature and constant volume, of 1 mol of the charged species (electrons) from one position to the other, such that

$$\Delta G_{cell} = \mu_{e^-}^{w} - \mu_{e^-}^{r} \tag{3-4}$$

Equating Equations 3-2 and 3-4, and using $z_{e^-} = -1$ gives:

$$F \cdot U_{MV} = \mu_{e^-}^{r} - \mu_{e^-}^{w} \tag{3-5}$$

At the reference electrode, the reaction $AgCl + e^- = Ag + Cl^-$ can occur in either direction depending on the ΔG values. At equilibrium for a reaction at constant T and P:

$$dG = 0 = \sum \mu_i dn_i \tag{3-6}$$

Here, μ is the chemical potential and *dn* is the change in moles. Thus, the reference electrode reaction at equilibrium gives:

$$0 = \mu_{Ag}^{r} + \mu_{Cl^-,probe}^{r} - \mu_{AgCl}^{r} - \mu_{e^-}^{r} \tag{3-7}$$

Here, Cl^- is the concentration of Cl^- in the sealed reference electrode. Similarly, for the working electrode reaction of $MV^{2+} + e^- = MV^+$, the working electrode reaction at equilibrium gives:

$$0 = \mu_{MV^+}^{w} - \mu_{MV^{2+}}^{w} - \mu_{e^-}^{w} \tag{3-8}$$

Substituting Equations 3-7 and 3-8 into 3-5, gives the expression of U_{MV} as a function of chemical potentials of different species:

$$F \cdot U_{MV} = (\mu_{Ag} + \mu_{Cl^-,probe} - \mu_{AgCl} - \mu_{MV^+} + \mu_{MV^{2+}}) \quad (3\text{-}9)$$

Note that in Equation 3-9, the MV concentrations are those surrounding the working electrode and they are assumed to be well mixed and represented by the corresponding concentrations in the bulk solution. The chemical potential for each species in Equation 3-9 can be expressed as

$$\mu_{MV^{2+}} = \mu_{MV^{2+}}{}^0 + \mathrm{R} \cdot \mathrm{T} \cdot \ln \frac{[MV^{2+}]}{[MV^{2+0}]} \quad \text{with } MV^{2+0} = 1M \quad (3\text{-}10)$$

$$\mu_{MV^+} = \mu_{MV^+}{}^0 + \mathrm{R} \cdot \mathrm{T} \cdot \ln \frac{[MV^+]}{[MV^{+0}]} \quad \text{with } MV^{+0} = 1M \quad (3\text{-}11)$$

$$\mu_{\mathrm{Ag}} = \mu_{\mathrm{Ag}}{}^0 \quad (3\text{-}12)$$

$$\mu_{\mathrm{AgCl}} = \mu_{\mathrm{AgCl}}{}^0 \quad (3\text{-}13)$$

$$\mu_{Cl^-,probe} = \mu_{Cl^-}{}^0 + \mathrm{R} \cdot \mathrm{T} \cdot \ln \frac{[Cl^-,probe]}{[Cl^{-0}]} \quad \text{with } Cl^{-0} = 3.4M \quad (3\text{-}14)$$

It should be noted that $Cl^-_{,\mathrm{probe}}$ is 3.4 M (the Cl^- concentration of the sealed reference electrode) such that $\mu_{Cl-,probe} = \mu_{Cl^{-0}}$. R_g is the universal gas constant (8.314 J / (mol · K)) and T is the absolute temperature (310.15K) for the reaction conditions.

Substituting Equations 3-10 to 3-14 into Equation 3-9 gives

$$F \cdot U_{MV} = \mu_{\mathrm{Ag}}{}^0 + \mu_{Cl^-}{}^0 - \mu_{\mathrm{AgCl}}{}^0 - \mu_{MV^+}{}^0 - \mathrm{R} \cdot \mathrm{T} \cdot \ln[MV^+] + \mu_{MV^{2+}}{}^0 + \mathrm{R} \cdot \mathrm{T} \cdot \ln[MV^{2+}] \quad (3\text{-}15)$$

Both MV concentrations in Equation 3-15 have units of M. In addition, the expression for the standard cell potential can be expressed as

$$F \cdot U_{\theta 1} = \mu_{Ag_\theta} - \mu_{AgCl_\theta} - \mu_{MVCl_\theta} + \mu_{MVCl_{2\theta}} \quad (3\text{-}16)$$

Substituting Equation 3-16 into 3-15 gives

$$F \cdot U_{MV} = F \cdot U_{\theta 1} - \mathrm{R} \cdot \mathrm{T} \ln \frac{[MV^+]}{[MV^{2+}]} \quad (3\text{-}17)$$

Finally, combining Equations 3-3 and 3-17 at equilibrium (ΔG_{system}=0) gives

$$F \cdot U_{external\ power} = F \cdot U_{\theta 1} - \mathrm{R} \cdot \mathrm{T} \ln \frac{[MV^+]}{[MV^{2+}]} \quad (3\text{-}18)$$

Similarly, for the reduction of MV^+ to MV^0, the following equation is also obtained.

$$F \cdot U_{external\ power} = F \cdot U_{\theta 2} - \mathrm{R} \cdot \mathrm{T} \ln \frac{[MV^0]}{[MV^+]} \quad (3\text{-}19)$$

$U_{\theta 1}$ and $U_{\theta 2}$ are standard potentials for reaction 1 and 2 where $U_{\theta 1}$ = -0.646V and $U_{\theta 2}$ = -0.960V relative to the Ag/AgCl reference electrode (at 3.4 M AgCl).

As previously reported, $MVCl_2$ has very little dissociation [93]. This adds an additional constraint on the system. Thus, the dissociation equilibrium constant (K) can be used to express the concentration relation between MV^{2+} and $MVCl_2$ where $K = [MV^{2+}][Cl^-_{soln}]^2/[MVCl_2]$. It should be noted that the Cl^- concentration is the concentration in the bulk solution surrounding the working electrode, which for this study is 0.1M. Since the Cl^- concentration in the bulk will

not change appreciably due to any $MVCl_2$ dissociation ($MVCl_2$ added is 1000 times smaller than Cl^- concentration), Cl^-_{soln} will essentially be constant at 0.1M. Rearranging K gives

$$[MVCl_2] = \frac{[MV^{2+}]\cdot[0.1M]^2}{K} \tag{3-20}$$

Additionally, due to 0.1 mM $MVCl_2$ being initially added to the system, the balance for all MV species is

$$0.0001M = [MV^{2+}] + [MV^{+}] + [MV^{0}] + [MVCl_2] \tag{3-21}$$

Substituting Equation 3-20 into Equation 3-21 gives

$$0.0001M = [MV^{2+}] \cdot (1 + \frac{[0.1M]^2}{K}) + [MV^{+}] + [MV^{0}] \tag{3-22}$$

Equations 3-18, 3-19, 3-20 and 3-22 were used to solve for the concentrations of $MVCl_2$, MV^{2+}, MV^{+}, and MV^0 at various values of $U_{external\ power}$ based on a given value of K. The MV^{+} experimental data in Figure 3.5 was used to find the K that fit the MV^{+} data with the least error. The best fit was with $K = 5.6\text{x}10^{-5}\ M^2$. This value is consistent with the literature that states that the dissociation is very small.

The model was able to fit the data very well and capture the bell-shaped curve of the MV^{+} data. Figure 3.5 also shows the predicted concentrations of $MVCl_2$, MV^{2+} and MV^0 as a function of applied external power. An interesting component associated with the model shown in Figure 3.5 is the low dissociation of $MVCl_2$ that leads to essentially negligible MV^{2+} in solution at all external power values. Only $MVCl_2$ is appreciable at low external power values. In contrast, MV^{+} and MV^0 can reach concentrations at various external power values that are the same magnitude as the initial $MVCl_2$ added to the solution. This finding leads to further

questions as to the effects of MV^{2+}, MV^{+}, and MV^{0} on cell toxicity since MV^{2+} will likely be lower than these other species. Obviously, the amount of Cl^{-} in the system will affect the equilibrium amount of MV^{2+} associated with the dissociation constraint.

The small difference between the model and the experimental MV^{+} concentration at -900 mV and -800 mV could be due to side reactions of MV^{+} such as dimerization and reaction with O_2 [88]. Dimerization effects have been shown to be reduced by using low MV^{+} concentrations in a 9:1 DMF:H_2O solution [94, 95]. This solution was used for this study but it appears that side reactions may not be completely eliminated. The dimerization is more likely when the MV^{+} concentration is higher. The O_2 generated in the anodic chamber was likely eliminated by purging N_2. Still it was a possibility that trace amounts of O_2 could enter the tubing connecting the flow cell in the UV-spectrophotomer to the chamber. The tubing was selected with a low O_2 permeability (2.804×10^{-7} cm^3/s) [92] but there could still be trace amounts of O_2 because the reaction time was as long as 15×10^3 s. The side reactions were not obvious when MV^{+} was in low concentration, but it may have a larger influence when MV^{+} is at a higher concentration.

3.2.2.2 Influence of K and $Cl^{-}_{,soln}$ on model.

The influence of the parameters K and the concentration of Cl^{-} in the solution on the prediction of the MV^{+} concentration were studied using the model in Excel. Results are demonstrated in Figures 3.6 and Figure 3.7

In Figure 3.6, the influence of K on the MV^{+} concentration when the concentration of Cl^{-} in the solution equals 0.1M is shown. As noted, as K increase, the plot will also expand to a less negative applied potential region with a higher peak value. An increase in the K value only

reduces the energy requirement for the first reduction (represented by right side of figure) but has little influence on the second reduction (represented by left side of figure). Although K is fixed and can only be adjusted by temperature, Figure 3.6 hypothetically shows what would happen if $MVCl_2$ could completely dissociate (large K represented by 1 x 10^4 M^2). In Figure 3.6, it is also obvious how incorrectly accounting for the equilibrium can provide inaccurate predictions. Thus, any electrode system analysis for electron mediators should make sure that equilibrium constraints are properly accounted for.

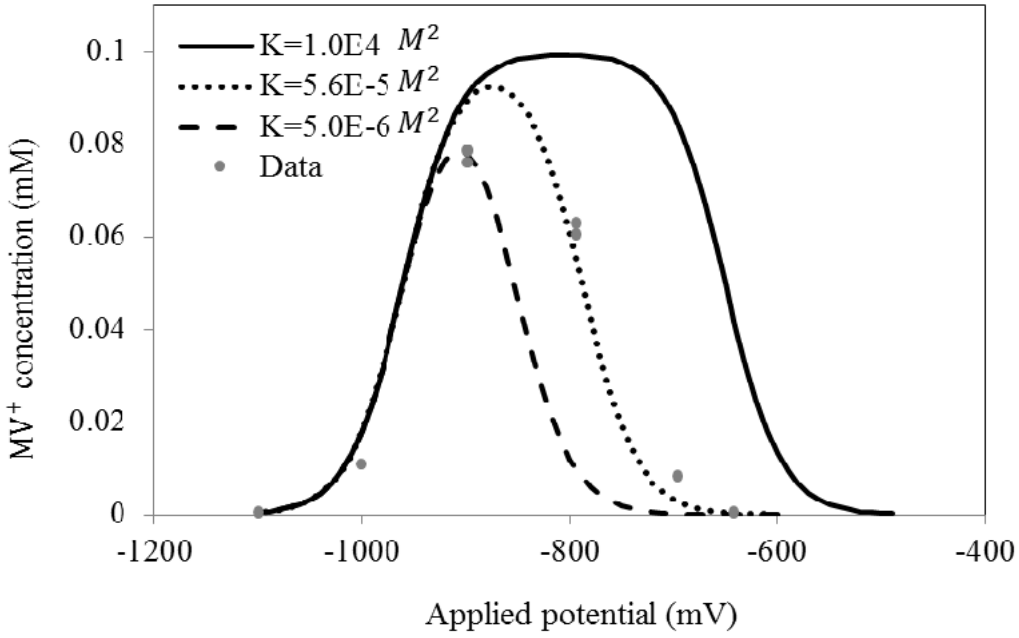

Figure 3.6 Influence of K on relationship of MV concentration change with potential

As shown in Figure 3.7, as Cl^-_{soln} decreases, the plot will also expand to a less negative applied potential region with a higher peak value. A decrease in Cl^-_{soln} reduces the energy requirement for the first reduction but has little influence on the second reduction. Unlike K, Cl^-_{soln} can be adjusted through experimental design. Thus, reducing Cl^-_{soln} would be beneficial

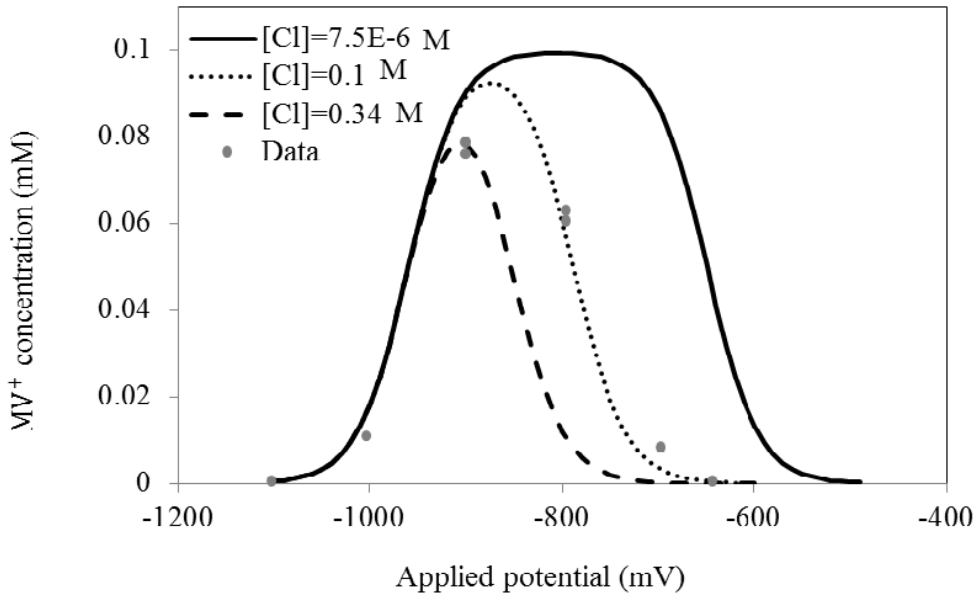

Figure 3.7 Figure 3.8 Influence of Cl^-_{sol} on relationship of MV concentration change with potential

to reduce the amount of applied energy needed to reduce MV^{2+} to MV^+. This reduced energy input would improve the economics. In addition, a lower applied energy would also likely reduce the H^+ reduction on the electrode, leading to better electron efficiency (see Chapter 5).

3.3 Discussion and conclusions

MV has three redox states and they can be converted to each other via redox reactions. Among the three species, MV^{2+} has no ability to donate electrons but the strongest ability to take electrons. As previously stated in Chapter 2, some studies have stated the MV (without identifying the species) is toxic to bacteria but other studies have shown positive effects. One working hypothesis is that MV^{2+} is potentially toxic to bacteria by taking electrons from bacteria

and depleting the ATP. For MV^+, MV^+ was the partially reduced species and it can only donate one electron per MV^+. An advantage for MV^+ is the lower potential and less energy required to electrochemically reduce MV^+. MV^0 has the strongest reducing power and it can donate two electrons per MV^0. Nevertheless, MV^0 requires more energy to be reduced and the reduction of MV^+ to MV^0 would compete with the reduction of H^+ and consume more energy. Moreover, reduction from MV^+ to MV^0 is not as reversible as the reduction from MV^{2+} to MV^+ [33], which has an adverse influence on the continuous applications. With these distinctive properties of the three MV species, a system should be designed for the most suitable species instead of randomly using all three species together. Controlling the species of MV in the solution is beneficial to maximize the beneficial species and maximize the beneficial effect that the species has on the desired product.

Thermodynamic studies also have significant importance in the applications of continuous production and system scale-up and new product exploration. Early MV thermodynamic research focused on the measurement of equilibrium potential for the two step reduction of MV [84]. Shebadeh et.al [85] presented the equilibrium constant values for homogeneous chemical reactions between MV and macrocyclic hosts. MV thermodynamic work is of significant importance but little has been done, especially the thermodynamic work for MV in an electrode system. Thermodynamics of MV in an electrode system is quite different from the thermodynamics in a homogeneous solution, because the external power provided by the electrode can largely influence the whole system.

In this study, MV was electrochemically reduced at different potentials. Any potential more negative than - 650 mV can drive the reduction of MV^{2+} to MV^+. Additionally, any

potential more negative than -1100 mV can completely reduce all MV^{2+} to MV^{0}. At potentials between -650 mV and -1100 mV, the concentration of MV^{+} equilibrated at a certain value and the value is a function of the external potential applied to the system. A thermodynamic model was built in this study to relate the equilibrium concentration of MV^{+} to the external power applied to the system.

With this model, the three species concentrations can be calculated once the external power is given, or the other way around. With this model, a system can potentially be designed to control the desired MV species by choosing an optimal potential. However, thermodynamic predictions will change with various conditions like pH, Cl^{-} (for this application), temperature, and electron mediators used. Although this model is limited to this specific experimental system with MV, the methods and model can provide guidance for similar studies at other conditions or for other electron mediators. This thermodynamic study not only provides the analysis of the minimum required external energy input to reduce MV^{2+} in the solution to useable MV species that can donate electrons, but also provides guidance on the applied potential needed to control the types of MV species that are present.

4 KINETIC STUDY

The understanding of the kinetics of electron mediator reduction is one of the most important fundamental principles that need to be addressed in order to design industrial applications. The rate of the desired reaction and the total yield of desired product could be limited if the rate of recycling the electron mediator is slower than that needed for an enzyme or cellular system. When choosing electron mediators to couple with cells, the maximum rate in which electron mediators donate electrons should be greater than the rate of electron consumption by bio organisms so that the organism is the limiting step. Identification of the kinetic mechanism and quantification of kinetic parameters for reducing agents are keys to gaining understanding required for future implementation of BERs.

MV has been used as electron donors for chemical [13, 96] and biological processes [12, 36, 77] in fundamental studies. The kinetics of MV reduction was always considered as diffusion limiting in cyclic voltammetry studies based on the limiting current measurement in stagnant solution [75, 79, 97] such that the kinetic-limiting reaction rates were not studied. For commercial biofuels production, it is important to know the kinetic-limiting reaction rate to aid in the design or analysis of potential commercial systems. In this study, the kinetics of MV reduction in the absence of diffusion limitations was studied using a well-stirred system.

4.1 **Materials and method**

Experiments for the kinetic study were part of the same studies outlined in Chapter 3. Thus, the materials and methods were previously discussed in Chapter 3. The kinetic parameters were obtained from the Chapter 3 results of the concentration of MV^+ with time as described below. The MV^+ concentration was taken every 60 seconds until the end of the experiment.

4.2 **Experimental data**

In Chapter 3 studies, MV^{2+} was electrochemically reduced at a potential of -1100 mV and the results showing the MV^+ concentration with time appear in Figure 4.1 for three studies. During the study, the pH of the system was initially adjusted to 7 and maintained around

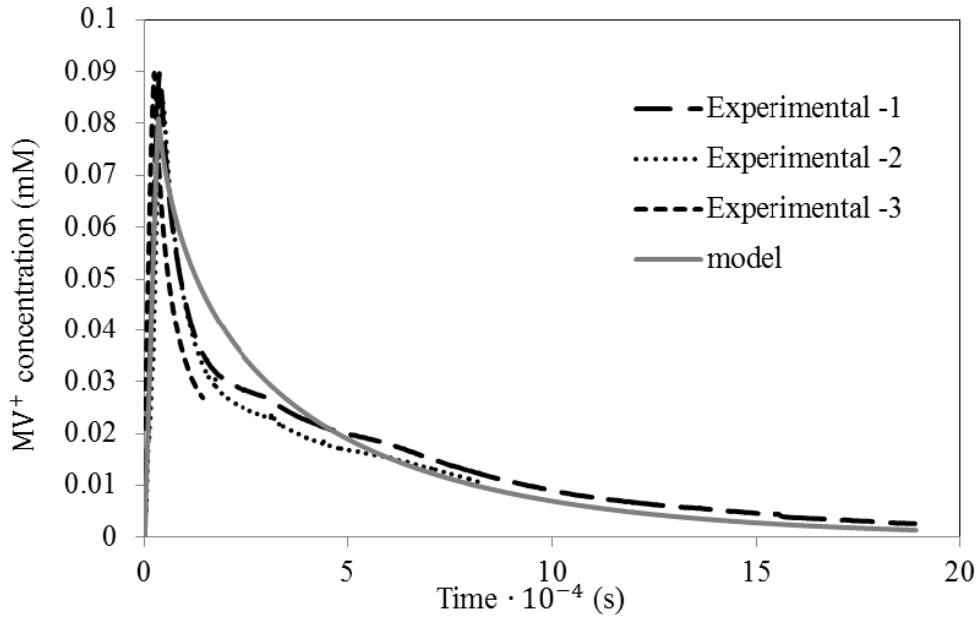

Figure 4.1 MV^+ concentration with time

7 throughout the experiment. The MV^+ concentration first increased nearly linearly, reached a mean peak value of 0.087 mM, then the MV^+ concentration began to decrease. Figure 4.1 shows a slower rate for the MV^+ concentration decrease than the increase. Also, the decrease was not linear and the rate of decrease declined as the reduction went on.

4.3 **Kinetic model**

4.3.1 Model development

The study involving the applied potential of -1100 mV was chosen for the kinetic analysis because only at a potential more negative than -1100 mV, both of the two steps of MV reduction will fully occur such that the reverse reactions of both reduction steps were considered negligible in the model development. For example, at a potential of -900 mV, MV^{2+} was fully reduced to MV^+ but the reaction between MV^+ and MV^0 reached an equilibrium which requires the reverse reaction to be taken into account and this increases the complexity of the model. Thus, this model is the first development towards a more detailed model that could include reversibility and applied voltage effects.

The MV reduction from MV^{2+} to MV^+, then to MV^0 is a two-step reaction, shown in Chapter 2. In this study, an electrode was used to electrochemically reduce MV, and the electrochemical reduction occurred on the surface of the electrode. Thus, each step of MV reduction was a surface reaction. Surface reactions are generally composed of three stages: reactant adsorption, surface reaction, and product desorption as shown in Figure 4.2. MV^{2+} first adsorbs onto the electrode surface and then MV^{2+} reacts with electrons provided by the cathode

on the surface to form MV^{+}. MV^{+} can either desorb from the cathode or further react with another electron and form MV^{0}. MV^{0} can also desorb from the electrode.

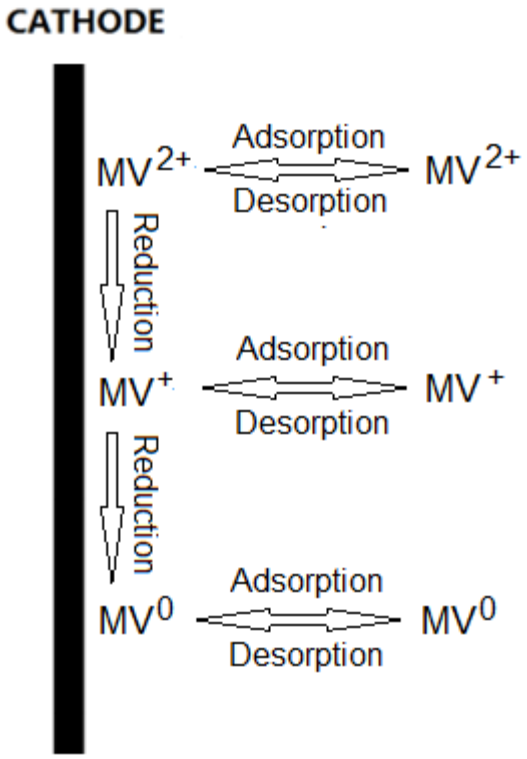

Figure 4.2 Mechanism of electrochemically reduction of MV

The detailed kinetic scheme is demonstrated as six elementary steps as follows

$MVCl_2 \leftrightarrow MV^{2+} + 2 \cdot Cl^{-}$ Dissociation equilibrium in solution (4-1)

$MV^{2+} + S \leftrightarrow (MV^{2+} - S)$ MV^{2+} adsorption/desorption (4-2)

$(MV^{2+} - S) \leftrightarrow (MV^{+} - S)$ MV^{2+} surface reaction (4-3)

$$(MV^{+} - S) \leftrightarrow MV^{+} + S \qquad MV^{+} \text{ adsorption/desorption} \tag{4-4}$$

$$(MV^{+} - S) \leftrightarrow (MV^{0} - S) \qquad MV^{+} \text{ surface reaction} \tag{4-5}$$

$$(MV^{0} - S) \leftrightarrow MV^{0} + S \qquad MV^{0} \text{ adsorption/desorption} \tag{4-6}$$

Noted that the concentration of MV^{2+} is in equilibrium with $MVCl_2$ as

$$K \cdot C_{MVCl_2} = C_{MV^{2+}soln} \cdot C_{Cl^{-}soln}{}^{2} \tag{4-7}$$

Thus, for every mole of $MVCl_2$ initially put in the solution, there are only $K' = \left(\frac{K}{[0.1M]^2+K}\right) =$ $5.57\text{x}10^{-3}$ moles MV^{2+} initially present (K=5.6 x 10^{-5} in Chapter 3) and the actual

$$C_{MV^{2+}soln} = K' \cdot (C_{MVCl_2} + C_{MV^{2+}soln}) \tag{4-8}$$

To simplify the model, let $C_{MV^{2+}total} = C_{MVCl_2} + C_{MV^{2+}soln}$. Any of these steps can be the rate limiting step in the process. Assuming a well-mixed system and no mass transfer limitations, the mole balance for each species can be expressed as follows:

$$\frac{1}{V}\frac{d}{dt}N_{MV^{2+}-S} = kf1 \cdot K' \cdot C_{MV^{2+}total} \cdot \theta_v - kr1 \cdot \theta_{MV^{2+}} - k2 \cdot \theta_{MV^{2+}} \tag{4-9}$$

$$\frac{1}{V}\frac{d}{dt}N_{MV^{+}-S} = k2 \cdot \theta_{MV^{2+}} - kf3 \cdot \theta_{MV^{+}} + kr3 \cdot C_{MV^{+}} \cdot \theta_v - k4 \cdot \theta_{MV^{+}} \tag{4-10}$$

$$\frac{1}{V}\frac{d}{dt}N_{MV^{0}-S} = k4 \cdot \theta_{MV^{+}} - kf5 \cdot \theta_{MV^{0}} + kr5 \cdot C_{MV^{0}} \cdot \theta_v \tag{4-11}$$

$$\frac{1}{V}\frac{d}{dt}N_{MV^{+}} = kf3 \cdot \theta_{MV^{+}} - kr3 \cdot C_{MV^{+}} \cdot \theta_v \tag{4-12}$$

$$\frac{1}{V}\frac{d}{dt}N_{MV^{0}} = kf5 \cdot \theta_{MV^{0}} - kr5 \cdot C_{MV^{0}} \cdot \theta_v \tag{4-13}$$

As for the change of the total MV^{2+} (MV^{2+} + $MVCl_2$) in the solution, the change consists of two parts

$$\frac{1}{V}\frac{d}{dt}N_{MV^{2+}soln} = -kf1 \cdot K' \cdot C_{MV^{2+}total} \cdot \theta_v + kr1 \cdot \theta_{MV^{2+}} + kf_{dissociation} \cdot (1 - K') \cdot C_{MV^{2+}total} - kr_{dissociation} \cdot K' \cdot C_{MV^{2+}total} \cdot C_{Cl^-}{}^2 \quad (4\text{-}14)$$

$$\frac{1}{V}\frac{d}{dt}N_{MVCl_2} = -kf_{dissociation} \cdot (1 - K') \cdot C_{MV^{2+}total} + kr_{dissociation} \cdot K' \cdot C_{MV^{2+}total} \cdot C_{Cl^-}{}^2 \quad (4\text{-}15)$$

The sum of the Equations 4-14 and 4-15 gives the total concentration change of MV^{2+} in solution

$$\frac{1}{V}\frac{d}{dt}N_{MV^{2+}total} = -kf1 \cdot K' \cdot C_{MV^{2+}total} \cdot \theta_v + kr1 \cdot \theta_{MV^{2+}} \quad (4\text{-}16)$$

It should be noted that for the study, the rate laws on the right sides of the equations have units of mM/s. For this study, the volume (V) is 200 ml. In the rate laws, $\theta_{MV^{2+}}$, $\theta_{MV^{+}}$, and $\theta_{MV^{0}}$ are the fractions of reactive sites on the electrode occupied by MV^{2+}, MV^{+}, and MV^{0} respectively. θ_v is the fraction of vacant reactive sites (denoted as S in Equations 4-2, 4-4, and 4-6). In developing the equations, it was assumed that the surface reaction steps were irreversible since MV^{2+} completely disappeared as shown in Figure 4.1. If Equations 4-9 to 4-11 are assumed to be at pseudo-steady state, then

$$kf1 \cdot K' \cdot C_{MV^{2+}} \cdot \theta_v - kr1 \cdot \theta_{MV^{2+}} - k2 \cdot \theta_{MV^{2+}} \approx 0 \quad (4\text{-}17)$$

$$k2 \cdot \theta_{MV^{2+}} - kf3 \cdot \theta_{MV^{+}} + kr3 \cdot C_{MV^{+}} \cdot \theta_v - k4 \cdot \theta_{MV^{+}} \approx 0 \quad (4\text{-}18)$$

$$k4 \cdot \theta_{MV^{+}} - kf5 \cdot \theta_{MV^{0}} + kr5 \cdot C_{MV^{0}} \cdot \theta_v \approx 0 \quad (4\text{-}19)$$

From the site balance on the surface of the electrode, $\theta_v = 1 - \theta_{MV^{2+}} - \theta_{MV^{+}} - \theta_{MV^{0}}$. Substituting the site balance into Equations 4-17 to 4-19 and solving individually for $\theta_{MV^{2+}}$, $\theta_{MV^{+}}$, and $\theta_{MV^{0}}$ gives:

$$\theta_{MV^{2+}} = \frac{C_{MV^{2+}_{total}}}{(K'_{mv23}+K'_{mv22}+1)\cdot C_{MV^{2+}_{total}}+(K'_{mv12}+K'_{mv11})\cdot C_{MV^{+}}+K'_{mv0}\cdot C_{MV^{0}}+K'_{0}} \quad (4\text{-}20)$$

$$\theta_{MV^{+}} = \frac{K'_{mv22}\cdot C_{MV^{2+}_{total}}+K'_{mv11}\cdot C_{MV^{+}}}{(K'_{mv23}+K'_{mv22}+1)\cdot C_{MV^{2+}_{total}}+(K'_{mv12}+K'_{mv11})\cdot C_{MV^{+}}+K'_{mv0}\cdot C_{MV^{0}}+K'_{0}} \quad (4\text{-}21)$$

$$\theta_{MV^{0}} = \frac{K'_{mv23}\cdot C_{MV^{2+}_{total}}+K'_{mv12}\cdot C_{MV^{+}}+K'_{mv0}\cdot C_{MV^{0}}}{(K'_{mv23}+K'_{mv22}+1)\cdot C_{MV^{2+}_{total}}+(K'_{mv12}+K'_{mv11})\cdot C_{MV^{+}}+K'_{mv0}\cdot C_{MV^{0}}+K'_{0}} \quad (4\text{-}22)$$

In these expressions, the Ks are combinations of different rate constants as listed in Table 4.1 below. It should be noted that in the table, $Kmv21 = K' \cdot kf1 \cdot kr5 \cdot (k4 + kr3)$ and this parameter is combined with other parameters to reduce the number of unknown parameters. Substituting Equations 4-17 to 4-19 into Equations 4-12, 4-13 and 4-16 provides three simplified expressions for predicting solution concentrations of MV species with time which are

$$\frac{d}{dt}C_{MV^{2+}_{total}} = -k2 \cdot \theta_{MV^{2+}} \quad (4\text{-}23)$$

$$\frac{d}{dt}C_{MV^{+}} = k2 \cdot \theta_{MV^{2+}} - k4 \cdot \theta_{MV^{+}} \quad (4\text{-}24)$$

$$\frac{d}{dt}C_{MV^{0}} = k4 \cdot \theta_{MV^{+}} \quad (4\text{-}25)$$

Table 4-1 Expressions for different K values as a function of rate constants

K expression
$K'0 = kf5 \cdot (kf3 + k4) \cdot (kr1 + k2)) / Kmv21$
$K'mv22 = K' \cdot k2 \cdot kf1 \cdot kf5 / Kmv21$
$K'mv23 = K' \cdot k2 \cdot k4 \cdot kf1 / Kmv21$
$K'mv11 = kr3 \cdot kf5 \cdot (kr1 + k2) / Kmv21$
$K'mv12 = k4 \cdot kr3 \cdot (kr1 + k2) / Kmv21$
$K'mv0 = kr5 \cdot (kf3 + k4) \cdot (kr1 + k2) / Kmv21$

Since V was constant during the experiments, the above equations were derived for constant V. The expressions for $\theta_{MV^{2+}}$, $\theta_{MV^{+}}$, and $\theta_{MV^{0}}$ can be substituted into Equations 4-23 to 4-25 to obtain rate expressions as functions of MV^{2+}, MV^{+}, and MV^{0} concentrations. For example,

$$\frac{d}{dt}C_{MV^{+}} = k2 \cdot \frac{C_{MV^{2+}_{total}}}{(K'mv23+K'mv22+1)\cdot C_{MV^{2+}_{total}}+(K'mv12+K'mv11)\cdot C_{MV^{+}}+K'mv0\cdot C_{MV^{0}}+K'mv0} - k4 \cdot \frac{K'mv22\cdot C_{MV^{2+}_{total}}+K'mv11\cdot C_{MV^{+}}}{(K'mv23+K'mv22+1)\cdot C_{MV^{2+}_{total}}+(K'mv12+K'mv11)\cdot C_{MV^{+}}+K'mv0\cdot C_{MV^{0}}+K'mv0} \quad (4\text{-}26)$$

4.3.2 Regression

The concentrations of three species at every second were calculated using the three differential equations using a numerical methods approach that minimized the square of the errors. A time step of 1s was used and each of the derivatives of the differential equations (Equations 4-23 to 4-25) was approximated as $\Delta C_{MV}/\Delta t$. For example, using initial guesses of the

parameters and the concentrations at time zero ($C_{MV^{2+}total} = 0.1$ mM, $C_{MV^{+}} = C_{MV^{0}} = 0$ mM), $\theta_{MV^{2+}}$, $\theta_{MV^{+}}$, and $\theta_{MV^{0}}$ were calculated and the values of $C_{MV^{2+}}$, $C_{MV^{+}}$ and $C_{MV^{0}}$ were then calculated at 60 s. This method was continued to predict the concentrations and fractions of the three MV species with time. If a higher accuracy is desired, smaller time steps could be chosen but it was observed that time steps of 1 s and 60 s gave similar results. The rate laws were based on mM/s because this unit provided a larger number than other units (e.g. M/s) for the regression analysis. For example, a number of the magnitude of 0.1 can provide a higher accuracy than a number of the magnitude of 10^{-4}.

The calculated concentration of MV^{+} at every 60s was compared to the experimental data because the experimental data was taken every 60s. The square of the difference between the calculated concentration and the experimental data was calculated at each 60s interval. Excel was used to obtain the best fit for the parameters by minimizing the sum of the square of the differences. The regression was performed step by step. The initial step used a high convergence and constraint value (e.g. 1) and the second step used a lower value (e.g. 0.1). The high convergence and constraint value provided a rough estimate of the parameters. Then, these parameter estimates were used as initial values with the lower convergence and constraint value to provide more accurate parameters. This was repeated several times until there was not a significant change in the parameters. Sometimes, the regression failed in Excel due to initial guesses and a better initial value was used to enable the regression to solve.

As shown in Equation 4-26, the general kinetic function of the MV^{+} concentration change with time is a complicated function with eight unknown parameters (the six in Table 4-1, k2, and k4). Simplification of the equation would be beneficial for regression of the various stages of the

experimental data as long as critical model details are not sacrificed. Simplification is also beneficial to reduce the number of model parameters while still capturing the essence of the model.

4.3.2.1 Model regression of initial stage-Stage 1

When MV^{2+} is first added to the system and during the initial time when MV^{2+} is reduced, the concentration of $MV^{2+}{}_{total}$ is abundant relative to the other MV species. Thus, the first term of Equation 4-26 is much greater than the second term such that the second term can be neglected during regression of data during early times. Additionally, it was assumed that the term $(K'_{mv23} + K'_{mv22} + 1) \cdot C_{MV^{2+}total}$ was initially much bigger than $(K'_{mv12} + K'_{mv11}) \cdot C_{MV^{+}}$, $K'_{mv0} \cdot C_{MV^{0}}$ and K'_{mv0}. Thus, Equation 4-26 was approximated as $\frac{d}{dt} C_{MV^{+}} = k2 \cdot \frac{1}{(K'_{mv23}+K'_{mv22}+1)}$ for the initial data. The zero-order rate signifies that the concentration of MV^{+} with time is linear which is consistent with Figure 4.1. Fitting the initial experimental data of Experiment-1 in Figure 4.1 (shown as Figure 4.3 during the first 1500 seconds) gives $k2 \cdot \frac{1}{(K'_{mv23}+K'_{mv22}+1)} = 2.58 \times 10^{-5}$ mM/s. The fit of the data during the first 1500 seconds with the simplified linear model is plotted in Figure 4.3. As shown, the fit is reasonable, thus validating the general model assumptions for the early part of the data. This $k2 \cdot \frac{1}{(K'_{mv23}+K'_{mv22}+1)}$ value was used as the initial estimate for further fitting the entire data set as described below.

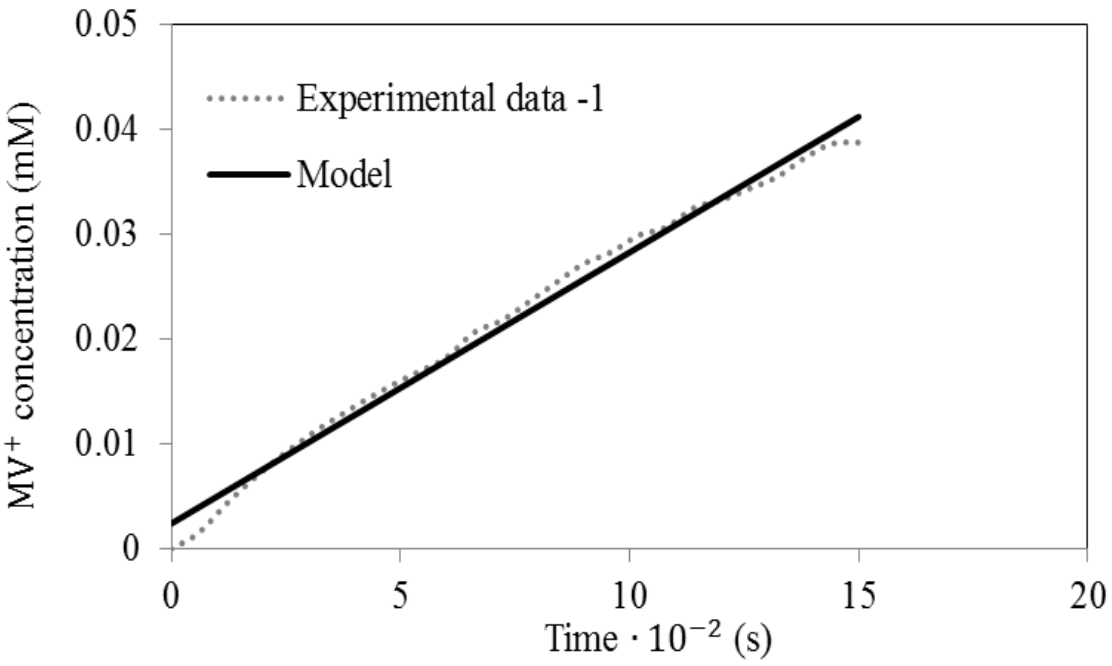

Figure 4.3 Preliminary fitting of MV^+ concentration

4.3.2.2 Model regression of middle stage-Stage 2

As MV^{2+}_{total} was gradually consumed and MV^+ and MV^0 were continuously produced, the concentrations of all three MV species in the solution were likely to be the same magnitude. Thus, none of the four terms $((K'_{mv23} + K'_{mv22} + 1) \cdot C_{MV^{2+}total}$, $(K'_{mv12} + K'_{mv11}) \cdot C_{MV^+}$, $K'_{mv0} \cdot C_{MV^0}$ and $K'_{mv0})$ in the denominator of the kinetic equation are likely not negligible. Thus, initial regression for this stage is not feasible to provide initial parameter estimates.

4.3.2.3 Model regression of final stage-Stage 3

As the reduction went on, the MV^{2+}_{total} concentration became less important since the MV^+ and MV^0 concentrations increased. Thus, in the latter part of the experiment, the $(K'_{mv23} +$

$K'_{mv22} + 1) \cdot C_{MV^{2+}total}$ term is negligible compared to the other terms. Also, it can be assumed that the first kinetic term of Equation 4-26 is negligible compared to the second term. Thus, the kinetic model can be reduced to:

$$\frac{d}{dt} C_{MV^+} = -k4 \cdot \frac{K'_{mv11} \cdot C_{MV^+}}{(K'_{mv12} + K'_{mv11}) \cdot C_{MV^+} + K'_{mv0} \cdot C_{MV^0} + K'_0} \quad (4\text{-}27)$$

This expression was fit to the Experiment-1 data from time 14 x 10^4 s to the end of the experiment using the regression method described above. The model with the fitted parameters is plotted in Figure 4.4.

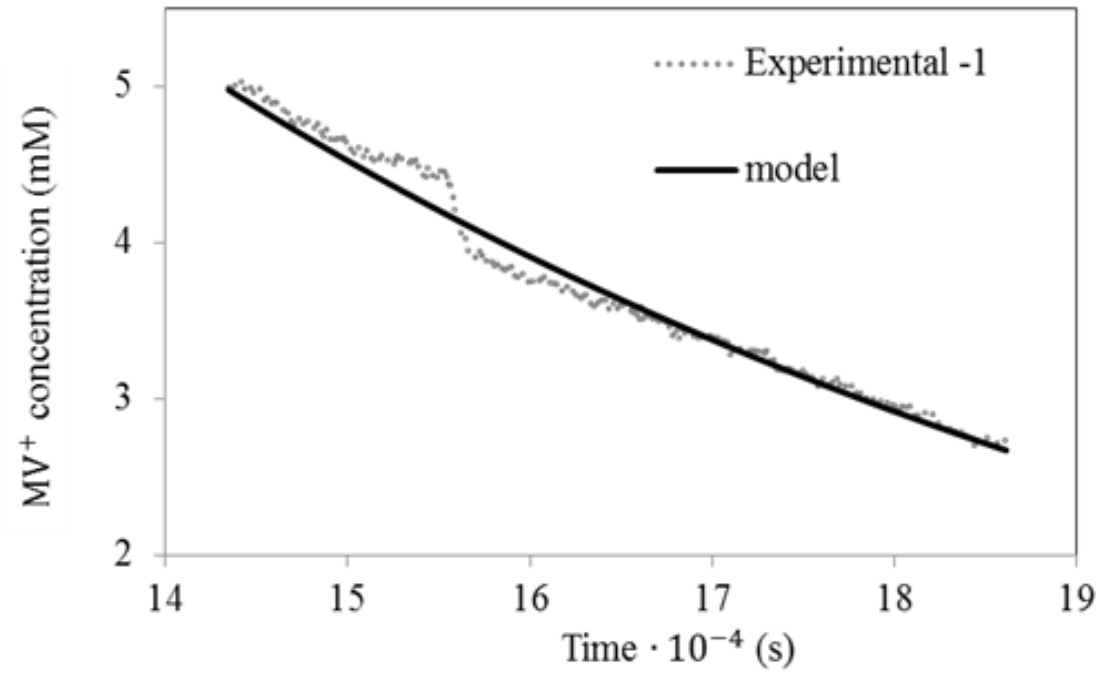

Figure 4.4 Preliminary fitting of latter part of MV^+ data

The values of parameters from the preliminary fitting are listed in Table 4-2. Since the values of K'_0 and K'_{mv12} are essentially zero in the preliminary fitting, these two parameters were eliminated from the model and the full model was reduced to a six-parameter model.

Table 4-2 Preliminary fitting values

Parameters	
K'_0	0.00
K'_{mv12}	0.00
K'_{mv11}	7.03×10^{-5}
K'_{mv0}	8.90×10^{-2}
k4 (mM/s)	5.53×10^{-3}

4.3.2.4 Full regression

The six-parameter model was fit to the entire experimental data of Experiment -1 (Figure 4.1) since this experiment was conducted for a long time. Even with constraints and preliminary parameters from the simplification discussed above, there were still random guessed initial values needed to solve the model. For example, K'_{mv22} and K'_{mv23} were assumed and then k2 was obtained using the regressed value shown in Figure 4.3. Several different initial values were tested and the parameters either converged to the same final parameters or the convergence failed. This demonstrated that the parameters noted in this work were independent of the initial guesses. The results of the regression are shown in Figure 4.1 with the model parameters listed in Table 4-3. The model shows general agreement with the experimental data and captures the formation and consumption of MV^+.

As previously stated, the K_i values shown in Table 4-3 are combinations of various rate constants. k2 and k4 are the forward rate constants for the reduction of MV^{2+} and MV^{+}, respectively. From Table 4-3, the rate constant of the MV^{+} reduction (k2) was much larger than

Table 4-3 Parameters for Experiment-1

Parameters	
K'_{mv23}	7.81×10^{-3}
K'_{mv22}	5.81×10^{-4}
K'_{mv11}	1.44×10^{-5}
K'_{mv0}	2.13×10^{-2}
k2 (mM/s)	2.83×10^{-5}
k4 (mM/s)	2.77×10^{-3}

that of MV^{2+} reduction (k4). This can be expected since it is easier to reduce MV^{2+} than MV^{+} based on the standard potentials described in Chapter 3. It should be noted that the parameters are only specific for the potential of -1100 mV and are only for the specific graphite electrode used in this study. Further studies would need to be conducted to include applied voltage and electrode characteristics in the model. It would also be advantageous to expand the model to include the reversible reactions to capture the data shown in Chapter 3 (Figure 3.2) at different potentials in which the MV^{+} concentration reached an equilibrium state. The model shown in this chapter provides an initial step towards developing a more rigorous model that includes reversibility along with the effects of voltage. The parameter values in the model can be influenced by the system conditions such as the electron mediator type, electrode material,

electrode surface structure, and potential applied to the system. Obviously, a model that captures these influences would be beneficial.

4.4 **Simplification and modification of model**

The experimental data revealed that the reduction of MV^+ appeared to have two regimes and the transition occurred at around 15 x 10^3 s. In the first regime, the MV^+ reduction rate was faster than the rate in the second regime. The decrease in the rate in the second regime showed that something was likely interfering with the MV^+ reduction. Potential side reactions or adverse factors that become important during the latter part of the experiment could be possibilities since such side reactions were not considered in the kinetic model. Thus, it is feasible that the model could be incorrect during the latter portion of the studies when the MV^+ concentration becomes smaller. For example, it may be possible the H^+ (which produces H_2 on the electrode) is more competitive for the vacant sites as the MV^+ concentration decreases.

Based on the above findings, the kinetic model was refit to the data (Experiments 1-3) from time 0s to time 15 x 10^3 s to provide a better estimate of the parameters before the transition occurred. Prior to the fit, the model was further simplified based on the model analysis noted in Section 4.3 using just Experiment-1 data. Originally, the full model had eight unknown parameters although two of them (K_0' and K'_{mv12}) were eliminated from the model based on the preliminary fit. Simplification of the model is beneficial to further reduce unknown parameters while trying to maintain the integrity of the model. In the initial regression, the values of K'_{mv23} and K'_{mv22} were negligible compared to 1 in the denominator terms in Equations 4-20 to 4-22. With all of these assumptions, Equations 4-20 to 4-22 were simplified as:

$$\theta_{MV^{2+}} = \frac{C_{MV^{2+}_{total}}}{C_{MV^{2+}_{total}} + K'_{mv11} \cdot C_{MV^{+}} + K'_{mv0} \cdot C_{MV^{0}}} \quad (4\text{-}28)$$

$$\theta_{MV^{+}} = \frac{K'_{mv22} \cdot C_{MV^{2+}_{total}} + K'_{mv11} \cdot C_{MV^{+}}}{C_{MV^{2+}_{total}} + K'_{mv11} \cdot C_{MV^{+}} + K'_{mv0} \cdot C_{MV^{0}}} \quad (4\text{-}29)$$

$$\theta_{MV^{0}} = \frac{K'_{mv23} \cdot C_{MV^{2+}_{total}} + K'_{mv0} \cdot C_{MV^{0}}}{C_{MV^{2+}_{total}} + K'_{mv11} \cdot C_{MV^{+}} + K'_{mv0} \cdot C_{MV^{0}}} \quad (4\text{-}30)$$

Thus, the simplified model based on the above simplified equations and Equation 4-24 was:

$$\frac{d}{dt} C_{MV^{+}} = k2 \cdot \frac{C_{MV^{2+}_{total}}}{C_{MV^{2+}_{total}} + K'_{mv11} \cdot C_{MV^{+}} + K'_{mv0} \cdot C_{MV^{0}}} - k4 \cdot \frac{K'_{mv22} \cdot C_{MV^{2+}_{total}} + K'_{mv11} \cdot C_{MV^{+}}}{C_{MV^{2+}_{total}} + K'_{mv11} \cdot C_{MV^{+}} + K'_{mv0} \cdot C_{MV^{0}}} \quad (4\text{-}31)$$

Equations 4-23 and 4-25 were also similarly simplified for MV^{2+} and MV^{0}. The simplified model now has five parameters instead of six. The parameter values from the previously fitted model were used as the initial value guesses and regression results are demonstrated in Figure 4.5 for regression of the combined data from all three experiments. Comparing the model and the experimental data revealed that the model predicted the change of MV^{+} with time with reasonable accuracy for the data of all three experiments. The overall agreement captured the essence of the MV^{+} concentration change with time. The parameter values from the fitting of the five-parameter model are shown in Table 4-4 for regressing the combined data and the individual data for each experiment.

Although there is some variation in the regressed parameters for each individual experiment, the values of the five parameters still demonstrated reasonable repeatability. Comparing all individual fitted parameters to the combined parameters, the maximum variation was 5% for K'_{mv22}, 34% for K'_{mv11}, 0% for K'_{mv0}, 23% for k2 and 3% for k4. K'_{mv11} and k2 values were the most sensitive parameters but both of them varied less than 40%. Based on the

difficulty of placing the reference electrode in the same position relative to the working electrode for each experiment, this variation is reasonable.

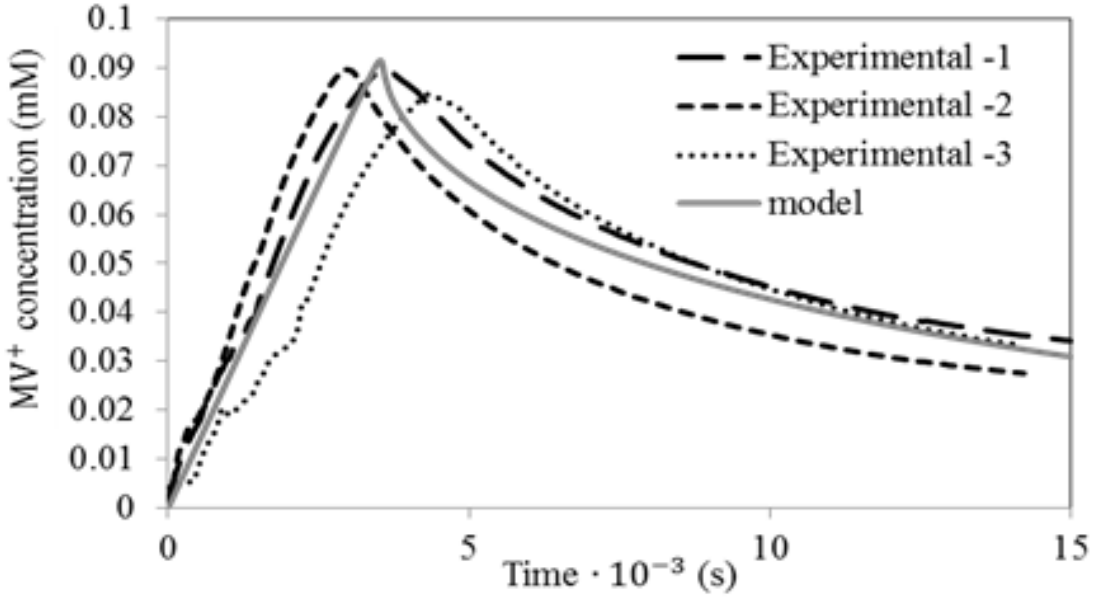

Figure 4.5 Fitting data with experimental data from time 0s to 15 x 10^3 s using the five-parameter model

Table 4-4 Parameter values for five-parameter model

Parameters	Combined	Experiment 1	Experiment 2	Experiment 3
K'_{mv22}	5.56 x 10^{-4}	5.47 x 10^{-4}	5.55 x 10^{-4}	5.28 x 10^{-4}
K'_{mv11}	2.60 x 10^{-5}	2.12 x 10^{-5}	3.44 x 10^{-5}	2.55 x 10^{-5}
K'_{mv0}	2.10 x 10^{-2}	2.10 x 10^{-2}	2.10 x 10^{-2}	2.10 x 10^{-2}
k2 (mM/s)	2.83 x 10^{-5}	2.84 x 10^{-5}	3.37 x 10^{-5}	2.18 x 10^{-5}
k4 (mM/s)	3.24 x 10^{-3}	3.25 x 10^{-3}	3.24 x 10^{-3}	3.34 x 10^{-3}

To assess whether the five-parameter model was justified instead of the six-parameter model, the six-parameter model was also fit to the same data set (Experiments 1 to 3 from time 0s to 15 x 10^3 s) and the difference between the six-parameter model and the five-parameter model was small enough to demonstrate that the simplification of the model was valid for the time from 0s to 15 x 10^3 s. The five-parameter and six-parameter models are shown in Figure 4.6 for comparison.

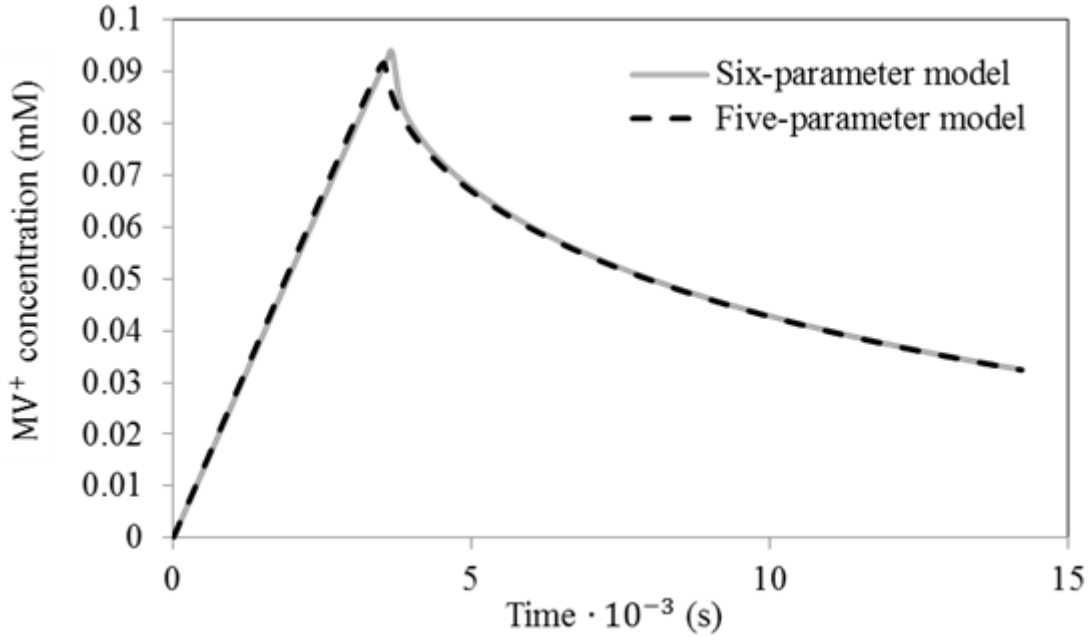

Figure 4.6 Comparison of the six-parameter model and the five-parameter model

A comparison of the new parameter values (Table 4-4) for the 5-parameter model (using all experimental data for partial time range of up to 15 x 10^3 s) with the earlier parameter values (Table 4-3) for the 6-parameter model (using only Experiment-1 data for the entire time range) is shown in Table 4-5. Most of the parameter values changed less than 10% except for the values of K'_{mv11} and k4. Referring to Equation 4-31, the rate of MV^+ concentration change after time 5 x

Table 4-5 Comparison of six-parameter values and five-parameter values

	Six-parameter model	Five-parameter model	Difference
K'_{mv23}	7.81 x 10^{-3}	Assumed 0	
K'_{mv22}	5.81 x 10^{-4}	5.56 x 10^{-4}	-4.46%
K'_{mv11}	1.44 x 10^{-5}	2.60 x 10^{-5}	80.9%
K'_{mv0}	2.13 x 10^{-2}	2.10 x 10^{-2}	-1.3%
k2 (mM/s)	2.83 x 10^{-5}	2.83 x 10^{-5}	0.1%
k4 (mM/s)	2.77 x 10^{-3}	3.24 x 10^{-3}	17.2%

10^3 s can be simplified based on the following assumptions. First, after time 5 x 10^3 s, all MV^{2+} is gone such that the concentration of MV^{2+}_{total} is approximately zero. Then, Equation 4-31 can be simplified and rearranged to $\frac{d}{dt}C_{MV^+} = -k4 \cdot \frac{C_{MV^+}}{C_{MV^+} + \frac{K'_{mv0}}{K'_{mv11}} \cdot C_{MV^0}}$. Second, the value of $\frac{K'_{mv0}}{K'_{mv11}}$ has a magnitude of 10^3 (independent of Cl^- concentration) and $\frac{K'_{mv0}}{K'_{mv11}} \cdot C_{MV^0}$ at time 5 x 10^3 s is approximately 26. This value is three orders of magnitude higher than C_{MV^+} with a value of 6.7 x 10^{-2} at 5 x 10^3 s. Therefore, further simplification leads to $\frac{d}{dt}C_{MV^+} = -k4 \cdot \frac{K'_{mv11}}{K'_{mv0}} \frac{C_{MV^+}}{C_{MV^0}}$ at times greater than 5 x 10^3 s. The value for $k4 \cdot \frac{K'_{mv11}}{K'_{mv0}}$ in the six-parameter model was 1.87 x 10^{-6}, which is approximately 1/2 the value of for the five-parameter model. Thus, this is why there is a faster

reduction of MV^+ for the five-parameter model than the six-parameter model. It can be seen that the decay of MV^+ is sensitive to the combination of the three parameters noted above.

The five-parameter and six-parameter model with the parameters of Table 4-5 is shown with the data of Experiment-1 in Figure 4.7 to show the models in comparison to data of later

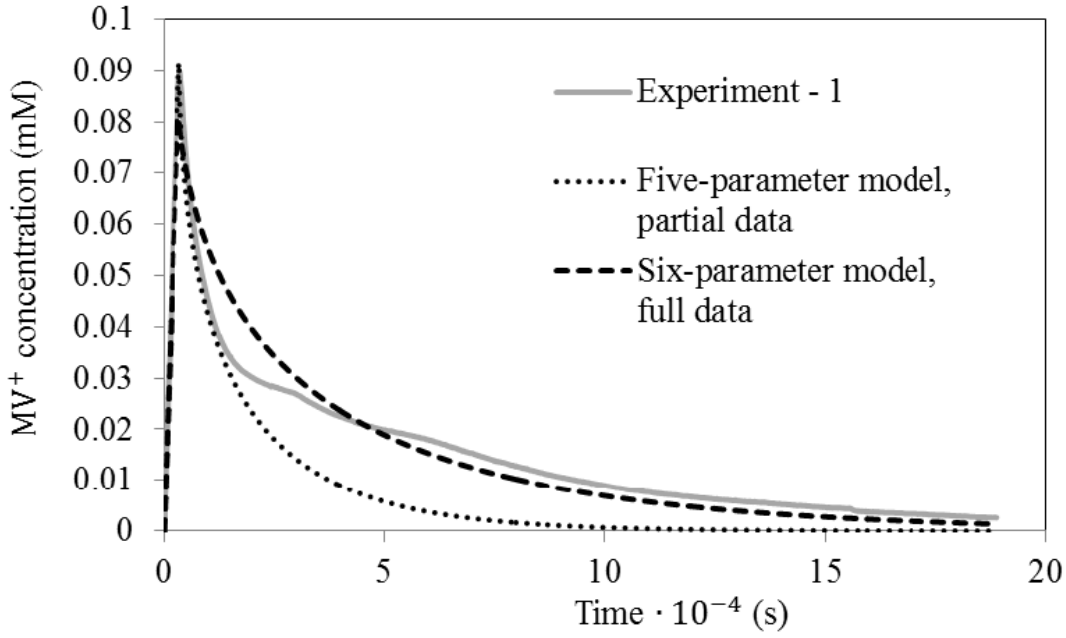

Figure 4.7 Comparison of experimental data with the justified model.

times. Figure 4.7 shows that the five-parameter model predicted the concentration change of MV^+ very well before time 15 x 10^3 s but significantly underestimated the MV^+ concentration after time 15 x 10^3 s. Comparing the data with the model, the experimental data demonstrated that the reduction of MV^+ slowed down after time 15 x 10^3 s. Possible reasons are discussed in Section 4.5 and it appears that model needs to be modified to account for this transition in the

rate. It is beyond the scope of this work to account for the rate change beyond 15 x 10^3 s and future work would be beneficial to determine the cause. For the six-parameter model, the reduction rate for MV^+ is slower than the rate of the five-parameter model but the model overestimated the MV concentration from time 9 x 10^3 s to 45 x 10^3 s and underestimated MV^+ from time 45 x 10^3 s to the end of the experiment.

Further analysis based on the modified kinetic model was performed for a better understanding of the reaction mechanism. The values of $\theta_{MV^{2+}}$ and θ_{MV^0} versus time were plotted in Figure 4.8 and the value of θ_{MV^+} versus time was plotted in Figure 4.9. Figure 4.8

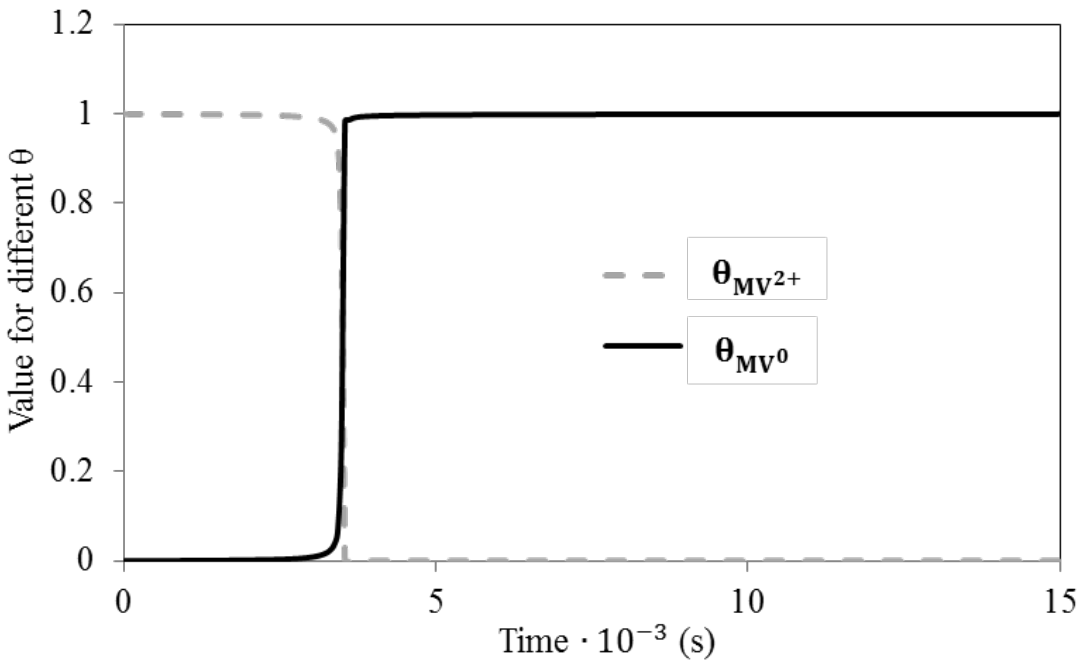

Figure 4.8 Chang of $\theta_{MV^{2+}}$ and θ_{MV^0} versus time.

indicated that the electrode surface was mostly occupied either by MV^{2+} or MV^0 and Figure 4.8 demonstrated that MV^+ only occupied up to 1.91% of the sites (but for only a short time). This

demonstrated that MV^+ only occupied up to 1.91% of the sites (but for only a short time). This showed that the graphite electrode surface has a stronger affinity to the MV^{2+} and MV^0 thanthe surface was occupied by MV^0 although the amount of MV^0 produced in the system was not abundant. MV^0 prefers to stay on the electrode surface than dissolve into the solution. This is MV^+. Figure 4.8 also showed that as time close to the end of the experiment, most of the sites on consistent with the finding that K'0 is extremely small (assumed zero compared to other terms in the model). From Table 4-1, K'0/K'mv0 = kf5/kr5 such that kf5/kr5 (desorption equilibrium constant for MV^0) is extremely small. This suggests that MV^0 prefers to stay absorbed on the electrode as it is formed, thus minimizing the opportunity for MV^+ to be reduced on the electrode. This can be one reason why the rate of MV^+ reduction is slower than the rate of MV^{2+} reduction.

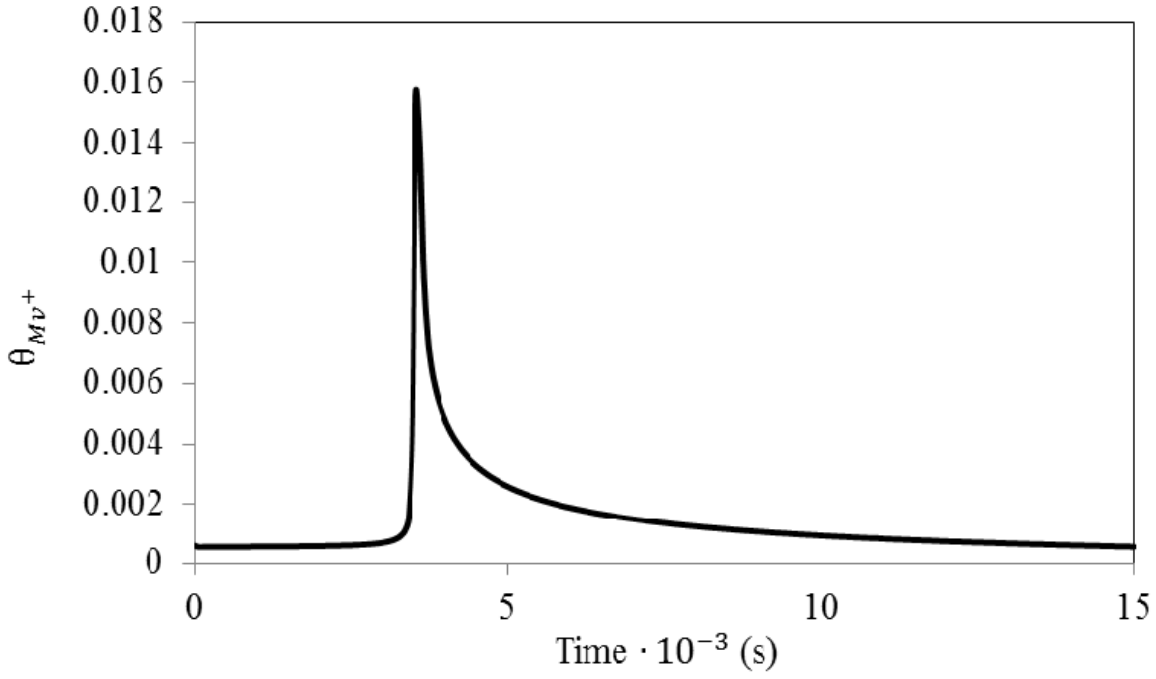

Figure 4.9 Chang of $\theta_{MV^{2+}}$ and θ_{MV^0} versus time.

4.5 **Discussion**

Kinetics of electron mediator reduction has significant importance for industrial application. Using electrochemically reduced MV species as an external electron mediator is a two-step procedure. Since MV species are reduced on the electrode, assessing the kinetic parameters for MV reduction was the objective in this chapter to enable comparison between rates of MV utilization by cells. In order to provide electrons and promote the use of MV in biological systems, recycling kinetics of electron mediators (e.g.MV) needs to be faster than the enzyme or cellular kinetics to eliminate electron mediator recycling from being the limiting step. Kinetics of MV reduction has been studied mostly in stagnant systems where diffusion was the rate-limiting step and the reaction rate was always expressed as the diffusion coefficient [75, 79, 97]. Obtaining kinetic parameters in a well-stirred system, like this study, provides an opportunity to address potential kinetic limitations of scaled-up applications. In industrial applications, a well-stirred system can also provide better mass transfer [98], faster reaction kinetics [99, 100] and a better product yield.

In this study, a kinetic model of MV^+ reduction (along with predicting MV^{2+}_{total}, MV^0, and the associated fractions of species on the electrode sites) in a well-stirred system was developed. The model estimated the concentration change of MV^+ with time but did not account for the transition in the MV^+ reduction rate beyond 15×10^3 s. There are several possible reasons for the transition. For example, H^+ reduction on the surface, which was neglected in the model, could be slow enough to be neglected during the reduction of MV^{2+} and the reduction of MV^+ when MV^+ is at a high concentration. However, when the MV^+ concentration becomes lower, the reduction of H^+ could became significant and compete with MV^+ on the surface to slow the MV^+

reduction. The true mechanism for the slow kinetic after time 15 x 10^3 s requires more experiments and critical analysis which can be achieved in future work.

From the discussion above, the affinity of MV^{2+} and MV^0 to the electrode was higher than the affinity of MV^+. The affinity of MV^{2+} and MV^0 can be compared using Equation 4-28 and 4-30. For a hypothetical situation in which the concentration of MV^{2+} and MV^0 are equal to each other with no MV^+ in the solution, $\theta_{MV^{2+}} = \frac{1}{1+K'_{mv0}}$ and K'_{mv0} can be neglected compared to 1, thus $\theta_{MV^{2+}} \approx 1$. As for θ_{MV^0}, $\theta_{MV^0} = \frac{K'_{mv23}+K'_{mv0}}{1+K'_{mv0}}$ which is a negligible value compared to $\theta_{MV^{2+}}$. Thus, the affinity of MV^{2+} is higher than MV^0 and higher than MV^+. A higher affinity of MV^{2+} is beneficial for future applications, because once MV^+ is converted by a bio organism back to MV^{2+}, MV^{2+} has a stronger ability to adsorb to the electrode surface and react with electrons provided by electrode.

As previously shown, the model predicted the MV^+ concentration well before 15 x 10^3 s and the parameter values were solved from fitting the model with the experimental data before 15 x 10^3 s. Although the parameters were specific for the experimental system at -1100 mV, the parameters can provide guidance towards design criteria for applications associated with electrochemical reactors. One application currently being explored is the use of electron mediators for biofuels production. The kinetic analysis provides information of the MV reduction rate (or electron transfer rate), which is valuable when assessing the feasibility of future cellular applications based on required cellular electron consumption rates. For the particular study of this work, experimental data indicated that the reduction of MV^{2+} was faster than the reduction of MV^+ even though the k4 had a higher value than k2. The reason might be

that the affinity of MV^+ to the electrode surface was too low that the concentration on the surface was very small and limited the reaction rate. A better engineering designed electrode might increase the affinity of MV^+ and increase the rate of MV^+ reduction (essentially two orders of magnitude compared to MV^{2+} reduction) if MV^0 is the desirable species in the system.

As discussed above, the first reduction of MV was faster than the second reduction and the highest rate of MV^+ concentration change occurred at the beginning of the reduction. At initial time, the highest reduction rate is equal to $k2 = 2.83 \times 10^{-5}$ mM/s (since the active sites are essentially filled with MV^{2+}). As shown in Figure 3.2, this rate is likely on the same order as the studies for -800 to -1100 mV although the rate slows down quicker as the applied voltage goes from -1100 to -800 mV.

To address the issue as to whether the reduction rate is sufficient for biofuels applications, the rate of ethanol production for *Clostridium carboxidivorans P7* using syngas as the electron and carbon source, was 2.01×10^{-4} mM/s [63]. As reported [63], the bio organism utilized 12 moles of electrons to produce 1 mole of ethanol. Thus, the rate of electrons required ($R_{e\text{-},required}$) to fully produce ethanol is 2.41×10^{-3} mM/s. This is nearly two orders of magnitude higher than the highest rate of MV reduction. However, the study cited above was for an extremely low cell mass (averagely 0.6 g/L). In commercial reactors, the rate of ethanol production should be higher because a higher cell mass should be used (at least 10x), which leads to a result that the reduction of MV would be three orders of magnitude slower and thus would be the limiting step when using MV as electron mediators for biofuels production via cells.

From the other point of view, for a continuous stirred reactor at steady state, the amount of ethanol (in moles) removed from the reactor would equal the amount of ethanol produced such that

$$S = R_{ethanol} \cdot \tau \tag{4-32}$$

S is the ethanol concentration of the outlet stream which must be at least 1100 mM (50 g/L or 5 wt%) or higher for economical distillation. $R_{ethanol}$ is the production rate of ethanol and τ is the residence time (volume of reactor divided by liquid flow rate) for the reactor. From Equation 4-32, the expression for R is

$$R_{ethanol} = S / \tau \tag{4-33}$$

Assuming that it takes 12 moles of electrons to form 1 mole of ethanol, the rate of electrons required to produce ethanol from just MV becomes

$$R_{e^- required} = 12 \cdot S / \tau \tag{4-34}$$

The ratio of the rate of electrons required (assuming S = 1100 mM) to the rate of electrons supplied by MV (R_{MV} = 2.83 x 10^{-5} mM/s or 1.69 x 10^{-3} mM/min) versus τ is plotted in Figure 4.10. A value of 1 on the y-axis is when MV can supply enough electrons to produce ethanol without any other electron source.

The ratio of $R_{e-,required}$ over R_{MV} decreased as τ increased and when τ equaled 1 x 10^3 min, the value of $R_{e-,required}$ was nearly four orders of magnitude higher than the value of R_{MV}. Figure 4.10 demonstrated that the rate of electrons provided by MV was three orders of magnitude

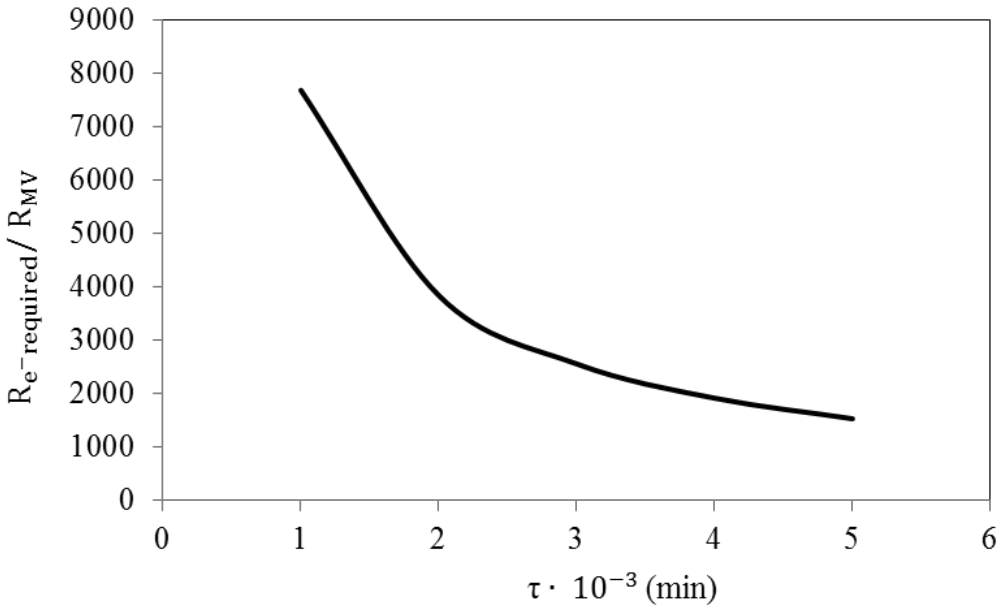

Figure 4.10 Ratio of the rate of electrons required to electrons supplied. τ is the residence time.

lower than the rate of the electrons required for bio-ethanol production which agreed with the previous analysis for *C. carboxidivorans P7*.

The above analysis demonstrated that using electrochemically reduced MV as an external electron mediator for biofuel production might not be feasible at a potential of -1100mV. The k2 and k4 are function of potential, and a more negative potential might increase the reduction rate according to electrochemical kinetic theory. However, a more negative potential would result in faster formation of H_2 and compete with the reduction of MV. Additionally more H_2 formation on the surface may result in the block of the pores on the surface and reduce the available surface active sites. The applied potential influence on the reduction rate in this study was complicated and requires further study to assess the full kinetics related to all experimental parameters (e.g. applied potential, electrode size, etc.).

It should be noted that this kinetic study didn't incorporate the H^+ adsorption on the surface and future studies could include the H^+ adsorption in a more comprehensive model. Reduction of H^+ has an open circuit potential of -642 mV vs Ag/AgCl and at an applied potential of -1100mV, H^+ was likely adsorbed on the electrode surface where it was reduced to H_2. Since the θ values for the three MV species shown in this chapter were obtained with the assumption that only MV^{2+}, MV^+, and MV^0 were absorbed, the inclusion of H^+ in a comprehensive model would lead to lower values of θ than the values in this study. However, the analysis shown in Figures 4.8 and 4.9 would only lower the values but not change the general conclusion that MV^+ has a much lower adsorption than MV^{2+} and MV^0. As shown in Equation 4-24, the concentration of MV^+ change was observed in the experiments and the product of a θ value and a rate constant (e.g. k2 or k4) was a specified value. Thus, the rate constants shown in this study may be underestimated and would be higher in a more comprehensive model that included the reduction of H_2. Higher k2 and k4 values would led to a higher reduction rate of MV species if H_2 reduction was prohibited in the future. With a modified material for the electrode, which can be toxic to H^+ but favored the reduction of MV, the reduction rate of MV can be higher.

As noted, k2 and k4 are a function of the surface area of the electrode. An electrode with larger surface area can increase the reduction rate of MV because in this study, nearly all surface sites were occupied either by MV^{2+} or MV^0 and more vacant sites can increase the concentration of MV^{2+} and MV^+ on the surface and increase the reduction rates. Specially, designing a nano-structured electrode with more sites per unit volume can drastically increase the surface area of the electrode and increase the reduction rate of MV. Also, as previously mentioned it may be possible to design an electrode that favors MV^+ adsorption (increasing electron supply rates two

orders of magnitude due to the k4 value compared to the k2 value) and minimizes H^+ adsorption. These changes could lead to a more favorable opportunity to produce biofuels from MV although this does not overcome the three order magnitude difficulty. In addition, studies with other electron mediators may find that other mediators are more favorable to use although these mediators would have to be utilized by the cells.

More kinetic studies should be conducted to test the kinetic parameters at different potentials before the conclusion of the feasibility of using MV as external electron mediator in commercial scale can be made. A more comprehensive kinetic model would also be helpful to predict the kinetic parameters at different potentials.

4.6 **Conclusions**

The kinetic model developed in this study provided information of the MV reduction rate which was valuable when assessing the feasibility of future cellular applications based on required cellular electron consumption rates. The model not only filled in the gaps in the kinetic research of MV, but also provided guidance in future similar studies for other electron mediators in different systems. From this study, MV seems to have a low reduction rate (compared to cellular needs) at the experimental settings studied. However, better engineering design, including an optimal potential, an electrode that favors MV^+ adsorption, and a larger electrode can increase the rate of MV reduction to favor the possible use of MV applications. In other applications, such as enzymatic systems that can utilize MV, the required electrons from MV may be less than for cellular systems such that MV could still possibly be a viable electron mediator.

5 EFFICIENCY STUDY

The coulombic efficiency is critical to assess the feasibility of using external power as an electron donor due to the high electricity price in some places (25.12 cents/kW·hr in Hawaii, 17.39 cents/ kW·hr in Connecticut [101]). The external power generates electrons; the electron mediators take electrons from the external power, transport the electrons to the bio organisms and bio organisms use the electrons to produce targeted products. The electron flow should ideally be 100 % efficient such that all electrons are used to produce the desired product. However, side reactions that also consume electrons without contributing to useful products can reduce the efficiency. Every electron comes with a price and a loss in electrons can lower the profit a commercial process. High electron efficiency is desirable and engineering analysis can help determine the factors that can increase the efficiency.

When using MV as an electron mediator in a biological system containing cells, the solution should be the medium optimal for cell growth and fermentation and not the 9:1 DMF: H_2O solution used in the studies of Chapters 3 and 4. The influence of the medium on the efficiency is necessary to help in medium optimization. A better medium design not only can reduce the electrons consumed by medium but also can help prevent side reactions that can alter the composition of medium and slow down the cell growth and fermentation.

5.1 -1100 mV efficiency analysis

The coulombic efficiency for this work is defined as the ratio of the electrons used to reduce MV species to the electrons supplied to the system via external electricity.

To assess the number of electrons consumed during MV reduction, one mole of MV^{2+} uses one mole of electrons to form MV^{+} and MV^{+} reduction requires one mole of electrons to form MV^{0}. To assess the number of electrons supplied to the system, integration of the current with respect to time can provide this estimate. The electrons consumed and provided were calculated separately.

5.1.1 Materials and methods

In this chapter, the -1100 mV studies in Chapters 4 using the BER system were used for the efficiency analysis. Additionally, an experiment was performed in the absence of MV to assess the current associated with the reduction of H^{+} under a potential of -1100 mV. For this latter experiment, 200 mL of 100 mM KCl solution was used in both the cathodic and anodic chambers. The pH was carefully controlled with the same pH control system and the pH before and after the reduction of H^{+} were both 7. The current was measured by the potentiostat assisted with a computer system every second.

5.1.2 Electrons consumed by MV species

Coulombic efficiency was analyzed based on the kinetic model built in Chapter 4 using the data from the three experiments. In Chapter 4, a kinetic model was developed from the experimental results for the -1100 mV studies from time 0s to time 15 x 10^{3} s. With the model,

the concentration change of all the three species of MV can be quantitatively predicted, though only the MV^+ concentration can be observed during the experiments. As discussed in Chapter 4, the concentration changes of $MV^{2+}{}_{total}$, MV^+, and MV^0 can be expressed as Equations 5-1, 5-2 and 5-3 as follows

$$\frac{d}{dt}C_{MV^{2+}total} = -k2 \cdot \theta_{MV^{2+}} \quad (5\text{-}1)$$

$$\frac{d}{dt}C_{MV^{+}} = k4 \cdot \theta_{MV^{2+}} - k4 \cdot \theta_{MV^{+}} \quad (5\text{-}2)$$

$$\frac{d}{dt}C_{MV^{0}} = k4 \cdot \theta_{MV^{+}} \quad (5\text{-}3)$$

The detailed expressions for $\theta_{MV^{2+}}$, $\theta_{MV^{+}}$, and $\theta_{MV^{0}}$ as a function of $C_{MV^{2+}}$, $C_{MV^{+}}$, $C_{MV^{0}}$ and rate constants can be found in Section 4.4 of Chapter 4.

Because MV^{2+} consumes one mole of electrons to form one mole of MV^+ and consumes two moles of electrons to form one mole of MV^0, the cumulative moles of electrons consumed ($N^{cons}{}_{e^-}$) with the reduction of MV species can be quantitatively expressed as

$$N_{e^-}^{cons} = \left(\frac{1\ mmole\ electrons}{1\ mmole\ MV^+\ produced}\right) \cdot C_{MV^+} \cdot V + \left(\frac{2\ mmoles\ electrons}{1\ mmoles\ MV^0\ produced}\right) * C_{MV^0} \cdot V \quad (5\text{-}4)$$

$N^{cons}{}_{e^-}$ has units of mmoles. As noted in Chapter 4, the concentration units for the predicted MV species are mM for the regressed parameters. For this study, V= 0.2 liters.

Using the kinetic parameters from Chapter 4 for each individual experiment at -1100 mV, the concentrations of all MV species were predicted with time and applied to Equation 5-4 to predict $N^{cons}{}_{e^-}$ versus time. The MV predictions for the three individual experiments are shown in Figure 5.1 for times up to 15 x 10^3 s. Later time data was not analyzed since the model was only

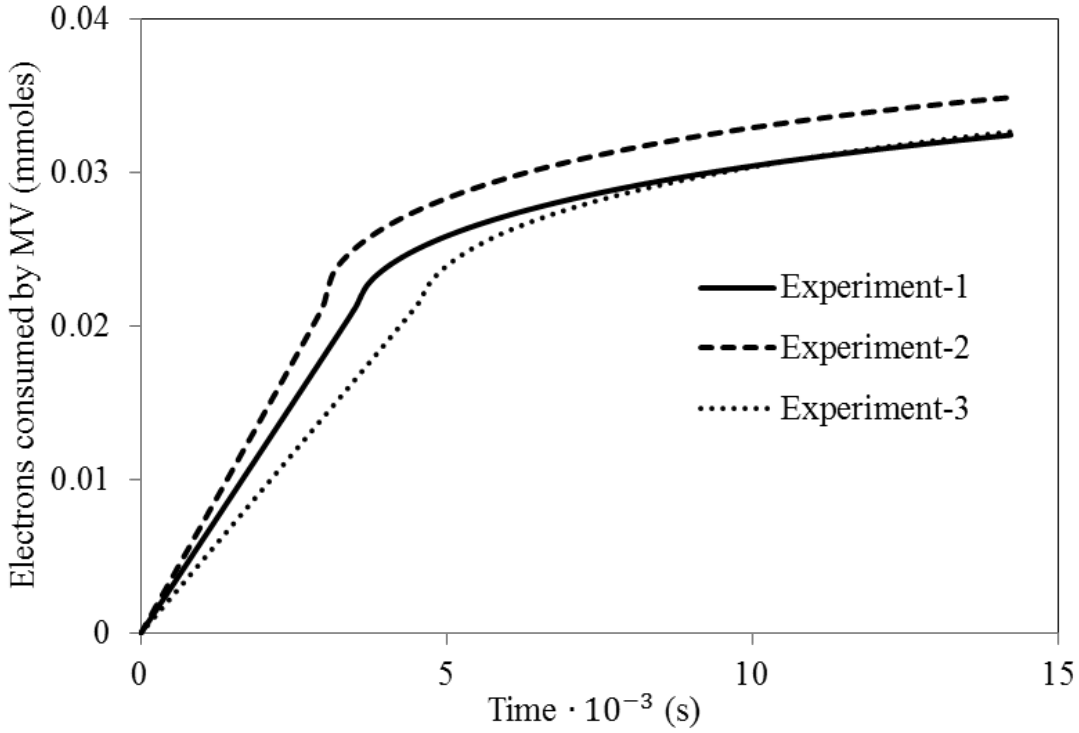

Figure 5.1 Cumulative electrons consumed by MV based on model using data from all three experiments

developed to describe the first 15 x 10^3 s. Generally, the increase of the cumulative electrons consumed by MV^+ and MV^0 has two regimes. In both regimes, the electron consumption rate was nearly linearly. The near-linear rate in the first regime (initial part of the study) was much faster than the near-linear rate in the second regime (latter part of the study). This demonstrated that electron consumption was much faster during MV^{2+} reduction as compared to MV^+ reduction and this agrees with the kinetic studies. In the kinetic studies in Chapter 4, the reduction of MV^{2+} (shown by the formation of MV^+) was much faster than the reduction of MV^+ (shown by the MV^+ concentration drop).

5.1.3 Electrons provided by the external power system

In order to determine coulombic efficiency as a function of time, the moles of electrons provided ($N^{prov}_{e^-}$) by the external power was calculated from the integration of current (i) with respect to time for each of the three experiments. Figure 5.2 shows the measured current as a function of time for the three -1100 mV experiments. The current for Experiment-2 had the highest value, the current for Experiment-3 had the lowest value and current for the Experiment-1 was between the two extreme. The difference among the three experiments increased from time 0s to 540s, and decreased from 540s to the end of the experiments.

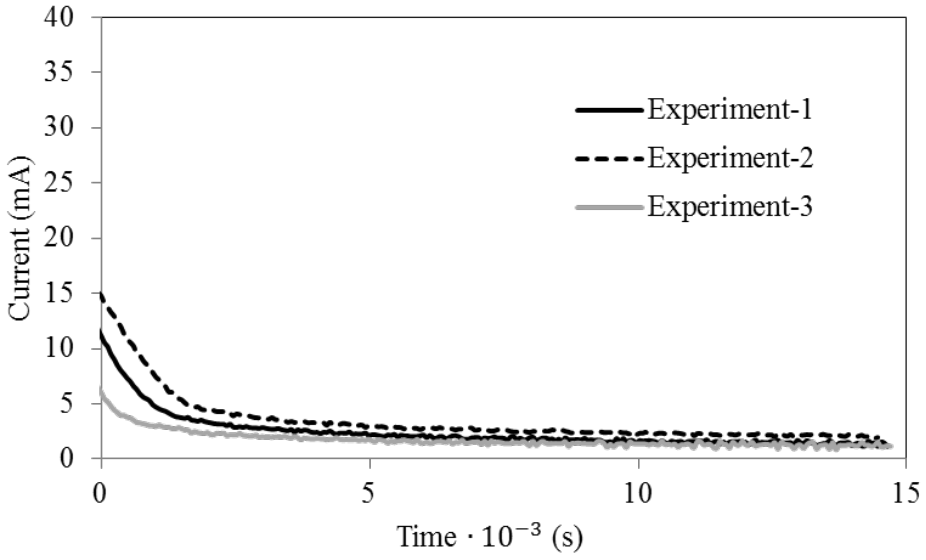

Figure 5.2 Current changes with time for Experiments 1-3.

The current measured in this study, shown in Figure 5.2, is the sum of the product of current density and the surface area of the electrode, which was

$$i_{total} = \sum i_{i,density} \cdot S_i \quad (5\text{-}5)$$

Here, i_{total} is the total current measured in this study, $i_{\text{i,density}}$ is the current density for a specific redox reaction *i* which is defined as the current per surface area (mA/cm^2) associated with redox reaction *i*. S_i is the surface area of the electrode that is utilized for redox reaction *i*. For the reduction of MV at potential of -1100mV, reduction of H^+ was also likely to occur. Thus, the current can be expressed as

$$i_{total,MV} = i_{H^+,density} \cdot S_{H^+} + i_{MV,density} \cdot S_{MV} \quad (5\text{-}6)$$

Here, $i_{,H^+,density}$ is the current density for the reduction of H^+ and $i_{MV,density}$ is the current density for the reduction of both MV^{2+} and MV^+. Both of the current densities are functions of the potential. S_{H^+} and S_{MV} are the surface areas occupied by the H^+ and MV species. Based on the study in Chapter 4 and assuming there are no vacant sites on the surface ($S_{total} = S_{H^+} + S_{MV}$), Equation 4-6 can be rearranged to

$$i_{total,MV} = [i_{H^+,density} \cdot \theta_{H^+} + i_{MV,density} \cdot (1 - \theta_{H^+})] \cdot S_{total} \quad (5\text{-}7)$$

Here, θ is the fraction of the total sites (S_{total}) that are occupied by the adsorbed species.

$i_{total,MV}$ values varied from the three experiments. In Equation 5-7, $i_{MV,density}$ and $i_{H^+,density}$ are functions of the over potential. The over potential is defined as the potential difference between the potential on the surface of the working electrode and the potential just outside the double layer. The double layer is used to describe the potential change within the distance from the working electrode to the edge of the double layer. The thickness of the double layer is a function of the size of the charged molecules, charge number of the ions, stirring rate, etc. It is desirable to place the reference electrode as close to the outer edge of the double layer as possible so that the applied voltage is equivalent to the overpotential. However, it's difficult to

place the reference electrode exactly at the same place every time. Thus, the change in the location of the reference electrode is a possible reason that the value of $i_{MV,density}$ among the three experiments was not the same.

Also, the θ_{H^+} and θ_{MV^+} were also subjects to change among the three experiments. Graphite electrodes used in this study have porous surface structure. H^+ is a small molecule which can diffuse into the small pores on the surface. As the reduction of H^+ occurred in the small pore, hydrogen would form inside the pores and the size of a H_2 molecule is double of the size of a H^+ molecule. H_2 molecules are more difficult to diffuse out and some of the H_2 molecules may remain in the pores and blocked the pore. Blocking the pores can reduce the total available surface area and changed the values of θ_{H^+} and θ_{MV^+}. This process of H_2 blocking the surface area can occur randomly among experiments, thus the value of θ_{H^+} and θ_{MV^+}could vary among each experiment.

For all three experiments, the incremental area under the curve (in mA·s) as a function of time was estimated using the trapezoid method individually for the three experiments. Dividing the integrated area by the Faraday's constant (F= 96.49 x 10^4 mA·s / mmol) gave the mmoles of electrons provided to the electrode as a function of time. The electrons provided as a function of time for the three experiments are shown in Figure 5.3. At the end of the experiment (15 x 10^3 s), electrons provided by the external power reached 0.425 mmoles for Experiment-1, 0.619 mmoles for Experiment-2 and 0.248 mmoles for Experiment-3. Due to the difference in the current, the highest amount of electrons provided (Experiment-2) was 150% higher than the lowest amount (Experiment-3).

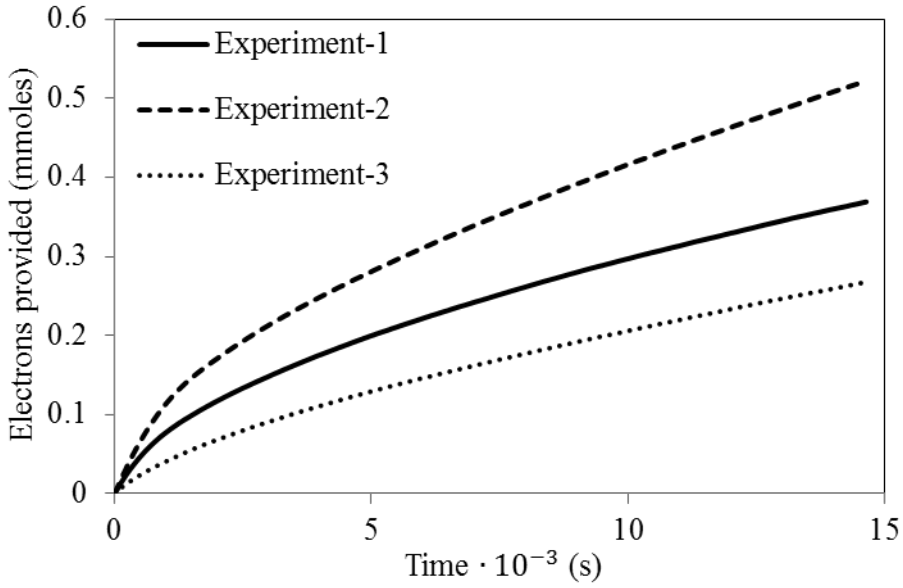

Figure 5.3 Electrons provided by external power source.

With both the information of electrons consumed by MV and electrons provided by the external power system, the coulombic efficiency (ε) can be calculated as ε= ($\frac{N_{e^-}^{cons}}{N_{e^-}^{prov}}$). The results are shown in Figure 5.4. The average ε for each of the three experiments was calculated to be 10.6%, 8.3% and 18.0% and the peak ε for each experiment was 13.1%, 10.4% and 21.7% for Experiment-1, Experiment-2, and Experiment-3, respectively. Although there was some difference in the predicted efficiencies, it is clear that for all three studies, most of the energy supplied to the system was likely wasted in side reactions instead of MV reduction. Compare to the direct electron transport with a efficiency as high as 85%, the efficiency of MV reduction is low. Since protons produced by water electrolysis in the anode chamber can be reduced to H_2 in the cathode chamber when the potential is -1100 mV, the reduction of H^+ can be one of the key side-reaction that consumes electrons and reduces the efficiency.

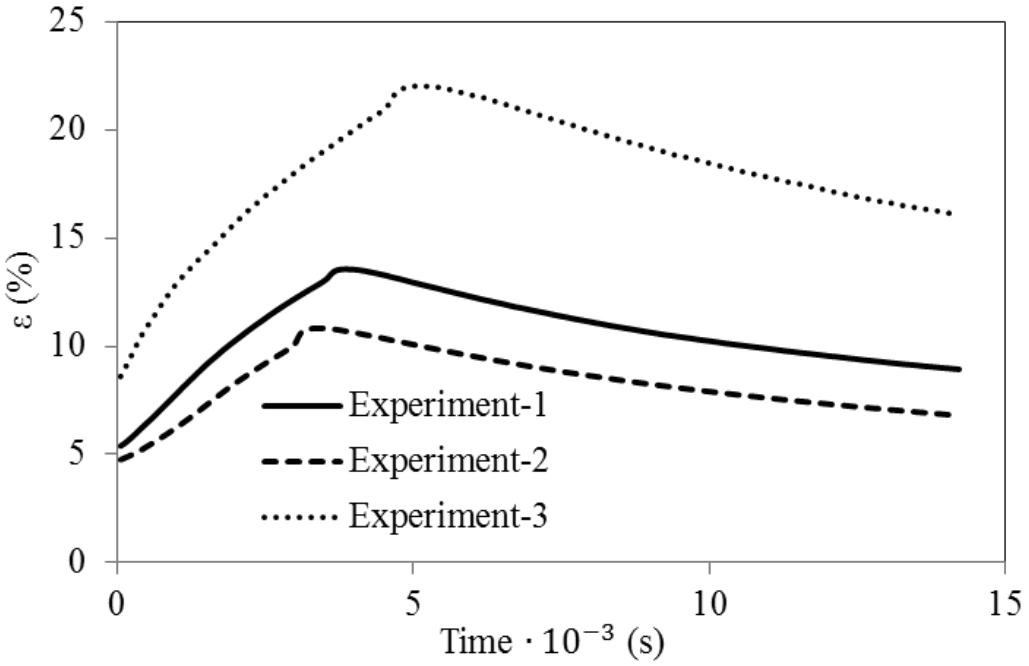

Figure 5.4 ε as a function of time.

To study whether H^+ likely played a significant role in the reduced MV efficiency, an analysis of the reduction of H^+ was explored with experiments with no MV in the solution. The results of the current with time are presented in Figure 5.5 along with the data for the three MV experiments. Figure 5.5 demonstrated that the current for the reduction of water in the absence of MV was at the same order of magnitude of the current for the reduction with MV present.

As discussed previously, the current for a system with MV can be expressed by Equation 5-7. For a system with no MV presents, only reduction of H^+ on the electrode occurred and the expression of current was

$$i_{total,H} = i_{H^+,density} \cdot S_{total} \tag{5-8}$$

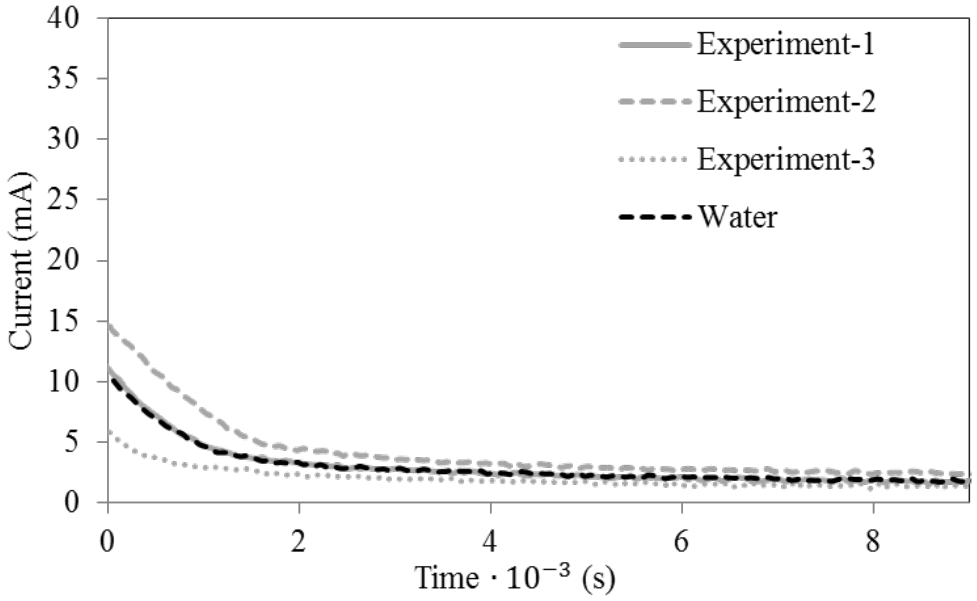

Figure 5.5 Comparison of current between reduction of MV and reduction of H^+

Thus, the difference between the current with MV and without MV was

$$\Delta i_{total} = i_{total,MV} - i_{total,H} \tag{5-9}$$

Substituting the Equation 5-7 and 5-8 into Equation 5-9 and rearranging gave

$$\Delta i_{total} = (i_{MV,density} - i_{H^+,density}) \cdot (1 - \theta_{H^+}) \cdot S_{total} \tag{5-10}$$

As shown in Figure 5.5, the current in the presence and absence of MV was on the same order of magnitude. When comparing the water study with Experiment-1, the currents were similar for a majority of the time (i.e. Δi_{total} is small). A small Δi_{total} indicates that ($i_{MV,density} - i_{H^+,density}$) is small and/or ($1 - \theta_{H^+,density}$) is small.

When $i_{MV,density} - i_{H^+,density}$ is small, the reduction of H^+ and MV has similar rates and the H^+ reduction is competitive to the reduction of MV. When $1 - \theta_{H^+,density}$ is small, most of the

surface area or surface active sites are occupied by H^+ and only a few are used for MV reduction. When both of the terms are small, the H^+ reduction is competitive in both the kinetic and the surface sites. This provides a plausible reason as to the low efficiency for MV reduction. Although the comparisons of Experiment-2 and Experiment-3 with the water experiment are not as easy to clarify, the above analysis provides a plausible reason for the low efficiency. Obviously, more experiments would provide better clarification. To increase the efficiency, it would be beneficial to design the electrode to minimize H^+ reduction.

If possible, it would be beneficial to operate at a potential where MV^{2+} reduction occurred and not MV^+ reduction since the rate of the first reduction is much faster (see Chapter 4) and would favorably compete with side reactions for the available electrons. The slower reduction of MV^+ does not compete as favorably with any potential side reactions. It should be noted that the applied voltage and the MV concentration can change these scenarios but the analysis in this chapter provides some insights regarding potential efficiency issues associated with utilizing MV for biological processes.

The efficiency analysis discussed above was only for a system with a DMF:H_2O solution. When using MV in a biological system, a specially designed medium should be used. The possibility of the reduction of medium species would unnecessarily occupy electrons provided by the external power and decrease the efficiency even further. The possibility of the reduction of medium was investigated as noted below to assess additional issues that may affect future applications of MV as an electron mediator in biological processes.

5.2 Medium reduction

5.2.1 Materials and method

5.2.1.1 Bio Electro Reactor (BER) for anaerobic systems

A BER similar to the one in Chapter 3 and 4 was used for the experiments. The major two differences for the BER in this chapter are:

1. Reference electrode. The reference electrode used in this chapter was the Ag/AgCl electrode (E255 Ag/AgCl wire electrode, Warner Instruments, Hamden, CT) instead of the sealed non-leaking reference electrode in Chapters 3 and 4. The potential of the reference electrode was controlled by maintaining a constant Cl^- concentration (100 mM) in the solution. The MV in the cathode chamber influenced the potential of the reference electrode, so the Ag/AgCl electrode had to be placed in the anodic chamber with a reference potential of 250 mV. For the studies of Chapters 3 and 4 with the sealed electrode, the MV did not affect the reference electrode. The wire reference electrode is not as suitable for quantitative studies because the potential between the reference and working electrode includes not just the over potential need to drive the electrochemical reaction but also other resistances. However, for the studies associated with the effects of the medium on MV reduction, the results from the wire electrode can still be utilized to provide general conclusions of medium effects.
2. pH control system. The pH probe and the pH buffer port in the pH control system were in the cathodic chamber instead of in the anodic chamber. This is in contrast to

the pH control system in the anode chamber for studies in Chapters 3 and 4 due to the limited number of liquid ports in each chamber (two for each chamber). However, the H^+ can easily move across the cation selective membrane. Thus, the placement of the pH control system had little influence.

Except for these two differences, the BER system used for the studies of this chapter was the same as the one used for the studies in Chapters 3 and 4.

5.2.1.2 Reduction of medium

Medium reduction in the presence of an applied voltage was studied using the modified medium for *Clostridium Ragsdalei* P11 (Oklahoma State University). The detailed compositions for stock solutions of minerals (Table 8-1), vitamins (Table 8-2), calcium (Table 8-3), trace metals (Table 8-4) are listed in the Appendix. The amounts of each component in the solution are shown for 1 liter stock solutions that were prepared in advance. For the experiments, both chambers contained 200 ml. In the anodic chamber, DI water with 100 mM (1.491g) KCl (Sigma) was used. In the cathodic chamber, either 5 ml mineral stock, 2ml vitamin stock, 2 ml trace metal stock, 2 ml calcium stock, or 0.1 g yeast extract were added to DI water for a total volume of 200 ml. As a control, DI water alone was used without the addition of any medium component.

The pH of the system was adjusted to pH 7 before every experiment but experiments were done before the pH control system was developed. The current of the experimental group and the control group was recorded with respect to time with the potentiostat described in Chapter 3 at a potential of -900 mV. This potential of -900 mV is different from the -900 mV in Chapter 3 because a different reference electrode was used. The electrons provided to the

electrode (N^{prov}_{e-}) as a function of time were calculated using the same method described in Section 5.1.3.

5.3 **Results and discussion - medium reduction**

There are four kinds of solutions in the optimal medium that are used for P11 growth: mineral solution, vitamin solution, trace metal solution, and calcium solution. Each solution, in the absence of MV, was studied to assess the effects of each solution on the electrons provided to the electrode. The results of N^{prov}_{e-} for water, water/calcium, water/yeast extract, water/minerals, water/vitamins, and water/metals are shown in Figure 5.4. Generally, every solution resulted in the flow of current. For water, the applied voltage can split water and form H_2 at the cathode, resulting in the flow of current. Although no significant bubbles were observed on the surface of electrode, the possibility of H_2 production is evident.

The rate of electrons provided (slope of data) by the electrode for each study were compared. Compared to the rate of electrons provided for water reduction, the rate for the metal solution was 266% higher, the rate for the mineral solution was 183% higher, the rate for the the vitamin solution was 147% higher and the rates for the yeast exact and calcium solutions were less than 115% higher. Based on the above analysis, the yeast extract and calcium solutions showed little reduction effects relative to the pure water study. However, as noted in Section 5.1.3, a similar current versus time doesn't exclude the possibility of the reduction of other species than H^+ reduction. However, it is likely that these solutions essentially do not contribute to current flow although this needs to be further studied.

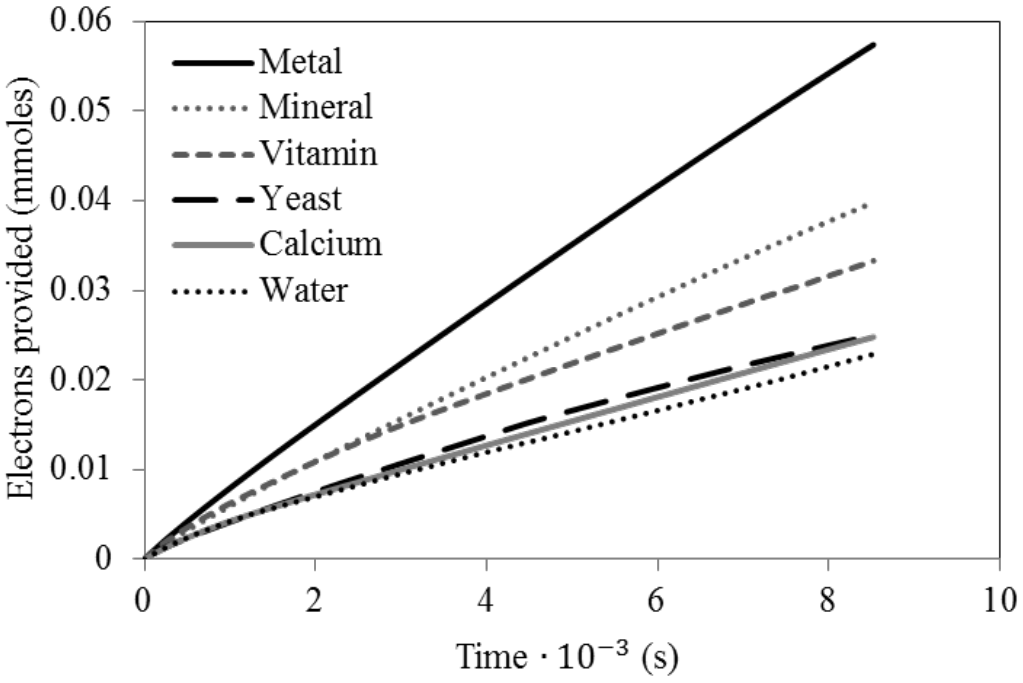

Figure 5.6 The comparison of current from reduction of medium with no MV.

The metal, mineral and vitamin solutions consumed more electrons than water only. However, the increase in the electron consumption could be caused by both the reduction of species in the medium and/or the pH drop. On the other hand, the pH drop would not occur without reduction of medium species reduction. Thus, the increase of the electron consumption was ultimately caused by the reduction of species in the solutions studied.

The composition of these solutions was carefully analyzed to find out the possible species in the solution. The metal solution contains 9 components as listed in Table 8-1 (Appendix). For $(NH_4)_2Fe(SO_4)_2$, Fe is in Fe^{2+} state which might be further reduced since the standard open circuit potential of this reduction is – 609 mV vs Ag/AgCl. As for Na_2MoO_4, Mo^{6+} can potentially be further reduced to five different species, Mo^{5+} [102], Mo^{4+}, Mo^{3+} [103], Mo^{2+}[103],

and Mo^{1+}[104]. also might be reduced due the reactivity of Se^{2+}. The high rate of electron usage of the metal solution may also be a result of the addition of electrolyte which reduces the resistance in the solution. However, the concentration of the electrolyte added to the solution is two orders of magnitude smaller than the calcium solution such that the influence of electrolytes is likely negligible since the calcium solution showed little difference than water alone.

As for the mineral solution, there are only two possible components that are in the oxidized state, KH_2PO_4 and $MgSO_4$. However, the reduction of these two species is likely not thermodynamically favorable at the applied voltage. However, the concentration of the electrolytes in the mineral solution was higher than the other stock solutions, thus the increase of current as a result of the minerals may be a result of electrolytes reducing the resistance. Since electrolytes can influence the current, then the mineral solution should have the biggest impact if no species in the solutions are reduced.

The reason for the effects of vitamins on the increase in current is unclear and this requires additional study.

These analyses are fundamentally theoretical analyses that serve as a guide for future modification of the medium for P11 when using P11 in an electrochemical system. By replacing components that are in their oxidized states with more reduced states, the reduction of medium species can be partly eliminated to enable more electrons to flow to MV or other electron carriers. However, it is critical that the modified medium should not have adverse effects on cell growth and fermentation for microorganisms. The redox state of the solution should also be carefully considered since the redox state can affect the fermentation [105].

Regarding pH and the need for pH control, any reduction besides H^+ on the cathode can result in the accumulation of H^+ in the solution. When 1mole of H^+ is produced on the anode, one mole of electrons would be donated to the cathode and one mole of electrons should be utilized on the cathode due to the electron balance. The one mole of electrons provided to the cathode would be used for H^+ reduction on the cathode and used for the reduction of any other species (e.g mineral or metals). If other species besides H^+ are reduced (e.g using 0.2 mole of electrons), then only 0.8 moles of H^+ would be reduced on the cathode and 0.2 moles of H^+ would remain in the solution. This would lower the pH while the species are being reduced.

This study was conducted before the development of pH control. Thus, if other species besides H^+ were reduced on the cathode, the pH in the system would drop, although no experimental results are available. From the thermodynamics of H^+ reduction at a lower pH, a lower applied potential is required to drive the H^+ reduction. Which is to say, when the applied potential remains the same, the reduction of H^+ would occur at a higher reduction rate as the pH decreases. Since the current is proportional to the reduction rate, a lower pH would lead to a higher current. Therefore, the reduction of other species besides H^+ not only contributes to the current by taking electrons from the cathode but also by lowering the pH.

From Figure 5.4, current can change by either increased electrolytes (likely observed with the mineral solution) or species reduction (likely observed with metals). For the reduction of species, it is not possible to determine what fraction of the increased current is due to a pH decrease and/or the increase in current consumption due to the added species.

5.4 **Conclusions**

The coulombic efficiency (ε) for MV reduction has been studied in this chapter. The ε is defined as the ratio of the electrons used to reduce MV species to the electrons supplied to the system via external electricity. The electrons consumed by MV reduction can be calculated using the kinetic model developed in Chapter 4 and the electrons supplied to the system can be calculated from the measured current.

The ε affects process economics. The coulombic efficiency study of MV reduction revealed that the complete electrochemical reduction of MV^{2+} to MV^{0} has a low overall average ε ranging from 8.3% to 18.0% with a peak ε ranging from 10.4% to 21.7%. The peak value for ε occurred near the peak value of the MV^{+} concentration which was the optimal operation point for MV reduction. A high ε is desirable for future applications. Currently, the best efficiency is when MV^{2+} reduction is occurring rather than when MV^{+} reduction is occurring. Formation of MV^{0} at a potential of -1100 mV has a low ε which means most of the electrons provided by the external power are wasted by side reactions or lost from the system; most of the electrons were not used in the MV reduction. Although the peak value of ε for MV^{+} reduction is not satisfactory, the system (electrode, reactor, etc.) used for this study is not optimized for a high ε. However, designing of a better electrode may enable the efficiency to be high for reduction of both MV^{2+} and MV^{+}. Using a better material instead of graphite which minimizes H^{+} reduction and medium reduction but favors MV reduction can increase the efficiency of the system. Therefore, engineering analysis and design is critical for optimizing systems.

On another note, the ε in this study is based on the solution of 9:1 H_2O: DMF at -1100 mV and when using MV in a biological system, medium is used. As demonstrated in the experimental results, the reduction of medium can contribute to the current and reduce the efficiency of MV reduction. Thus, in the presence of medium, the process should have an even lower efficiency than the predictions shown in Figure 5.4. Comparing with an efficiency of more than 85% for a biological process using electrons directly from electrodes [28, 29], the efficiency using MV as electron donor is low although there are still many design opportunities that can make this efficiency higher. Also, processes using external electron mediators in biological system possessed advantages including more available bio organisms for better yield and broader choice of product.

The low efficiency of MV reduction was likely because of the competition of H^+ reduction. As shown in Figure 5.5 the current difference between reduction with or without MV was small which meant the reduction of H^+ and MV had similar rates and/or most of the surface area or surface active sited were occupied by H^+ and only a few were used for MV reduction. Blocking the H^+ on the electrode surface by introducing a specially designed electrode would decrease the competition of H^+ and increase the efficiency. For example, if blocking the H^+ can free 99.9% percent of surface sites for MV reduction (if H^+ dominates the adsorption), then the rate of MV reduction can increase 1000 times, then the MV might be suitable for commercial application. Future work related to engineering analysis of the mechanism(s) of the competition between H^+ and MV would be beneficial for a better engineering designed system.

With regards to applications using bio organisms, the reduction of MV is only the first step in using MV as external electron donor in biological processes [36, 37]. After MV^{2+} is

reduced, the reduced MV species must transport into the bio organisms and then transfer electrons from MV to metabolic pathway(s). MV^{+} would then be oxidized back to MV^{2+} and MV^{2+} would have to transport out of the bio organisms and be reduced again on the electrode.

In summary, although the overall efficiency for the reduction of MV was lower than 22%, the engineering analysis performed in this study provides possibilities that the efficiency can be increased and MV can be used as an electron mediator. The efficiency can possibly be increased by specially designed electrodes which can block the reduction of H^{+} and favored the reduction of MV. The efficiency can also be increased by a better medium composition with replacement of oxidized species with more reduced species. The process of using MV as external electron donor is still promising but requires more research on the improvement of efficiency. Thus, it is critical that the system should be carefully designed and characterized for better application of MV.

6 CONCLUSIONS

6.1 Summary

The use of MV in biological studies has shown promising potential as an external electron mediator, although a better understanding of the underlying engineering principles would provide more guidance as to the potential use of MV in various applications. This study focused on the thermodynamic and kinetic characterization of MV in an electrode system to provide a foundation that can lead towards better control and design of biological systems utilizing extracellular electron mediators.

The thermodynamic study provides the analysis of the minimum required external energy input to reduce MV^{2+} in the solution to useable MV species that can donate electrons and provides guidance on the applied potential needed to control the types of MV species that are present. The kinetic analysis provides information of the MV reduction rate (or electron transfer rate), which is valuable when assessing the feasibility of future cellular applications based on required cellular electron consumption rates. For efficiency studies, where the electron efficiency is defined as the ratio of the electrons acquired by the reducing MV versus the electrons provided by external power, the efficiency helps in the analysis of the economic feasibility in future biofuel production with an electrode system.

6.2 **Discussion and future opportunities**

6.2.1 Electrode design

The electrode used in the system was made of graphite. With the graphite electrode, the kinetic and the coulombic efficiency of the MV reduction was not satisfactory for commercial applications. However, with the engineering analysis in this study, the electrode can be redesigned for better kinetics and efficiency in three ways.

First, as discussed in Chapter 4 and 5, the reduction of H^+ on the cathode likely lowered the kinetic rates of MV reduction and the coulombic efficiency of MV reduction. A better designed electrode that minimizes the side-reaction of H^+ reduction can increase both the kinetic and the coulombic efficiency. H^+ was likely adsorbed on the electrode surface where it was reduced to H_2 at an applied potential of -1100mV. As discussed in Chapter 4, the rate constants shown in this study may be underestimated and would be higher in a more comprehensive model that included the reduction of H_2. Higher k2 and k4 values would led to a higher reduction rate of MV species if H^+ reduction was prohibited in the future.

As for the efficiency, the reduction of protons consumes electrons that are provided by the external power, leading to a reduced efficiency. Higher coulombic efficiency would be achieved if H^+ reduction was eliminated.

The material of the electrode can also be carefully designed to reduce the reduction of H^+ and favor the reduction of MV. The material can either be designed to minimize the adsorption of H^+ on surface or designed to minimize the reduction of H^+ if H^+ is adsorbed on the surface.

Second, the affinity of MV species, especially MV^+, can be increased for better kinetics and efficiency. The electrode used in this study was a graphite electrode which had a porous surface structure. H^+ is a much smaller molecule than MV. H^+ can more easily diffuse into small pores compared to MV. With a specially designed electrode, the size of the pores can be controlled to maximize the amount of MV molecules that can interact with the electrode. More MV on the surface would lead to a higher reduction rate and a higher efficiency.

As demonstrated in Chapter 4, the fraction of surface sites occupied by MV^+ (θ_{MV^+}) had a peak value of 1.9% for a very short time and most of the surface sites were occupied by either MV^{2+} or MV^0. The rate constant for reduction of MV^+ was two orders of magnitude higher than the rate constant for reduction of MV^{2+}. If a specially designed electrode is designed to increase the affinity of MV^+ on the surface and increase the value of θ_{MV^+}, then the rate of the reduction of MV^+ can be largely increased by two orders of magnitude. Also, increasing the affinity of MV^+ can decrease the fraction of surface sites occupied by H^+ and reduce the negative effect of the reduction of H^+.

Third, the total surface area of the electrode can be increased to provide more active sites for surface reduction. As discussed in Chapter 4, the value of $\theta_{MV^{2+}}$ and θ_{MV^0} was approximately 1 most of the time which demonstrated that there were no vacant sites available. The rate constants k2 and k4 in Chapter 4, which are a function of the total surface sites, would increase if the total number of the sites increased. Thus, increasing the total surface sites can increase the reduction rate of the MV.

6.2.2 Control of MV species

Three MV species have distinctive properties and a system should be designed for the most suitable species instead of randomly using all three species together (like most existing studies). Controlling the species of MV in the solution is beneficial to maximize the positive effects that the species has on the desired product. As discussed in Chapter 2, MV^{2+} is potentially toxic to bio organisms but MV^{+} and MV^{0} both have promising potential to be effective electron mediators. According to the thermodynamic model developed, the toxicity of MV^{2+} can be assessed by measuring cell growth in the presence of primarily MV^{2+} by imposing a potential less negative than -650 mV to the system. In addition, the toxicity of any of the MV species on cell growth or product formation can be assessed by measuring cell growth in the presence of carefully controlled systems that produce the desired MV species.

Also, $MVCl_2$ has a low equilibrium constant ($5.6x10^{-5}$ M^2) which leads to a low concentration of free MV^{2+} in the solution. The free MV^{2+} concentration can be changed by varying the Cl^- concentration. It is unclear as to the impact of other anions on the free MV^{2+} concentration.

6.2.3 Medium design

The metal, mineral and vitamin solutions consumed more electrons than water alone. The medium analyses serves as a guide for future modification of the medium for P11 cells when using P11 in an electrochemical system. By replacing components that are in their oxidized states with more reduced states, the reduction of medium species can be partly eliminated to enable more electrons to flow to MV or other electron carriers. However, it is critical that the

modified medium should not have adverse effects on cell growth and fermentation for microorganisms. The redox state of the solution should also be carefully considered since the redox state can affect the fermentation [105]. An optimized medium would better support cellular growth and fermentation, and the medium would not contribute to the current and decrease the coulombic efficiency for the MV reduction.

6.2.4 Other electron mediators

The engineering analysis involving thermodynamics, kinetics and coulombic efficiency was performed using the electron mediator MV. The analysis provides guidance towards a better design for applications such as electron mediators for biofuel production and electron mediators for fuel cells. A similar engineering analysis of other successful electron mediators including NR, Benzyl viologen, 9,10-anthraquinone-2,6-disulfonic acid disodium salt (AQDS), safranine O, resazurin and humic acids would be beneficial.

6.3 Conclusion

Thermodynamic, kinetic and efficiency analysis had been performed in this study for electrochemical reduction of MV. These engineering analyses provides guidance for designing systems for better MV redox state control, quicker kinetics and a higher coloumbic efficiency. MV has possibiliities of applications such as microbial fuel cells, biofuels formation, and waste water treatment. However, engineering analysis of electron mediators is critical to provide better engineering control, design, and economic analysis for future applications.

7 REFERENCES

1. Administration UEI: **International Energy Outlook 2010**. 2010.
2. REN21: **Renewables 2010 global status report**. 2010.
3. Agency USEP: **Draft inventory of U.S. Greenhouse gas emissions and sinks:1990-2009**. 2011.
4. Potter MC: **Electrical effects accompanying the decomposition of organic compounds**. *Proceedings of the Royal Society of London* 1912, **84**:76.
5. Demirbas A: **Political, economic and environmental impacts of biofuels: A review**. *Applied Energy* 2009, **86**(Supplement 1):S108-S117.
6. Carolan MS: **ENVIRONMENTAL REVIEW: The Cost and Benefits of Biofuels: A Review of Recent Peer-Reviewed Research and a Sociological Look Ahead**. *Environmental Practice* 2009, **11**(01):17-24.
7. Salvi BL, Panwar NL: **Biodiesel resources and production technologies – A review**. *Renewable and Sustainable Energy Reviews* 2012, **16**(6):3680-3689.
8. Balat M, Balat H: **Recent trends in global production and utilization of bio-ethanol fuel**. *Applied Energy* 2009, **86**(11):2273-2282.
9. Serrano-Ruiz JC, Ramos-Fernandez EV, Sepulveda-Escribano A: **From biodiesel and bioethanol to liquid hydrocarbon fuels: new hydrotreating and advanced microbial technologies**. *Energy & Environmental Science* 2012, **5**(2):5638-5652.
10. Afionis S, Stringer LC: **European Union leadership in biofuels regulation: Europe as a normative power?** *Journal of Cleaner Production* 2012, **32**(0):114-123.
11. Yacobucci BD, Womach J: **Fuel ethanol: background and public policy issues**. In. Washington D.C.: Congressional Research Service; 2000.
12. Erbes DL, Burris RH: **The kinetics of methyl viologen oxidation and reduction by the hydrogenase from Clostridium pasteurianium**. *Biochimica et Biophysica Acta (BBA) - Enzymology* 1978, **525**(1):45-54.

13. Llobell A, Fernandez VM, López-Barea J: **Electron transfer between reduced methyl viologen and oxidized glutathione: A new assay of Saccharomyces cerevisiae glutathione reductase**. *Archives of Biochemistry and Biophysics* 1986, **250**(2):373-381.

14. Lan EI, Liao JC: **Metabolic engineering of cyanobacteria for 1-butanol production from carbon dioxide**. *Metabolic Engineering* 2011, **13**(4):353-363.

15. Palatnik JF, Valle EM, Carrillo N: **Oxidative stress causes ferredoxin-NADP+ reductase solubilization from the thylakoid membranes in methyl viologen-treated plants**. *Plant Physiology* 1997, **115**(4):1721-1727.

16. Panneerselvam A, Wilkins MR, DeLorme MJM, Atiyeh HK, Huhnke RL: **Effects of various reducing agents on syngas fermentation by clostridium ragsdalei**. *Biological Engineering* 2010, **2**(Compendex):135-144.

17. Aulenta F, Catervi A, Majone M, Panero S, Reale P, Rossetti S: **Electron transfer from a solid-state electrode assisted by methyl viologen sustains efficient microbial reductive dechlorination of TCE**. *Environmental Science and Technology* 2007, **41**(7):2554-2559.

18. Lymar SV, Hurst JK: **Electrogenic and electroneutral pathways for methyl viologen-mediated transmembrane oxidation-reduction across dihexadecylphosphate vesicular membranes**. *Journal of physical chemistry* 1994, **98**(Compendex):989-996.

19. Marshall CW, May HD: **Electrochemical evidence of direct electrode reduction by a thermophilic Gram-positive bacterium, Thermincola ferriacetica**. *Energy & Environmental Science* 2009, **2**(6):699-705.

20. Park DH, Zeikus JG: **Utilization of electrically reduced neutral red by Actinobacillus succinogenes: Physiological function of neutral red in membrane-driven fumarate reduction and energy conservation**. *The Journal of Bacteriology* 1999, **181**(8):2403-2410.

21. Wang K, Liu Y, Chen S: **Improved microbial electrocatalysis with neutral red immobilized electrode**. *Journal of Power Sources* 2011, **196**(1):164-168.

22. Delaney GM, Bennetto HP, Mason JR, Roller SD, Stirling JL, Thurston CF: **Electron-transfer coupling in microbial fuel cells. 2. performance of fuel cells containing selected microorganism—mediator—substrate combinations**. *Journal of chemical technology and biotechnology* 1984, **34**(1):13-27.

23. Bond DR, Holmes DE, Tender LM, Lovley DR: **Electrode-reducing microorganisms that harvest energy from marine sediments**. *Science* 2002, **295**(5554):483-485.

24. Sund C, McMasters S, Crittenden S, Harrell L, Sumner J: **Effect of electron mediators on current generation and fermentation in a microbial fuel cell**. *Applied Microbiology and Biotechnology* 2007, **76**(3):561-568.

25. Strehlitz B, Gründig B, Vorlop KD, Bartholmes P, Kotte H, Stottmeister U: **Artificial electron donors for nitrate and nitrite reductases usable as mediators in amperometric biosensors**. *Fresenius' Journal of Analytical Chemistry* 1994, **349**(8):676-678.

26. Damian A: **Direct electrochemical regeneration of NADH on Au, Cu and Pt-Au electrodes**. *Chemical and biochemical engineering quarterly* 2007, **21**(1):21-32.

27. Schroder U: **Anodic electron transfer mechanisms in microbial fuel cells and their energy efficiency**. *Physical Chemistry Chemical Physics* 2007, **9**(21):2619-2629.

28. Nevin KP, Woodard TL, Franks AE, Summers ZM, Lovley DR: **Microbial electrosynthesis: feeding microbes electricity to convert carbon dioxide and water to multicarbon extracellular organic compounds**. *MBio* 2010, **1**(2).

29. Nevin KP, Hensley SA, Franks AE, Summers ZM, Ou J, Woodard TL, Snoeyenbos-West OL, Lovley DR: **Electrosynthesis of organic compounds from carbon dioxide catalyzed by a diversity of acetogenic microorganisms**. *Applied Environmental Microbiology* 2011:AEM.02642-02610.

30. Huang L, Regan JM, Quan X: **Electron transfer mechanisms, new applications, and performance of biocathode microbial fuel cells**. *Bioresource Technology* 2011, **102**(1):316-323.

31. Rosenbaum M, Aulenta F, Villano M, Angenent LT: **Cathodes as electron donors for microbial metabolism: Which extracellular electron transfer mechanisms are involved?** *Bioresource Technology* 2011, **102**(1):324-333.

32. Tatsumi H, Takagi K, Fujita M, Kano K, Ikeda T: **Electrochemical study of reversible hydrogenase reaction of desulfovibrio vulgaris Cells with methyl viologen as an electron carrier**. *Analytical Chemistry* 1999, **71**(9):1753-1759.

33. Kim JY, Lee C, Park JW: **The kinetics of neutral methyl viologen in acidic H2O+DMF mixed solutions studied by cyclic voltammetry**. *Journal of Electroanalytical Chemistry* 2001, **504**(1):104-110.

34. Chongmok LEE BYKaJWP: **The kinetics of 2e--reduced viologens in acidic DMF + H2O mixed solutions by cyclic voltammetry: effect of substituents and solvent composition**. *Proceedings of the sixth asian conference on analytical sciences* 2001:p.a69.

35. Peguin S, Goma G, Delorme P, Soucaille P: **Metabolic flexibility of Clostridium acetobutylicum in response to methyl viologen addition**. *Applied Microbiology and Biotechnology* 1994, **42**(4):611-616.

36. Rao G, Mutharasan R: **Alcohol production by clostridium-acetobutylicum induced by methyl viologen**. *Biotechnology Letters* 1986, **8**(12):893-896.

37. Peguin S, Delorme P, Goma G, Soucaille P: **Enhanced alcohol yields in batch cultures of Clostridium acetobutylicum using a three-electrode potentiometric system with methyl viologen as electron carrier**. *Biotechnology Letters* 1994, **16**(3):269-274.

38. Tashiro Y, Shinto H, Hayashi M, Baba S-i, Kobayashi G, Sonomoto K: **Novel high-efficient butanol production from butyrate by non-growing Clostridium saccharoperbutylacetonicum N1-4 (ATCC 13564) with methyl viologen**. *Journal of Bioscience and Bioengineering* 2007, **104**(3):238-240.

39. Schubert C: **Can biofuels finally take center stage?** *Nature Biotechnology* 2006, **24**(7):777-784.

40. Kim S, Dale BE: **Global potential bioethanol production from wasted crops and crop residues**. *Biomass and Bioenergy* 2004, **26**(4):361-375.

41. Lewis RS, Tree, D.R., Hu, P., and Frankman, A.: **Syngas fermentation to ethanol: Challenges and opportunities**. In: *Biofuel and Bioenergy from Biowastes and Residues.* Edited by Khanal SK: American Society of Civil Engineers: Reston, VA; Apr 2010.

42. Shleser R: **Ethanol production in Hawaii**. *State of Hawaii, Energy Division, Department of Business, Economic Development and Tourism* 1994.

43. Kádár Z, de Vrije T, van Noorden G, Budde M, Szengyel Z, Réczey K, Claassen P: **Yields from glucose, xylose, and paper sludge hydrolysate during hydrogen production by the extreme thermophile Caldicellulosiruptor saccharolyticus**. *Applied Biochemistry and Biotechnology* 2004, **114**(1):497-508.

44. Yomano L, York S, Zhou S, Shanmugam K, Ingram L: **Re-engineering <i>Escherichia coli</i> for ethanol production**. *Biotechnology Letters* 2008, **30**(12):2097-2103.

45. Delgenes JP, Moletta R, Navarro JM: **Effects of lignocellulose degradation products on ethanol fermentations of glucose and xylose by Saccharomyces cerevisiae, Zymomonas mobilis, Pichia stipitis, and Candida shehatae**. *Enzyme and Microbial Technology* 1996, **19**(3):220-225.

46. Rogers P, Lee K, Skotnicki M, Tribe D: **Ethanol production by zymomonas mobiliszed microbial reactions**. In., vol. 23: Springer Berlin / Heidelberg; 1982: 37-84.

47. Hickman DA, Schmidt LD: **Production of syngas by direct catalytic oxidation of methane**. *Science* 1993, **259**(5093):343-346.

48. Pen˜a MA, Gómez JP, Fierro JLG: **New catalytic routes for syngas and hydrogen production**. *Applied Catalysis A: General* 1996, **144**(1–2):7-57.

49. Wilhelm DJ, Simbeck DR, Karp AD, Dickenson RL: **Syngas production for gas-to-liquids applications: technologies, issues and outlook**. *Fuel Processing Technology* 2001, **71**(1–3):139-148.

50. DOE US: **U.S. Department of Energy 2009 Annual Report**. 2009.

51. Subramani V, Gangwal SK: **A review of recent literature to search for an efficient catalytic process for the conversion of syngas to ethanol**. *Energy & Fuels* 2008, **22**(2):814-839.

52. Van Der Laan GP, Beenackers AACM: **Kinetics and selectivity of the Fischer–Tropsch synthesis: a literature review**. *Catalysis Reviews* 1999, **41**(3-4):255-318.

53. Davis BH: **Fischer-Tropsch synthesis: relationship between iron catalyst composition and process variables**. *Catalysis Today* 2003, **84**(1–2):83-98.

54. Iglesia E: **Design, synthesis, and use of cobalt-based Fischer-Tropsch synthesis catalysts**. *Applied Catalysis A: General* 1997, **161**(1–2):59-78.

55. Dry ME: **High quality diesel via the Fischer–Tropsch process – a review**. *Journal of Chemical Technology & Biotechnology* 2002, **77**(1):43-50.

56. Klasson KT, Ackerson MD, Clausen EC, Gaddy JL: **Bioconversion of synthesis gas into liquid or gaseous fuels**. *Enzyme and Microbial Technology* 1992, **14**(8):602-608.

57. Abrini J, Naveau H, Nyns E-J: **Clostridium autoethanogenum an anaerobic bacterium that produces ethanol from carbon monoxide**. *Archives of Microbiology* 1994, **161**(4):345-351.

58. Chang IS, Kim BH, Lovitt RW, Bang JS: **Effect of CO partial pressure on cell-recycled continuous CO fermentation by Eubacterium limosum KIST612**. *Process Biochemistry* 2001, **37**(4):411-421.

59. Ahmed A, Lewis RS: **Fermentation of biomass-generated synthesis gas: Effects of nitric oxide**. *Biotechnology and Bioengineering* 2007, **97**(5):1080-1086.

60. Misoph M, Drake HL: **Effect of CO2 on the fermentation capacities of the acetogen Peptostreptococcus productus U-1**. *Journey of Bacteriology* 1996, **178**(11):3140-3145.

61. Henstra AM, Sipma J, Rinzema A, Stams AJM: **Microbiology of synthesis gas fermentation for biofuel production**. *Current Opinion in Biotechnology* 2007, **18**(3):200-206.

62. Kundiyana DK, Huhnke RL, Wilkins MR: **Syngas fermentation in a 100-L pilot scale fermentor: Design and process considerations**. *Journal of Bioscience and Bioengineering* 2010, **110**(6):724-724.

63. Hurst KM, Lewis RS: **Carbon monoxide partial pressure effects on the metabolic process of syngas fermentation**. *Biochemical Engineering Journal* 2010, **48**(2):159-165.

64. Drake HL, Daniel SL: **Physiology of the thermophilic acetogen Moorella thermoacetica**. *Research in Microbiology* 2004, **155**(6):422-436.

65. Thrash JC, Van Trump JI, Weber KA, Miller E, Achenbach LA, Coates JD: **Electrochemical stimulation of microbial perchlorate reduction**. *Environmental Science and Technology* 2007, **41**(5):1740-1746.

66. Wingard Jr LB, Shaw CH, Castner JF: **Bioelectrohemical fuel cells**. *Enzyme and Microbial Technology* 1982, **4**(3):137-142.

67. Sakai S, Yagishita T: **Microbial production of hydrogen and ethanol from glycerol-containing wastes discharged from a biodiesel fuel production plant in a bioelectrochemical reactor with thionine**. *Biotechnology and Bioengineering* 2007, **98**(2):340-348.

68. Rozendal RA, Hamelers HVM, Rabaey K, Keller J, Buisman CJN: **Towards practical implementation of bioelectrochemical wastewater treatment**. *Trends in Biotechnology* 2008, **26**(8):450-459.

69. Hussain A, Al-Rawajfeh AE, Alsaraierh H: **ChemInform abstract: membrane bio reactors (MBR) in waste water rreatment (a review of the recent patents)**. *ChemInform* 2011, **42**(20):no-no.

70. Sakai H, Nakagawa T, Tokita Y, Hatazawa T, Ikeda T, Tsujimura S, Kano K: **A high-power glucose/oxygen biofuel cell operating under quiescent conditions**. *Energy & Environmental Science* 2009, **2**(1):133-138.

71. Mehta V, Cooper JS: **Review and analysis of PEM fuel cell design and manufacturing**. *Journal of Power Sources* 2003, **114**(1):32-53.

72. Zalc JM, Löffler DG: **Fuel processing for PEM fuel cells: transport and kinetic issues of system design**. *Journal of Power Sources* 2002, **111**(1):58-64.

73. Shin KM, Watt GD, Zhang B, Harb JN, Harrison RG, Kim SI, Kim SJ: **Electrochemical analysis of the reduction of ferritin using oxidized methyl viologen**. *Journal of Electroanalytical Chemistry* 2006, **598**(Compendex):22-26.

74. Surareungchai W, Turner APF, Saini S: **Kinetics of electron transfer of a bioelectrochemical reaction in binary organic solvent-water media**. In*: 1995; Stockholm, Sweden*. IEEE: 478-480.

75. Monk PMS, Hodgkinson NM: **Charge-transfer complexes of the viologens: effects of complexation and the rate of electron transfer to methyl viologen**. *Electrochimica Acta* 1998, **43**(Compendex):245-255.

76. Mohammad M: **Methyl viologen neutral MV. 1. Preparation and some properties**. *The Journal of Organic Chemistry* 1987, **52**(13):2779-2782.

77. Kim S, Yun S-E, Kang C: **Electrochemical evaluation of the reaction rate between methyl viologen mediator and diaphorase enzyme for the electrocatalytic reduction of NAD+ and digital simulation for its voltammetric responses**. *Journal of Electroanalytical Chemistry* 1999, **465**(Compendex):153-159.

78. Andrew mills PDaTR: **Kinetic Study of the Reduction of Water to Hufrogen by Reduced Methyl viologen mediated by Platinised Alumina**. *Journey of Chemical Society* 1990, **86**(9):7.

79. Asada K, Neubauer C, Heber U, Schreiber U: **Methyl Viologen-Dependent Cyclic Electron Transport in Spinach Chloroplasts in the Absence of Oxygen**. *Plant and Cell Physiology* 1990, **31**(4):557-564.

80. McLachlan KL, Crumbliss AL: **The use of the methyl viologen neutral species as a mediator**. *Journal of electroanalytical chemistry and interfacial electrochemistry* 1990, **295**(1-2):113-122.

81. Park JW, Choi MH, Park KK: **Electrocatalytic reduction of benzoylformic acid mediated by methyl viologen**. *Tetrahedron Letters* 1995, **36**(Compendex):2637-2637.

82. Kim M-H, Yun S-E: **Construction of an electro-enzymatic bioreactor for the production of -mandelate from benzoylformate**. *Biotechnology Letters* 2004, **26**(1):21-26.

83. Park DH, Laivenieks M, Guettler MV, Jain MK, Zeikus JG: **Microbial utilization of electrically reduced neutral red as the sole electron donor for growth and metabolite production**. *Applied and Environmental Microbiology* 1999, **65**(Compendex):2912-2917.

84. Prince RC, Linkletter SJG, Dutton PL: **The thermodynamic properties of some commonly used oxidation reduction mediators inhibitors and dyes as determined by polarography** *Biochimica et Biophysica Acta* 1981, **635**(1):132-148.

85. Mizyed S, Shehab M, Marji D: **A thermodynamic study of the charge transfer complexes of MV with some macrocyclic hosts**. *Journal of Inclusion Phenomena and Macrocyclic Chemistry* 2011, **70**(1):109-113.

86. Maier VE, Shafirovich VY: **Kinetics of the reduction of methyl viologen with hydrogen on a colloidal Pt catalyst**. *Kinetics and Catalysis* 1988, **29**(Compendex):417-420.

87. Tsukahara K, Wilkins RG: **Kinetics of reduction of eight viologens by dithionite ion**. *Journal of the American Chemical Society* 1985, **107**(9):2632-2635.

88. Thorneley RNF: **A convenient electrochemical preparation of reduced methyl viologen and a kinetic study of the reaction with oxygen using an anaerobic stopped-flow apparatus**. *Biochimica et Biophysica Acta (BBA) - Bioenergetics* 1974, **333**(3):487-496.

89. Monk PMS, Hodgkinson NM, Partridge RD: **The colours of charge-transfer complexes of methyl viologen: effects of donor, ionic strength and solvent**. *Dyes and Pigments* 1999, **43**(3):241-251.

90. Schroder U, Wadhawan JD, Compton RG, Marken F, Suarez PAZ, Consorti CS, de Souza RF, Dupont J: **Water-induced accelerated ion diffusion: voltammetric studies in 1-methyl-3-[2,6-(S)-dimethylocten-2-yl]imidazolium tetrafluoroborate, 1-butyl-3-methylimidazolium tetrafluoroborate and hexafluorophosphate ionic liquids**. *New Journal of Chemistry* 2000, **24**(12):1009-1015.

91. Lee LYC, Hurst JK, Politi M, Kurihara K, Fendler JH: **Photoinduced diffusion of methyl viologen across anionic surfactant vesicle bilayers**. *Journal of the American Chemical Society* 1983, **105**(3):370-373.

92. **Masterflex Tubing Application Guide Brochure** [http://www.coleparmer.com/] Jan 2012

93. **Paraquat dichloride** [http://sitem.herts.ac.uk/aeru/footprint/en/Reports/1524.htm] March 2012

94. Wolszczak M, Stradowski C: **Methylviologen cation radiacal, its dimer and complex in various media**. *International Journal of Radiation Applications and Instrumentation Part C Radiation Physics and Chemistry* 1989, **33**(4):355-359.

95. Quintela PA, Diaz A, Kaifer AE: **Dimerization of the methylviologen cation radical in anionic micellar and polyelectrolyte solutions**. *Langmuir* 1988, **4**(3):663-667.

96. Bauer R, Werner HAF: **Investigation of the Electron Transfer Mechanism Between Methyl Viologen Radicals and Protons Via a Noble Metal Catalyst**. In: *Studies in Surface Science and Catalysis.* Edited by L. Guczi FS, P T, vol. Volume 75: Elsevier; 1993: 2173-2176.

97. Park YS, Um SY, Yoon KB: **Charge-Transfer Interaction of Methyl Viologen with Zeolite Framework and Dramatic Blue Shift of Methyl Viologen−Arene Charge-Transfer Band upon Increasing the Size of Alkali Metal Cation**. *Journal of the American Chemical Society* 1999, **121**(13):3193-3200.

98. Johnson DL, Saito H, Polejes JD, Hougen OA: **Effects of bubbling and stirring on mass transfer coefficients in liquids**. *AIChE Journal* 1957, **3**(3):411-417.

99. Miller JD, Wan R-Y: **Reaction kinetics for the leaching of MnO2 by sulfur dioxide**. *Hydrometallurgy* 1983, **10**(2):219-242.

100. Vysniauskas A, Bishnoi PR: **A kinetic study of methane hydrate formation**. *Chemical Engineering Science* 1983, **38**(7):1061-1072.

101. Administration EI: **Electric Sales and Revenue.** 2011.

102. Xiao Z, Bruck MA, Doyle C, Enemark JH, Grittini C, Gable RW, Wedd AG, Young CG: **Dioxomolybdenum(VI) complexes of tripodal nitrogen-donor Ligands: syntheses and spectroscopic, structural, and electrochemical studies, including the generation of EPR-active molybdenum(V) species in solution**. *Inorganic Chemistry* 1995, **34**(24):5950-5962.

103. Dilworth JR, Neaves BD, Pickett CJ, Chatt J, Zubieta JA: **Electrochemical generation of sulfur-ligated molybdenum(II) and molybdenum(III) substrate binding sites. Preparation and crystal structures of [MoCl(S2CNEt2)2(Ph2PCH2CH2PPh2)][BF4] and [MoCl(S2CNEt2)2(PPh2Me)2][PF6] and the mechanism of their electrochemical reduction**. *Inorganic Chemistry* 1983, **22**(24):3524-3529.

104. Nocera DG, Gray HB: **Electrochemical reduction of molybdenum(II) and tungsten(II) halide cluster ions. Electrogenerated chemiluminescence of tetradecachlorohexamolybdate(2-) ion**. *Journal of the American Chemical Society* 1984, **106**(3):824-825.

105. Hu P: **Thermodynamic, Sulfide, Redox Potential, and pH Effects on Syngas Fermentation**. Provo: Brigham Young University; 2011.

8 APPENDIX

8.1 Composition of the medium for P11

Table 8-8-1 Composition of mineral stock solution

Minerals stock solution	Unit (g/L)
Potassium Chloride	10
Potassium Phosphate Monobasic (KH_2PO_4)	10
Magnesium sulfate	20

Table 8-8-2 Composition of vitamin stock solution

Vitamin stock solution	Unit (g/L)
Pyridoxine hydrochloride	0.01
Thiamine hydrochloride	0.005
Riboflavin	0.005
D-Pantothenic acid hemicalcium salt	0.005
Thioctic acid	0.005
p-(4)-Aminobenzoic Acid	0.005

Table 8-8-3 Composition of vitamin stock solution - continued

Vitamin stock solution	Unit (g/L)
Nicotinic acid	0.005
Vitamin B12	0.005
d-Biotin	0.002
Folic acid	0.002
2-mercaptoethanesulfonic acid sodium salt (MESNA)	0.01

Table 8-8-4 Composition of trace metal stock solution

Trace Metal Stock Solution (ml per liter)	Unit (g/L)
Nitrilotriacetic acid	2
Manganese sulfate monohydrate	1
Ferrous ammonium sulfate	0.8
Cobalt chloride hexahydrate	0.2
Zinc sulfate heptahydrate	1
Nickel chloride	0.2
Sodium molybdate dehydrate	0.02
Sodium selenite anhydrous	0.1
Sodium tungstate dehydrate	0.2

Table 8-8-5 Composition of calcium stock solution

Calcium Stock Solution (ml per liter)	Unit (g/L)
Calcium chloride dehydrate	10